Manuscript prepared for Earth Surf. Dynam.
with version 2015/04/24 7.83 Copernicus papers of the LATEX class copernicus.cls.
Date: 16 June 2016

# Reconstruction of North American drainage basins and river discharge since the Last Glacial Maximum

Andrew D. Wickert[1]

[1]Department of Earth Sciences and Saint Anthony Falls Laboratory, University of Minnesota, Minneapolis, MN, USA

*Correspondence to:* A. D. Wickert (awickert@umn.edu)

**Abstract.** Over the last glacial cycle, ice sheets and the resultant glacial isostatic adjustment (GIA) rearranged river systems. As these riverine threads that tied the ice sheets to the sea were stretched, severed, and restructured, they also shrank and swelled with the pulse of meltwater inputs and time-varying drainage basin areas, and sometimes delivered enough meltwater to the oceans in the right places to influence global climate. Here I present a general method to compute past river flow paths, drainage basin geometries, and river discharges, by combining models of past ice-sheets, glacial isostatic adjustment, and climate. The result is a time series of synthetic paleohydrographs and drainage basin maps from the Last Glacial Maximum to present for nine major drainage basins – the Mississippi, Rio Grande, Colorado, Columbia, Mackenzie, Hudson Bay, Saint Lawrence, Hudson, and Susquehanna. These are based on five published reconstructions of the North American ice sheets. I compare these maps with drainage reconstructions based purely on field data, such as river deposits and terraces, isotopic records, mineral provenance markers, glacial moraine histories, and evidence of ice-stream and esker flow directions. The sharp boundaries of the reconstructed past drainage basins complement the flexurally-smoothed GIA signal more often used to validate ice-sheet reconstructions, and provide a complementary framework to reduce nonuniqueness in model reconstructions of the North American ice sheet complex.

## 1 Introduction

At the time of Last Glacial Maximum (LGM) ice extent, ca. 30 ka to 19.5 ka (Clark et al., 2009; Lambeck et al., 2014), North American drainage configurations and river discharge were dramatically different from those at present. Ice advance rerouted rivers (e.g., Ridge, 1997; Curry, 1998; Blumentritt et al., 2009), and ice streams fed temporarily-enlarged drainage basins (Dyke and Prest, 1987; Patterson, 1998; Margold et al., 2014, 2015). The growth of the ice-sheets changed atmospheric circulation (Kutzbach and Wright, 1985; Ullman et al., 2014) by generating up to 3.5–4 km of high-albedo ice-surface topography (e.g., Peltier, 2004; Tarasov et al., 2012; Peltier et al., 2015; Ivanović et al., 2015) that influenced global climate and therefore patterns of drainage-basin-scale water balance and river discharge to the oceans.

Reconstructions of past ice-sheet thickness have proliferated (e.g., Tushingham and Peltier, 1991; Lambeck et al., 2002; Peltier, 2004; Tarasov et al., 2006, 2012; Gregoire et al., 2012; Argus et al., 2014; Peltier et al., 2015), but are evaluated using limited (Tarasov et al., 2006, 2012) to no (all others) geologic evidence for past drainage patterns. All but the G12 model (Gregoire et al., 2012) were tuned or calibrated terminal moraine positions and records of glacial isostatic adjustment, with the latter being a response with a characteristic two-dimensional flexural half-wavelength of 500–850 km over the high-flexural-rigidity Canadian Shield provence that was covered by the ice sheet (Vening Meinesz, 1931; Kirby and Swain, 2009; Tesauro et al., 2012). G12 (Gregoire et al., 2012) was built to roughly match ice-sheet outlines and evolve more freely. Flow-routing calculations (e.g., Metz et al., 2011; Schwanghart and Scherler, 2014) are deterministic and can be used to produce time-series of drainage pathways predicted by each reconstructed ice-sheet and its associated glacial isostatic adjustment (GIA) history, forming the necessary links between the reconstructed ice-sheet and measurable geomorphic and sedimentary records. Furthermore, the discrete boundaries of drainage basins are sensitive to ice geometry in a way that is distinct from the broad GIA response, and therefore can provide a partly-independent check on the accuracy of any given ice-sheet reconstruction (Wickert et al., 2013).

On a global scale, climate change during deglaciation may have been forced by meltwater delivery to the oceans, especially at the time of the Younger Dryas (e.g., Broecker et al., 1989). The global climate system is highly sensitive to the locations of meltwater inputs to the oceans (e.g., Tarasov and Peltier, 2005; Murton et al., 2010; Condron and Winsor, 2012; Carlson and Clark, 2012). Geologic data provide a timeline of meltwater delivery to one basin or another (e.g., Ridge, 1997; Licciardi et al., 1999; Clark et al., 2001; Flower et al., 2004; Knox, 2007; Rittenour et al., 2007; Carlson et al., 2009; Breckenridge and Johnson, 2009; Murton et al., 2010; Hoffman et al., 2012; Williams et al., 2012; Breckenridge, 2015), with some types of data, such as oxygen isotopes, being able to be analyzed to produce reconstructions of meltwater discharge (Moore et al., 2000; Carlson et al., 2007a; Carlson, 2009; Obbink et al., 2010; Wickert et al., 2013). The relationships between geological data in different parts of the continent must be connected by conservation of ice-sheet mass and glaciological continuity of ice flow. Continental-scale meltwater routing calculations that connect data and models address both of these concerns by using quantified ice-sheet thickness and ensuring that water that is not sent to one basin is sent to another.

In general, there exists a lack of recognition of the importance of Pleistocene drainage rearrangement on river systems. In spite of the broad knowledge that river systems and drainage basins have changed significantly since the LGM (Dyke and Prest, 1987; Wright, 1987; Teller, 1990a, b; Marshall and Clarke, 1999; Patterson, 1997, 1998; Licciardi et al., 1999; Overeem et al., 2005; Tarasov et al., 2006; Wickert, 2014b; Ullman et al., 2014; Margold et al., 2014; Ullman et al., 2015; Margold et al., 2015), many studies do not include any clear picture of drainage basin evolution. This results in representations of the modern drainage network wholly or partially in place of glacial-

stage drainage basins (e.g., Blum et al., 2000; Sionneau et al., 2008; Montero-Serrano et al., 2009; Sionneau et al., 2010; Kujau et al., 2010; Lewis and Teller, 2006; Tripsanas et al., 2007, 2014; Rittenour et al., 2003, 2005, 2007; Knox, 2007) that help to propagate a lack of consciousness about the continental-scale hydrologic changes that occurred, even in cases when the study acknowledges in the text that past drainage pathways were different. The best current Cenozoic history of Mississippi River drainage does not attempt to place its northern drainage basin boundary during the Pleistocene (Galloway et al., 2011). Model-based studies likewise either test a range of possible drainage basin areas (Overeem et al., 2005) or assume that the rivers have remained unchanged (Roberts et al., 2012). In the former case, this can lead to less-precise calculations of sediment transport and deposition. In the latter case, this violates the underlying assumptions used to compute erosion and infer spatially-distributed uplift. Paleoclimate general circulation model reconstructions of past climate (e.g., Liu et al., 2009, 2012; He et al., 2013) maintain static drainage basins in spite of climate sensitivity on patterns of meltwater routing, and this has just begun to be addressed (Ivanović et al., 2015). All of these scenarios highlight the need for an improved community-wide understanding of the ice-age effects on the continental-scale river systems of North America that provides the necessary backdrop to understand the present-day rivers, their origins, and their evolution.

Here, I focus primarily on nine North American river basins. These are (counterclockwise from North) the Mackenzie River, Columbia River, Colorado River, Rio Grande, Mississippi River, Susquehanna River, Hudson River, Saint Lawrence River, and Hudson Bay/Hudson Strait. These rivers span a north–south gradient of catchments that were dramatically and directly impacted by Quaternary glaciation and those that were far from the ice sheet, and together constitute a reasonably representative set of rivers from which the continental-scale hydrologic impact of glaciation on North American drainage basins can be surmised.

The present work is inspired by the dual and connected needs for (1) an appropriate mapping tool for data–model intercomparison, and (2) maps of the past drainage basins of North America to inform geologic studies. I first present a standardized and automated method to extract past drainage pathways and river discharges from combinations of ice-sheet, GIA (Mitrovica and Milne, 2003; Kendall et al., 2005), and climate (Liu et al., 2009; He, 2011) reconstructions. I then apply this method to four ice-sheet models: the old but still-relevant ICE-3G (Tushingham and Peltier, 1991); the "industry standard" ICE-5G (Peltier, 2004); the ANU model, developed by a separate research group (Lambeck et al., 2002), the ice-physics-based "G12" model (Gregoire et al., 2012), and the new ICE-6G (Argus et al., 2014; Peltier et al., 2015). I then compare the resultant drainage basin evolution and synthetic paleohydrographs against onshore and offshore geologic data, including data-driven reconstructions of North American drainage basins.

## 2 Methods: Automated Drainage Reconstruction

River systems in North America have responded to synchronous and linked changes in climate, ice extent, and sea level, with the latter including GIA-induced variability. Addressing this connected climate–ice–solid-Earth system is necessary to accurately reconstruct drainage. Ice advances and retreats blocked drainage pathways and rerouted rivers (Tight, 1903; Ver Steeg, 1946; Bluemle, 1972; Teller, 1973; Licciardi et al., 1999; Teller et al., 2002; Carlson and Clark, 2012; Prince and Spotila, 2013). Ice-sheet retreat left behind large isostatic depressions that held proglacial lakes, such as the massive Glacial Lake Agassiz (e.g., Breckenridge, 2015), and strongly affected drainage patterns (e.g, Fisher and Souch, 1998). Even the subtle ($\sim$20–60 m) forebulges of continental ice-sheets have been hypothesized to play major roles in drainage rearrangement (Anderson, 1988). This is especially true of the generally low-relief North American cratonal interior, where ice-sheets and GIA have been significant drivers of large-scale topographic slopes.

The drainage basin and paleohydrologic reconstructions are a combination of four inputs: (1) a digital elevation model (DEM) with high enough resolution to resolve the valleys of major river systems, (2) a prescribed ice-sheet history, (3) a model of the GIA response to that ice history, and (4) a past water balance based on general circulation model (GCM) outputs that have been offset to fit modern data at the present time step (Fig. 1). These factors together allow us to generate synthetic river discharge histories that can be compared with geologic data.

This analysis produced three major end products. The first is a spatially-distributed map of estimated mean river discharges since the Last Glacial Maximum. The second is a gridded product of river discharges to the sea, designed for coupling with general circulation models to investigate the feedbacks between ice melt, ocean circulation, and climate (see Ivanović et al., 2014). The third is a set of major drainage basin extents and a time-series of their discharges into the ocean.

The drainage analyses were performed using GRASS GIS (Neteler et al., 2012; GRASS Development Team, 2012), a free and open-source GIS software that has efficient data management, computational, and hydrologic tools. GRASS GIS is fully scriptable, and the Python source code to automate these analyses has been released under the GNU General Public License (GPL) version 3 and is made available to the public at the University of Minnesota Earth-surface GitHub organizational repository, at https://github.com/umn-earth-surface/ice-age-rivers.

### 2.1 Surface elevations for flow-routing

Water and ice flow downslope following a routing surface, $Z_r$, that is given by:

$$Z_r = Z_{m,b} + H_i + \Delta Z_b \tag{1}$$

$Z_b$ is the reference (i.e., modern) land-surface elevation (subscript "$b$" stands for "modern glacier bed" or "modern bare (i.e., ice-free) ground"), $H_i$ is the ice thickness, and $\Delta Z_b$ represents changes between the past and modern land-surface (glacier-bed) elevation. Together, $Z_b + \Delta Z_b$ give the con-
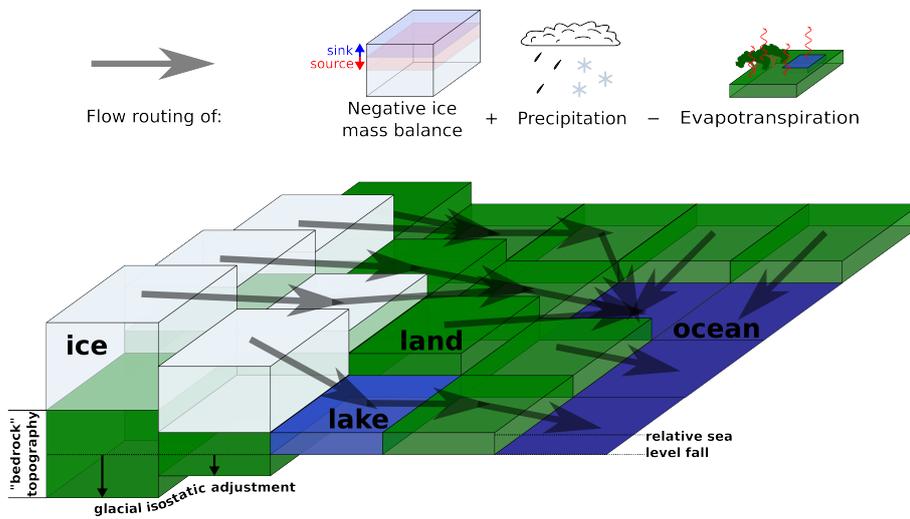
**Figure 1.** Meltwater and meteoric (precipitation minus evapotranspiration) water are routed to the coast, across a surface formed by the sum of present-day topography, glacial isostatic adjustment, and ice sheet thickness.

temporaneous glacier bed elevation field. When this $(Z_{m,b} + \Delta Z_b)$ surface is summed with ice thickness, $H_i$, the resulting routing surface, $Z_r$, combines ice-free land-surface elevations and the elevations of the surface of the ice-sheet. This ice-sheet surface is chosen for the flow-routing calculations because this is what generates the driving stress for ice flow (cf. Cuffey and Paterson, 2010), and therefore sets ice divides and meltwater pathways. If one wanted to compute subglacial water routing instead, an alternate approach is to drive flow by the subglacial pressure gradient to simulate meltwater routing through subglacial streams and tunnel channels (e.g., Wright, 1973), and this could be accomplished by multiplying $H_i$ by $\rho_i/\rho_w$, where the latter are the densities of ice and water, respectively (e.g., Livingstone et al., 2015).

### 2.1.1 DEM and grid resolution

$Z_b$ is modern land-surface elevation. The primary modern elevation data set for flow routing is the GEBCO_08 30-arcsecond DEM (British Oceanographic Data Centre, 2010). GEBCO provides the highest resolution combined topography and bathymetry data sets currently available. 30 arcseconds corresponds to a North–South cell size of 927 m, and a East–West cell size that ranges from 895 m at 15°N, the southern extent of the analysis region, to 81 m at 85°N, the northern extent. The GEBCO_08 grid is used in all areas except beneath the Greenland Ice Sheet, where the subglacial topography is interpolated from the etopo1 1-arcminute global topographic data set (Amante and Eakins, 2009).

This sub-kilometer resolution over the ice-free Earth is required to resolve flow inside the km-scale valleys of the major rivers that drain North America, and is therefore critical to accurately calculate river networks. More coarsely-gridded drainage routing can send water from the modern

Upper Missouri River basin, for example, towards the Arctic Ocean. However, even these high-resolution calculations exhibit some small deviations from mapped drainage basin extents. Examples of this, such as in the Arrowhead region of Minnesota where the Saint Louis River is believed to have progressively captured Upper Mississippi drainage near Savanna Portage (van Hise and Leith, 1911), indicate that still-higher resolution elevation data will continue to improve flow-routing calculations near headwaters streams, a scale-dependence given by the relationship between channel geometry, river discharge, and drainage area (Leopold and Maddock, 1953).

Raster grid cell area, $A_c$, is a function of latitude, and this is an important conversion factor for changing scalar quantities in cells, such as ice thickness, into a measure of volume. Using the simplifying assumption that Earth is perfectly spherical,

$$A_c = (R_E \delta\theta) \left( R_E \cos\left(\theta - \frac{\pi}{2}\right) \delta\varphi \right) \tag{2}$$

Here, $R_E$ is the mean radius of Earth, $\theta$ is again colatitude, and $\varphi$ is again east-longitude (i.e., degrees east of Greenwich). $\delta\theta$ is cell north–south extent, and $\delta\varphi$ is cell east-west extent; in the simulations presented here, both of these extents equal 30 arcseconds. These areas are computed at a latitude $\lambda$ corresponding to the north–south midpoint of the cell, with the implicit assumption that the cells are small enough that the north–south difference in cell size can be approximated to be linear such that a straight mean accurately represents the whole. For the GEBCO_08 30-arcsecond grid that is used here, this approximation generates errors of <0.3%.

### 2.1.2 Ice-sheet history

$H_i$, ice-sheet thickness, is provided by pre-generated ice-sheet reconstructions. These are produced at a coarser resolution than the 30-arcsecond flow-routing grid, and therefore are interpolated using an iterative nearest-neighbor approach to remove stepwise discontinuities. This smoothing works successively from 1/3 the native resolution to 30 arcseconds, and is necessary because some coarse ice-sheet reconstructions contain multi-cell interior plateaus and several-hundred-meter cliffs at their termini that would otherwise introduce artifacts in the flow-routing calculations. For a 1-degree grid, this requires 5 iterations and leads to smoothing over a half-degree distance (∼40–50 km) outside of a given cell. While this somewhat smears the ice-sheet boundary (see, e.g., "ICE-6G" vs. "From data" in Figures 7 and 8), it does not significantly change its fit to the published ice-margin chronology (Dyke et al., 2003; Dyke, 2004).

I use five ice models, four of which were created based on geophysical data, and one of which was generated using a numerical model of ice-sheet physics. In the former, ice-sheet thickness evolution was determined by inverting for global sea level data by combining (1) the total water mass contained within the ice-sheets, causing global mean sea level fall, and (2) calculations of the GIA process, which created deviations from the mean sea level history. Most notable among these deviations is that due to postglacial rebound, i.e., the local deformation of the lithosphere and mantle due to

the weight of the ice, which is a key indicator of the presence of major past ice-sheets. However, postglacial rebound rates are a function of both time-evolving ice-sheet thickness and solid Earth (lithosphere and mantle) rheology. That this one rate is a function of two only partly-constrained variables introduces an element of uncertainty into GIA-based inversions (Mitrovica, 1996). Ice physics, on the other hand, are most sensitive to the paleoclimate forcing and basal conditions (e.g., topography, roughness, sedimentary cover, geothermal heat flux) (Tarasov et al., 2006; Cuffey and Paterson, 2010). Here, I investigate four geophysically-based ice-sheet reconstruction (Tushingham and Peltier, 1991; Lambeck et al., 2002; Peltier, 2004; Argus et al., 2014; Peltier et al., 2015) and one ice-physics based reconstruction (Gregoire et al., 2012), with the latter being allowed to evolve more freely than the tuned model reconstructions of, e.g., Tarasov et al. (2006) and Tarasov et al. (2012).

ICE-3G (Tushingham and Peltier, 1991) was one of the earliest widely-used ice-sheet reconstructions. It was constructed to constrain ice thickness as much as possible with measurements of glacial isostatic adjustment from radiocarbon-dated sea level markers. While it does not include enough ice to reproduce the full magnitude of the observed LGM global sea level fall (Austermann et al., 2013; Lambeck et al., 2014), it provides a counterpoint to the more recent ice-sheet reconstructions, all of which include a much more massive North American ice-sheet complex (Figure 2).

ICE-5G (Peltier, 2004) has been often considered the "industry standard" global ice-sheet and GIA reconstruction. It was also built by combining geological data and geophysical inversions, and is an update to ICE-3G. It contains a very thick north–south-oriented ice dome over western Canada (Argus and Peltier, 2010) that is not located where glacial geological evidence would place the Keewatin dome. This causes its meltwater discharge to the coast to fail to match isotopic records from the Mississippi River drainage basin (Wickert et al., 2013), and in any case, seems unlikely as the ice-sheet would slide and thin over the soft Western Interior Seaway sediments east of the Canadian Rockies. Nevertheless, ICE-5G remains widely-used and matches many observations of GIA and sea-level (Peltier, 2004).

ICE-6G (here, shorthand for ICE-6G_C) (Argus et al., 2014; Peltier et al., 2015) is the successor to ICE-5G. It has been shown to improve agreement with present-day GIA measurements, and was built to match geologic evidence for the locations of the ice domes and ice-sheet outlines (Patterson, 1998; Dyke et al., 2003; Dyke, 2004). As ICE-6G is so new, it has not been extensively tested outside of the group that developed it (Argus and Peltier, 2010; Argus et al., 2014; Peltier et al., 2015).

Lambeck et al. (2002) developed the Australian National University (ANU) ice-sheet model, also based on field data constraining sea level and GIA. This model differs from ICE-3G and ICE-5G in that it was developed regionally, and these regions were later combined into a more global picture of ice-sheet evolution.

To produce the G12 ice model, Gregoire et al. (2012) simulated North American ice-sheet evolution from the LGM to present using the Glimmer community ice-sheet model (Glimmer–CISM)

(Rutt et al., 2009). Glimmer–CISM is a thermomechanical model of ice deformation and dynamics that uses the shallow ice approximation for its driving stresses. While the shallow ice approximation neglects higher-order (i.e., less-important) stresses, it generally closely approximates those models that do include higher-order terms, and its computational efficiency makes it a viable option for long-term simulations (Rutt et al., 2009), such as the Gregoire et al. (2012) LGM–present study. One of its major features is a collapse of the ice saddle between the Laurentide and Cordilleran Ice Sheets at ca. 11.6 ka. Geological data, on the other hand, place the major phase of saddle collapse during the Bølling-Allerød warm period, ca. 14.5–12.9 ka Williams et al. (2012); Dyke et al. (2003); Dyke (2004), and possibly beginning as early as ∼17.0 ka (John et al., 1996; Clague and James, 2002; Carlson and Clark, 2012). While Gregoire et al. (2012) shifted their chronology to compare their Laurentide–Cordilleran ice-saddle collapse to the geologic record of Meltwater Pulse 1A (Fairbanks, 1989; Deschamps et al., 2012), I use their model ages as direct geologic age, such that the results presented here are linked in time with the effects of their climate forcings on their ice sheet. Most importantly, the ice dynamics contained within Glimmer–CISM provide it a set of tools to match reality that place it in a different category than the GIA-based models.

**2.1.3 Change in land-surface elevation: glacial isostatic adjustment**

$\Delta Z_b$, change in land-surface (glacier bed) elevation, is here provided by the combination of changes in local relative sea level. At the Last Glacial Maximum, ice-volume equivalent global mean sea level was 130–135 m lower than present, but local relative sea level was highly variable due to the effects of GIA (Lambeck et al., 2014). GIA comprises deformational, gravitational, and rotational effects of ice-age loading. The deformational component is the local flexural isostatic response to changes in ice and water loading. The gravitational component is in response to redistribution of mass (and hence, gravitational potential) across the surface of Earth, and this is amplified by the water self-gravitation feedback (e.g., Mitrovica and Milne, 2003). The rotational component is also the response to changing near-surface mass distributions that perturb the moment of inertia and produce true polar wander that causes the equatorial bulge to migrate, first in the form of seawater and later in the form of solid Earth material. These three components feed back into one another, and therefore are solved numerically through iteration.

The gravitationally self-consistent sea level theory applied here and its numerical implementation are described by Mitrovica and Milne (2003) and Kendall et al. (2005), respectively, who calculate the GIA effects of changing ice and water masses. The calculations are performed using a pseudo-spectral algorithm that, for this work, is truncated at spherical harmonic degree and order 256. This satisfies the Nyquist flexural wavenumber for the solid Earth models employed, meaning that the wavelength of the spectral representation is always less than half of the flexural wavelength (Vening Meinesz, 1931) of the lithosphere in the solid Earth model. Satisfaction of this condition allows the solutions to be interpolated to an arbitrarily high resolution without concerns about aliasing.
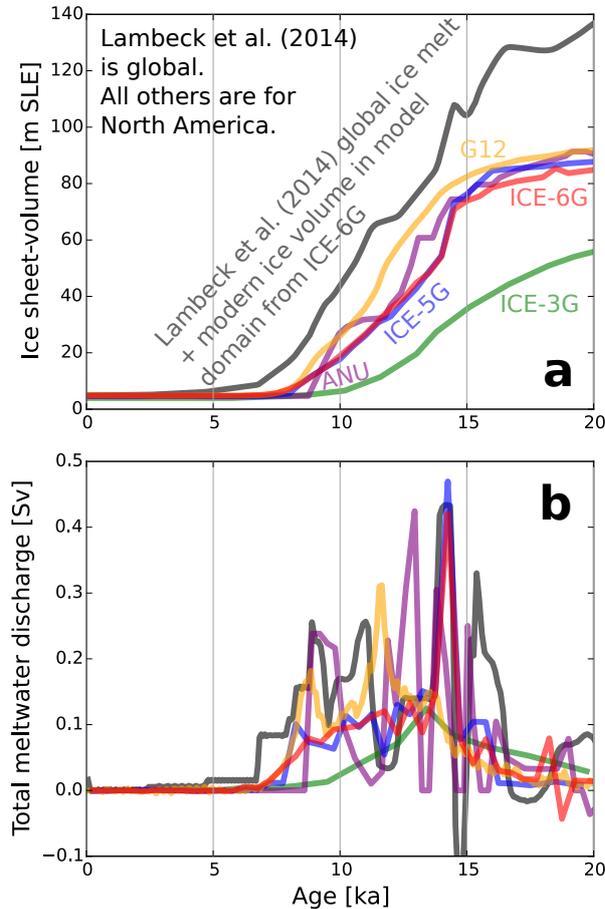
**Figure 2.** Ice volume histories over the North American computational region for each of the examined ice-sheet reconstructions (colors), along with the full global ice-volume estimate of Lambeck et al. (2014) (gray) shifted for easier comparison to match the same ice volume as ICE-6G in the North American region at the modern time-step. **a.** Cumulative change in ice volume within the computational domain, which here contains the entire North American ice-sheet complex and part of Greenland. These ice volumes are represented in meters sea-level equivalent (SLE), assuming a constant ocean surface area of $3.62 \times 10^8$ km$^2$ (after Marshall and Clarke, 1999). **b.** Total meltwater discharge over the computational domain for each ice-sheet reconstruction. ICE-5G and ICE-6G have a noticeable peak during Meltwater Pulse 1A (MWP-1A), 14.65–14.31 ka Deschamps et al. (2012). Though the time-scale of their numerical model is shifted, Gregoire et al. (2012) also consider their meltwater peak, due to collapse of the ice saddle between the Cordilleran and Laurentide ice sheets, to represent MWP-1A. The vertical axis is in Sverdrups, where 1 Sv is $10^6$ m$^3$ s$^{-1}$.

ICE-3G, ICE-5G, ICE-6G, and ANU were each calibrated to match sea level data based on specific 1D models of solid Earth viscoelasticity (Tushingham and Peltier, 1991; Lambeck et al., 2002; Peltier, 2004; Argus et al., 2014; Peltier et al., 2015); Argus and Peltier (2010, p. 699) provide a succinct review of the VM$n$ models. I use each ice reconstruction's respective spherically symmetric Earth model to simulate its response to these loads – VM1 for ICE-3G, VM2 for ICE-5G, VM5a for ICE-6G, and an unnamed model for ANU. G12 was built using a simplified model of isostatic response to glacial loading, and was run only for North America. I pair it with VM2, and *a posteriori* enforce a total global ice-sheet volume (and therefore ice-volume equivalent global mean sea level history) equal to that of ICE-5G. Among these solid Earth models, VM1 is a two-layer model with a viscosity that increases at the transition zone. VM2 includes a large number of layers with a large increase in viscosity at the 660-km discontinuity and gradually-increasing viscosity in the lower mantle towards the core–mantle boundary; these layers underly a 90 km thick elastic lithosphere in the most recent version of VM2, which is used here (Peltier, 2004). Below 100 km, VM5a is a simplification of VM2; above 100 km, it includes a 60-km thick lithosphere over a 40-km thick layer with a viscosity of $10^{22}$ Pa s. The ANU solid Earth model has a higher viscosity contrast between the upper and lower mantle than VM2, placing it in better agreement with geophysical inferences of the upper mantle–lower mantle viscosity contrast based on observations of the long-wavelength geoid (Hager and Richards, 1989), and employs a 65 km thick elastic lithosphere. One may note that all of the lithospheric elastic thicknesses are characteristic of cratonal regions; this is because the Laurentide and Fennoscandian ice sheets nucleated and grew across old, thick cratonal lithosphere, and a cratonal value for elastic thickness therefore provides the best fit to near-field data that record GIA.

I initiate the GIA modeling of G12 in equilibrium at the LGM, and ANU slightly before the LGM. This is a potential source of error: while the sea-level records of Lambeck et al. (2014) indicate that global ice mass was grew only slightly between 30 and 20 ka, providing enough time to approach isostatic equilibrium, this is only ∼2 $e$-folding time-scales towards isostatic equilibrium based on data from the Ångerman River and Hudson Bay (Mitrovica and Forte, 2004; Nordman et al., 2015). Therefore, it is very likely that the North American Ice Sheet complex was not yet in isostatic equilibrium at the LGM. ICE-5G includes hypothesized ice-sheet growth since 120 ka. This start point is during the last interglacial (MIS 5e), when global mean sea level peaked 5.5–7.5 meters above its present level (Hay et al., 2014) though with some significant variability, as indicated by ancient beaches and modeling studies (Hearty et al., 2007; Rohling et al., 2007; Dutton and Lambeck, 2012; Hay et al., 2014; Dutton et al., 2015). ICE-3G was initiated at the last interglacial as well, with ice being grown in the same pattern as it retreated, except more slowly and in reverse.

Our flow-routing calculations neglect geomorphic change for three major reasons. First, significant changes in Lake Agassiz outflow directions occurred as a precursor to spillway incision (Teller et al., 2002), meaning that ice-sheet geometry and GIA are the primary drivers of drainage change.

Second, while process-based landscape evolution models exist (cf. Tucker and Whipple, 2002; Will-
goose, 2005; Tucker and Hancock, 2010), the thresholded and highly nonlinear relationships be-
tween flow, erosion, sediment transport, and deposition, means that these models may predict a very
wide range of potential landscape responses with sufficient uncertainty as to reduce their predictive
capability. This would leave changing the DEM's by hand as an option (as was done by Tarasov and
Peltier, 2005), but considering incomplete knowledge of past topography and my desire to, at least
at this stage, separate the calculations from the field work against which they are checked, I choose
to use modern topography while acknowledging that this is an approximation.

## 2.2 Water balance: precipitation, evapotranspiration, and ice melt

Each cell in the flow-routing grid domain can act as a source of water to continental drainage systems.
Water balance over each cell is a sum of precipitation gains, $P$, evapotranspiration losses, $ET$, and
changes in water-equivalent thickness of the ice-sheet reconstruction, $(dH_i/dt) * (\rho_i/\rho_w)$. When
multiplied by the cell area, $A_c$ (Eq. 2), the result is an expression for volumetric incoming water
discharge, $Q_{\text{in}}$ (Eq. 3).

$$Q_{\text{in}} = A_c \left( P - ET - \frac{\rho_i}{\rho_w} \frac{\Delta h_i}{\Delta t} \right) \tag{3}$$

### 2.2.1 Global precipitation and evapotranspiration

Precipitation and evapotranspiration inputs changed through time (Fig. 3). These changes were cal-
culated by Liu et al. (2009) and He (2011) using a continuous LGM (22 ka) to present run of the
National Center for Atmospheric Research (NCAR) Community Climate System Model version 3
(CCSM3) (Collins et al., 2006). This simulation, called TraCE-21K, was run at 3.5 degree resolu-
tion, and used ICE-5G/VM2 as its ice sheet and paleotopography input. Therefore, the only fully
self-consistent calculations presented here are from the ICE-5G/VM2 reconstruction. I spherically
interpolated (following Dierckx, 1993) the results to 0.25 degree (15 arcminute) resolution to match
the assembled modern data products (below).

The low resolution CCSM3 contains systematic biases that produce a $\sim$1 mm/day positive pre-
cipitation anomaly in western North America and a $\sim$1 mm/day negative precipitation anomaly in
eastern North America (Yeager et al., 2006). To correct for this and other possible model biases, I as-
sembled modern precipitation and evapotranspiration fields, computed the difference between each
time step of TraCE-21K and its modern time step, and summed the modern compilations with the
computed TraCE-21K difference from modern. I could find no global evapotranspiration product,
and global precipitation products were coarse, often at 2.5-degree resolution ($\sim$280-km cells at the
equator) (Xie and Arkin, 1997; Chen et al., 2002; Adler et al., 2003). Therefore, I generated my own
global data product compilations as mean rates from 2000 to 2004, for consistency with prior work
(Wickert et al., 2013), at 0.25° resolution.

I derived the precipitation data by stitching together three data products. The CRU TS3.21 0.5° precipitation product provided precipitation over the global continents except Antarctica (expanded from the work of Harris et al., 2014), and this was smoothed and spherically interpolated (following Dierckx, 1993) to 0.25° resolution. The HOAPS-3 satellite-derived precipitation data product (0.25° resolution) was used for the oceans north of the Antarctic region (Andersson et al., 2010). Gaps of 2° or less between these data sets were filled by an interpolation of them. The remainder of the globe, primarily the Antarctic region, was filled by the CMAP reanalysis data set (Xie and Arkin, 1997), interpolated from 2.5° resolution to 0.25° resolution.

Our modern evapotranspiration rates for the continents (except Antarctica) are based on calculations using the MODerate-resolution Imaging Spectroradiometer (MODIS) instruments that are mounted on the Aqua and Terra satellites (Mu et al., 2007, 2011), available at 30-arcsecond resolution. The oceanic evaporation data are from HOAPS-3 and at 0.25° resolution (Andersson et al., 2010). Analysis of the HOAPS-3 data product shows that it has an ~10% error, with a global 0.2–0.5 mm day$^{-1}$ excess evaporation (Andersson et al., 2011). These data sets were interpolated over the ice-free land surface and global oceans. Evapotranspiration rates for Greenland and Antarctica were taken from the 0-ka time step of the TraCE-21K simulation (Liu et al., 2009; He, 2011), spherically interpolated to 0.25° resolution and thresholded at 0 to prevent the interpolation method from generating negative evapotranspiration rates.
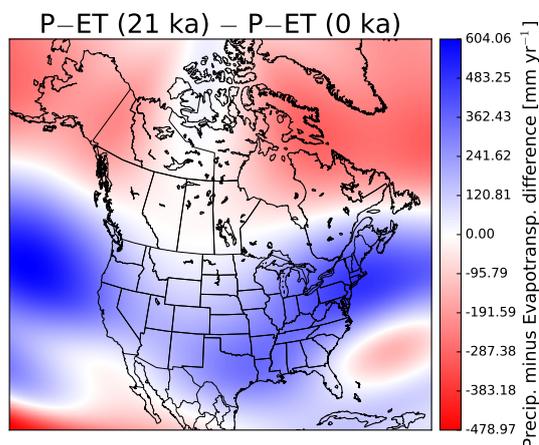
**Figure 3.** Modeled changes precipitation minus evapotranspiration between the Last Glacial Maximum and present. These differences were calculated with the TraCE-21K continuous LGM to present paleoclimate run (Liu et al., 2009; He, 2011) of the CCSM3 GCM (Collins et al., 2006). They are combined with ice mass balance to produce water inputs for computed paleodischarges

### 2.2.2 Ice melt and central differencing

Ice-sheet inputs to runoff are determined by differencing ice-sheet thicknesses at adjacent time steps for each of the ice models. These differences in ice-sheet height are converted to water discharges by (1) multiplying them by the DEM cell size ($\propto \cos(\text{latitude})$), (2) multiplying them by 0.917 as a conversion factor between ice and water density, and (3) dividing them by the time elapsed (Eq. 3).

Flow routing and drainage basins can be calculated only on time steps when the ice-sheet and GIA models provide surface topography (Section 2.3, below), but the ice-sheet contribution to runoff requires ice-sheet thickness to be differenced. This requires a choice of whether to allow central differencing and numerical diffusion in space (i.e., flow-routing) or time (i.e., melt rate). Melt rates change more gradually than near-instantaneous drainage rerouting events, and these rerouting events are critical to understanding climate impacts of ice melt (e.g., Broecker et al., 1989; Clark et al., 2001; Tarasov et al., 2006; Condron and Winsor, 2012). Therefore, I prefer numerical diffusion in time, and allow the gridded melt rate at each ice-sheet reconstruction time step to equal the averages of the melt rates calculated between this time step and those before and after it.

Time steps vary by model. ICE-3G (Tushingham and Peltier, 1991) and ANU (Lambeck et al., 2002) use irregular time steps separated by a ~1000 years (ICE-3G) and ~500 years (ANU). Time steps for ICE-5G are 1000 years from 32 to 17 ka, and 500 years thereafter (Peltier, 2004). All time steps for ICE-6G (Argus et al., 2014; Peltier et al., 2015) are 500 years. Model outputs from Gregoire et al. (2012) were provided at 10-year intervals, with GIA computed at uniform 100-year time-steps (Wickert et al., 2013), which are the same as those used here for the flow routing calculations. This means that the model outputs will generally average over short-term geologic events that are responsible for creating some of the major spillways and deposits (e.g., Kehew et al., 1994; Breckenridge, 2007; Murton et al., 2010).
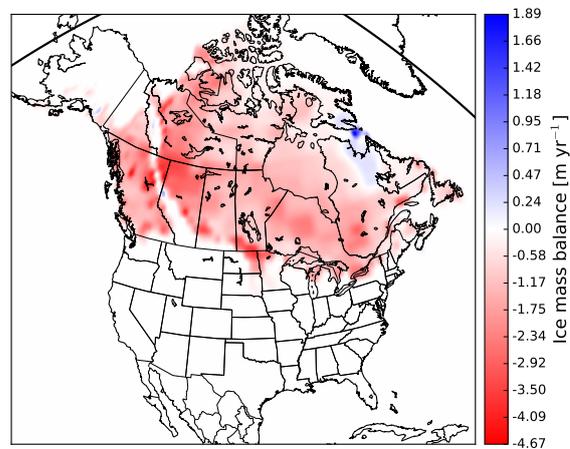
**Figure 4.** Ice-sheet melt is an important input to calculations of past water discharge. Ice surface mass balance shown here is for the ICE-6G (Argus et al., 2014; Peltier et al., 2015) between 14.5 and 14.0 ka.

### 2.2.3 Neglected terms: groundwater and lakes

375 While groundwater is a significant reservoir that affects river discharge, I assume that over the millennial time scales of interest to us, groundwater discharge will be in equilibrium with atmospheric inputs. Although ice-sheets can strongly influence groundwater discharge, modeling work by Lemieux et al. (2008) shows that the maximum net deglacial groundwater discharge across the whole North American continent is only ∼2.5% the modern Mississippi River discharge, and that

380 this spike was short-lived.

I do not include proglacial lakes in the continental water storage because the ice-sheet reconstructions discussed here (Tushingham and Peltier, 1991; Lambeck et al., 2002; Peltier, 2004; Gregoire et al., 2012; Peltier et al., 2015) do not. This means that these models implicitly include the lake-water volume within the ice mass. This deficiency affects the ability of the models to match the

385 observed record of ice-marginal geometry, as ice must be used in the models to represent the surface loads of these large lakes in the geologic past, and removes the potential effects of the lakes in driving ice-sheet retreat in mechanistic models. In this work, water is simply routed across proglacial-lake-producing depressions using a least-cost path algorithm (see Section 2.3).

### 2.3 Continental flow routing and accumulation

390 After defining the amount of flow each cell contributes to runoff, I used the time-evolving grids of surface elevation to compute drainage patterns across North America. I first specified that the drainage outlets must occur along the coast at that time step. I then routed flow down the $Z_r$ (Eq. 1) surface while computing accumulated discharge as (1) meteoric inputs only, (2) ice-sheet inputs only, and (3) combined total discharge. I computed this flow routing and accumulation using

395 "r.watershed", the high-efficiency least-cost path search algorithm of Metz et al. (2011), which is integrated into GRASS GIS (Metz et al., 2011; Neteler et al., 2012; GRASS Development Team, 2012).

### 2.3.1 Defining continent, ocean, and shore

Shorelines and topographic elevations changed dramatically since the Last Glacial Maximum, thus

400 requiring redefinition of the coastline on which river mouths appear at each time step. This could not be done by simply picking regions below sea-level, because this approach would, for example, cause flow to "disappear" into the below-sea-level Caribou sub-basin of Lake Superior and/or into regions around the ice margin that were isostatically depressed below sea-level. Therefore, I developed an algorithm to define as "ocean" only those regions that were below sea-level and contiguous with

405 the global ocean. First, I thresholded the topography-plus-ice flow-routing map, $Z_r$, at 0, to define a binary raster map of regions above and below sea level. Then, I converted this into a vector map. Using the topological analysis built into GRASS GIS, I looked only for areas that touched the map

edge and were below sea level, and chose these to be ocean. The remaining area was defined as continent and used as the flow-routing surface.

### 2.3.2 Flow routing and accumulation

410

The flow-routing calculations produce maps of (1) drainage direction, (2) meteoric water discharge, (3) meltwater discharge, and (4) total water discharge. These maps are spatially distributed, providing 30-arcsecond-resolution time-series of the time-averaged surface water discharge that is produced by each ice-model–solid-Earth-model combination.

415  The flow-routing algorithm I used, r.watershed (Metz et al., 2011), uses a least-cost path search algorithm that sets it apart from other drainage analyses in that it is capable of routing water through depressions without explicitly flooding them (see, e.g., Schwanghart and Scherler, 2014). This algorithm allows for rapid calculations to be carried out over a landscape that contains moving ice dams and isostatic depressions.

420  The ability of the Metz et al. (2011) algorithm to route water across local depressions also prevents both natural and artificial (human-built or DEM artifact) highs and lows in the landscape from stopping the flow routing. This is an advantage because flow-routing calculations without this feature fail unless they are performed on a hydrologically-corrected DEM (i.e., one in which the elevation is altered to produce the known drainage basins). Using a hydrologically-corrected DEM is a po-

425  tential source of error in reconstructions of the past because its actual terrain has been artificially changed (e.g., Grimaldi et al., 2007) in a way that may produce unexpected results when combined with surface deformation and ice-sheet thickness.

in spite of these advantages, the Metz et al. (2011) method causes internally drained regions to be amalgamated to drainage basins that flow to the coast. In the drainage calculations performed for

430  this work, the Great Basin is split between the Colorado River and Columbia River drainage basins. In part, this is realistic: outflow from Lake Bonneville entered Columbia River between 18.2±0.3 ka (McGee et al., 2012) and ∼17.5–17.4 ka (∼14.4–14.3 ^{14}C ka; calibrated with IntCal13: Reimer et al., 2013) (Godsey et al., 2005), with a massive <1-year flood from Lake Bonneville ending this period of inter-basin interchange. In part, this does not matter: a hydrologically-closed basin must

435  maintain a state in which precipitation equals evapotranspiration, and as such should not have a major effect on discharge calculations, outside of the aforementioned period of climate change during the end of the Pleistocene. But in part, this is the dissatisfying result of flow-routing calculations that are not coupled to a hydrologic model that can raise and lower the levels of lakes in closed basins, and a fundamental problem of any flow-routing approach that disconnects local hydrologic balances.

440  This dilemma over the Great Basin highlights a key question in how much to adjust the model by hand to fit data, versus how much to just allow the model to run. It would be possible to modify the flow-routing inputs to declare the Great Basin to be closed throughout part or all of the modeled

geologic past. The approach taken here is to leave the flow-routing grid unmodified in order to maintain distance between data and model (see the final paragraph in Section 2.1.3).

## 2.4 Distributed melt delivery to the coast

These methods also allow us to produce grids of meltwater discharge to the coast that are fully-distributed in space and time. These have been converted to GCM-input-appropriate spatial resolutions and used in preliminary work to connect ice melt and global ocean circulation and climate change (Ivanović et al., 2014). This is an improvement over "hosing" experiments (e.g., Meissner and Clark, 2006; Liu et al., 2012; Condron and Winsor, 2012), in which meltwater additions are prescribed to a patch of ocean in a way that need not be connected to patterns of continental runoff. These "hosing" experiments provide very useful intuition for the climate impacts of a major meltwater input event. Fully-distributed GCM meltwater inputs that are tied to paleodrainage histories, when coupled with models that can appropriately handle point sources of fresh water, create a more realistic ice-age ocean that is better-conditioned to respond to changes in meltwater inputs and can be used to connect models of ice-sheet history with their likely impacts on global climate. Code to produce these GCM inputs is also provided in the Github repository (https://github.com/umn-earth-surface/ice-age-rivers).

## 2.5 Drainage basins and river discharge

I compute time-evolving drainage patterns with a generalized algorithm that can overcome changes in shoreline geometry, river mouth positions, and difficulties in consistent topography-based flow reconstruction across the very subtle topography of the continental margins. These components are essential to connect glacial-stage rivers to their modern counterparts after 20,000 years of shoreline and topographic change due to evolving sea level and ice-sheet geometry.

First, I create a map of regions where I expect the mouth(s) of each river system to be. Each "river mouth region" (Fig. 5b) is defined by hand to accommodate the changing locations of river mouths with time as a function of sea level, ice cover, and GIA (Figure 6). This is especially important for drainage systems such as Hudson Strait and the Saint Lawrence River, which previously played host to ice streams and now are fully or partially inundated with seawater.

I then create a set of points at which each of the "major" rivers ($\geq$1000 m$^3$ s$^{-1}$ reconstructed discharge) reaches the coast. Wherever one of these river mouths is located inside a named region (Fig. 5), the program builds a drainage basin. Each drainage basin is labeled with the name of its respective river mouth region (e.g., "Mississippi" or "Columbia"). River mouth regions that contain more than one river mouth produce a named drainage basin that is an amalgamation of the drainage basins of all $\geq$1000 m$^3$ s$^{-1}$ rivers in the basin; this allows us, for example, to combine the Mississippi, Atchafalaya, and Red Rivers into a single broader basin flowing towards Louisiana, and to combine all of the major modern rivers that flow into Hudson Bay into a single basin, even though
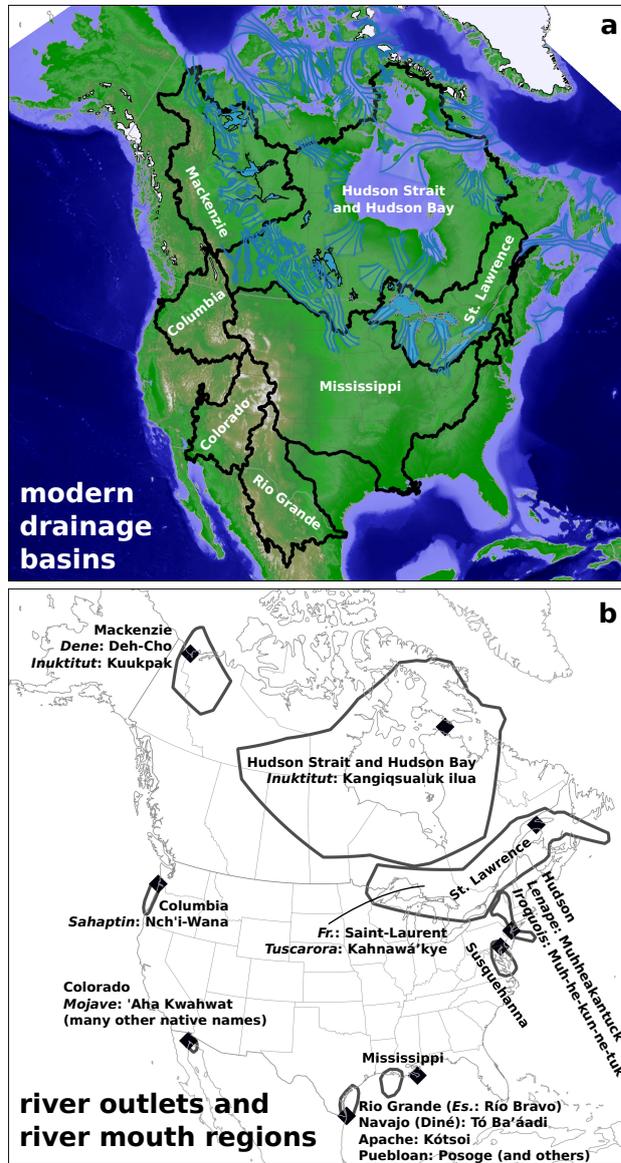
**Figure 5. a.** Modern drainage basin extents for the rivers involved in this study, with ice and lake extents from the 1 ka time step of the maps of Dyke (2004), elevation basemap from British Oceanographic Data Centre (2010), and modern drainage basins from Lehner et al. (2013). **b.** Modern river mouths alongside the river mouth regions used to define a flow path as part of a drainage basin (Section 2.5). Names are also given in European non-English languages where they are common, alongside a non-exhaustive set of common names in local languages. Note that the mouth of the Mississippi River lies entirely outside its river mouth region. This is because the topographically-routed flow (Metz et al., 2011) follows the course of the Atchafalaya River; the present course of the Mississippi runs counter to the regional topographic gradient because it is held in its old course by the Old River Control Structure (e.g., Harmar and Clifford, 2007).
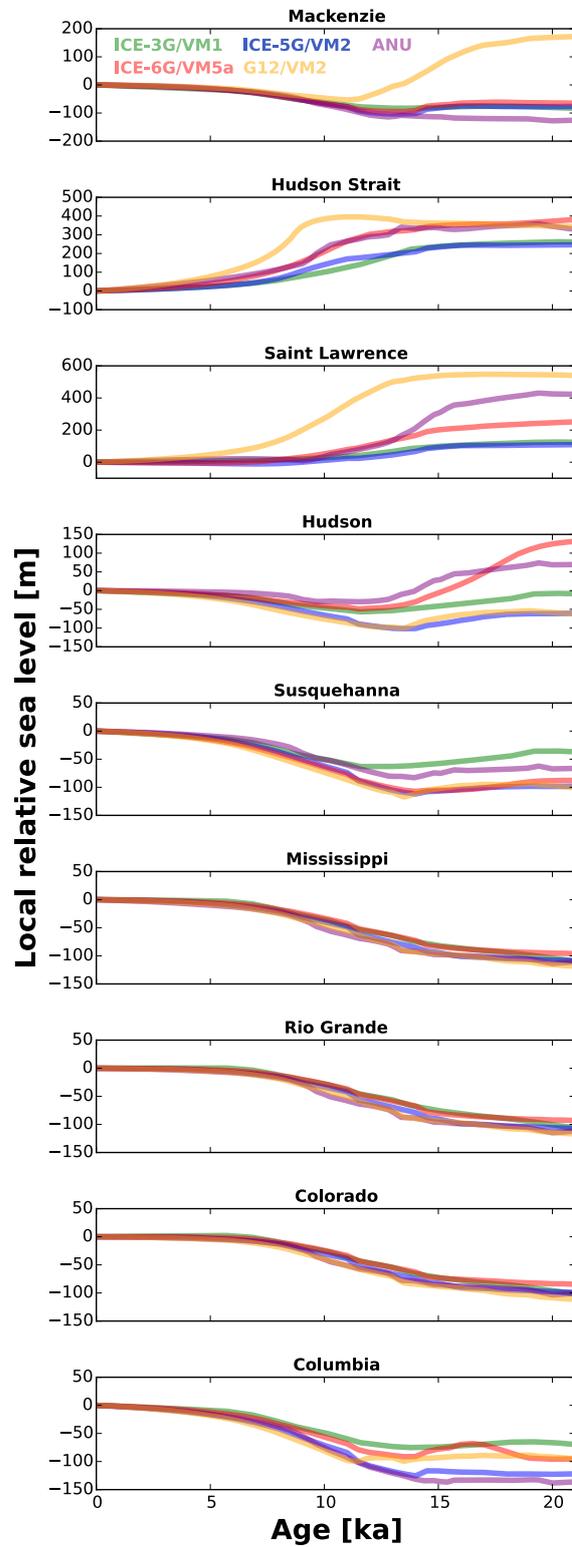
**Figure 6.** Sea level curves extracted from GIA models at the modern locations for the river mouths that are important to this study (Fig. 5). Wide variability highlights the different histories experienced by rivers formerly near (or under) thick ice, and those far from it.

their previous combined outlet in Hudson Strait is now inundated. If a particular river mouth region contains no river mouths with flow $\geq 1000$ m$^3$ s$^{-1}$, the program builds a drainage basin based on the highest-discharge coastal cell from the flow accumulation calculation.

After defining the major drainage basins, I sum (1) ice-sheet melt, (2) precipitation minus evapotranspiration, and (3) the sum of (1) and (2) across each basin. Each sum, respectively, provides ice-sheet meltwater discharge ($Q_i$), meteoric (seasonal precipitation minus evapotranspiration) discharge ($Q_m$), and total river discharge ($Q = Q_m + Q_i$). Many of these calculations provide discharges at the modern time step that are close to the modern pre-human-impact mean river discharge (Table 1, which also includes measured modern sediment discharges for reference). For some, however, the result differs somewhat due either to (1) the water balance maps not perfectly representing water delivery to the coast and/or (2) the incorporation of the internally-drained Great Basin into the Columbia River and Colorado River basins because the flow-routing algorithm (Metz et al., 2011) was set up to disallow internal drainage. To provide more realistic discharge histories while also being explicit about the raw outputs of the model, I rescaled discharge in each basin to match its modern value with the mean of the computed time steps between 3 ka and present, while also making note on the plots (Figs. 11–16) of the predicted uncorrected modern discharge. This correction may create a systematic underestimate of Columbia River discharge from 18.2±0.3 ka (McGee et al., 2012) to ∼17.5–17.4 ka (Godsey et al., 2005; Reimer et al., 2013), when waters from Lake Bonneville – part of the Great Basin – flowed into the Columbia River Basin.

## 3 Methods: Data-driven Drainage Reconstruction

A set of entirely data-driven drainage histories provides a necessary counterpoint to evaluate the model-based computed drainage basins and river discharge histories. I developed these in two different ways: as paleogeographic maps of drainage divide positions, and as a categorical river discharge history that defines periods of high and low flow.

I developed a set of data-driven drainage basin boundaries for each of the study basins (Figs. 7–10, lower right panels) based on several lines of evidence. The first is the modern drainage basin outlines of Lehner et al. (2013). The second is the ice-sheet margin chronology of Dyke et al. (2003); Dyke (2004), which, when lacking independent information, I use as an approximate set of contours of ice-sheet thickness. The ice divide could, however, have moved with time, offsetting it from the chronological contours, and Tarasov et al. (2012) and Gowan (2013) note that uncertainties exist in this deglaciation chronology. Therefore, a key third set of information comes from the evidence of ice streaming recently completed by Margold et al. (2014, 2015) and the mapped Canadian eskers from Storrar et al. (2013). As there are few chronological controls on when these ice-streams were active, ice divides are drawn between diverging ice-streams. While this is a potential source of error, it also may not be such a bad assumption: where there are chronological controls on ice-stream

**Table 1.** Modern drainage basin areas and water ($Q_w$) [cubic meters per second] and sediment ($Q_s$) [$10^6$ metric tons per year] discharges. Many of these were gathered and independently of the Milliman and Farnsworth (2013) compilation, and generally provide good agreement with their numbers.

| River | A [km$^2$] | $Q_w$ [m$^3$ s$^{-1}$] | $Q_s$ [Mt yr$^{-1}$] | Reference(s) |
|---|---|---|---|---|
| Mackenzie | $1.8 \times 10^6$ | 9910 | 128 | Carson et al. (1998) |
| Hudson Strait and Bay | $1.173 \times 10^6$ | 30,900[a] | ~1.1[a,b] | Schneider-Vieira et al. (1994); Bentley (2006) |
| Saint Lawrence[c] | $1.344 \times 10^{6[d]}$; $1.61 \times 10^{6[e]}$ | 12,000[d]; 14,400[e] | 3.6[d] | Holeman (1968); Doyon (1996); Dolgopolova and Isupova (2011); Environment Canada (2013) |
| Hudson River | $0.034 \times 10^6$ | 590 | 0.737 | Wall et al. (2008); Milliman and Farnsworth (2013) |
| Susquehanna | $0.0704 \times 10^6$ | 1082 | 5 | Gross et al. (1978); Kammerer (1990) |
| Mississippi[f] | $3.225 \times 10^6$ | 18,430[f] | 400[g], 210[i] | Kammerer (1990); Milliman and Farnsworth (2013) |
| Rio Grande | $0.870 \times 10^6$ | 570[g,h]; 22[i] | 20[g,h]; 0.66[i] | Gates et al. (2000); Milliman and Farnsworth (2013) |
| Colorado[j] | $0.637 \times 10^6$ | ~665[g,h]; 6.3[i] | 145[g,h], 0.1[i] | U.S. Bureau of Reclamation (1952); van Andel (1964) (as cited by Carriquiry and Sánchez, 1999); Kammerer (1990); Prairie and Callejo (2005); Nowak (2011); Milliman and Farnsworth (2013) |
| Columbia | $0.668 \times 10^6$ | 7500 | 7 | Milliman and Meade (1983); Kammerer (1990) |

[a] This is the sum of river inputs to Hudson Bay from pre-1975 data

[b] Modeled following Syvitski et al. (2003)

[c] Not including modern diversions into or out of the Great Lakes. These include the Chicago Diversion (out of the Great Lakes basin), and the Ogoki and Long Lake Diversions (into the Great Lakes basin). The drainage basin figures show the modern Great Lakes–Saint Lawrence drainage basin, which includes these diversions; as these are small compared to other sources of possible error, I have not returned the mapped Great Lakes–Saint Lawrence drainage basin to its pre-diversion state.

[d] The Great Lakes–Saint Lawrence drainage system alone

[e] Including inflow into the Saint Lawrence estuary from rivers other than the Saint Lawrence

[f] This is the sum of Mississippi River (Old River) discharge and drainage area, Mississippi River discharge and drainage area routed towards the Atchafalaya River, and the Atchafalaya-Red River system. Inclusion of the latter increases drainage area from $2.978 \times 10^6$ km$^3$ to $3.225 \times 10^6$ km$^2$ and discharge from 16,790 m$^3$ s$^{-1}$ to 18,430 m$^3$ s$^{-1}$.

[g] Before the installation of river control structures; all other values (including those on the same line) are modern unless indicated

[h] Before modern water withdrawals; these values are estimated based on the work of Gates et al. (2000) for the Rio Grande and Prairie and Callejo (2005) and Nowak (2011) for the Colorado River at Imperial Dam, which was summed with inputs from the Gila River (U.S. Bureau of Reclamation, 1952); see Cohen et al. (2001) for an earlier calculation of natural discharge to the Colorado River delta, and Schmidt et al. (2010) for a review of the 20th century human–river interaction that necessitated my approximation here. Modern values of water and sediment discharge are from Milliman and Farnsworth (2013).

[i] Modern discharge to the ocean.

[j] Modern discharge values are from Milliman and Farnsworth (2013); past estimates and the estimated sediment yield are from other sources.

reorganization, the changes in drainage tend to produce modest and localized changes in catchment area and/or outlet location (e.g., Stokes et al., 2009; Ross et al., 2009; Ó Cofaigh et al., 2010). Better chronologies often come from direct dating of ice-marginal positions (e.g., Licciardi et al., 1999; Dyke, 2004; Gowan, 2013), fluvial deposits (e.g., Bretz, 1969; Atwater, 1984; Ridge, 1997; Benito and O'Connor, 2003; Knox, 2007; Rittenour et al., 2007), and lacustrine deposits (e.g., Antevs, 1922; Kehew et al., 1994; Rayburn et al., 2005, 2007, 2011; Richard et al., 2005; Breckenridge, 2007; Breckenridge et al., 2012) and these provide the fourth layer to define drainage chronologies. The fifth layer of data comes from the offshore stratigraphic record (e.g., Andrews and Tedesco, 1992; Andrews et al., 1999; Flower et al., 2004; Carlson et al., 2007a, 2009; Williams et al., 2012; Maccali et al., 2013), which can be compiled into a paleohydrograph that may correlate with drainage basin area (Wickert et al., 2013), but outside of some information on provenance (Carlson et al., 2007a, 2009), can not independently indicate where the past drainage basin margins lie. All radiocarbon ages were recalibrated to calendar years BP using IntCal13 (Reimer et al., 2013).

While very detailed and well-dated geological constraints permit a quantitative approach to reconstruct past discharge (Licciardi et al., 1999; Carlson et al., 2007a; Carlson, 2009; Carlson et al., 2009; Obbink et al., 2010; Wickert et al., 2013), most interpretations are much more basic, simply showing when periods of high or low discharge may have existed due to changes in drainage basin area (e.g., Ridge, 1997), isotopic ratios (e.g., Andrews and Dunhill, 2004), and/or proglacial lake outlets (e.g., Teller and Leverington, 2004, and later revisions). I therefore first took the simplest approach to these records, defining them as simply "high discharge" (light and dark gray on Figs. 11–16) or "low discharge" (white background on Figs. 11–16). Dark gray indicates times for which there is geological evidence for a distinct period high flow, and light gray indicates the time over which data-based inferences indicate that enhanced flow would have occurred and/or when discharge would have been higher but not as high as during the time indicated by the dark gray regions. For example, Mississippi River discharge increased when Lake Agassiz flooded into it (one dark gray band), but was overall higher than present from the LGM until ∼12.9 ka due to ice-sheet input and a larger drainage basin area (light gray and dark gray).

## 4 Results

The result of the computational work is two major products: synthetic drainage basin and discharge histories. The former are summarized in four sets of maps of significant points in time since the Last Glacial Maximum (Figs. 7–10), with the full time-series of each reconstruction provided as a supplementary video. The latter are a set of reconstructed deglacial water discharges by drainage basin (Figs. 11–16), with Fig. 16 including the meltwater total discharge calculations of Licciardi et al. (1999) for comparison. These provide a spatially-distributed and quantified view of how rivers in North America have broadly changed over the past 20,000 years.

The counterpart to these computed histories are those that are driven by more direct interpretations of the data (e.g., Teller, 1990a; Licciardi et al., 1999; Carlson et al., 2007a; Carlson, 2009). I write, "counterpart" as opposed to "ground-truth" because these are also to some extent interpretations, based on limited data. Their key utility is that they offer a much simpler path from the raw data to the interpreted drainage basin extents and periods of high discharge, and one that can be more closely tied to geological fact. No age uncertainty is provided for these data-driven reconstructions: The maps display multiple events that coincide, assembled from disparate data sources, of which not all have well-quantified error. The periods of high and low discharge are marked with sharp lines even where chronological constraints are sparse, and should be viewed as a current geological best estimate. Nevertheless, the large-scale drainage basins noted on Figures 7–10, each of which displays an important time in deglacial history, display the current state of knowledge for that point in the geologic time scale, regardless of chronological error. Therefore, large-scale disagreements between the data-constrained drainage basin outlines and the model results at these key points in the geological time scale generally indicate a need to improve the model-based reconstructions. Mismatches between data-driven and model-driven discharge histories are less straightforward to attribute to model error, as they involves both drainage basin area and rates of ice-sheet melt, with the latter being less easily quantified by geological data. These potential mismatches are discussed below.

## 5 Discussion

### 5.1 Comparison with geologic evidence for varying drainage basin areas and discharge

Each of the river systems in this study experienced high flow and low flow at different times. The high flow could be due to meltwater inputs or drainage area expansion. These are often linked: ice-sheet advance into mid-continent drainage basins vastly increased their areas (Figs. 7–9). Figure 11 includes a brief description of each of these times, which is expanded upon in the following sections. The data-driven drainage histories (Section 3) through North America are updated from Wickert (2014b), with the dates for ice advance and retreat compiled by Licciardi et al. (1999) still broadly consistent with the modern state of knowledge. For the following chronology, all radiocarbon ages were calibrated (or recalibrated) using IntCal13 (Reimer et al., 2013). Current geologic evidence, while incomplete and subject to revision, provides a good picture of the broad changes in drainage across North America since the Last Glacial Maximum.

### 5.1.1 Drainage histories by river

The Mississippi, Hudson, and Susquehanna Rivers traded drainage inputs from the Great Lakes and their respective former ice lobes, resulting in a pattern of symmetric increases and decreases in discharge along the southern Laurentide margin. At the Last Glacial Maximum, the drainage area of the
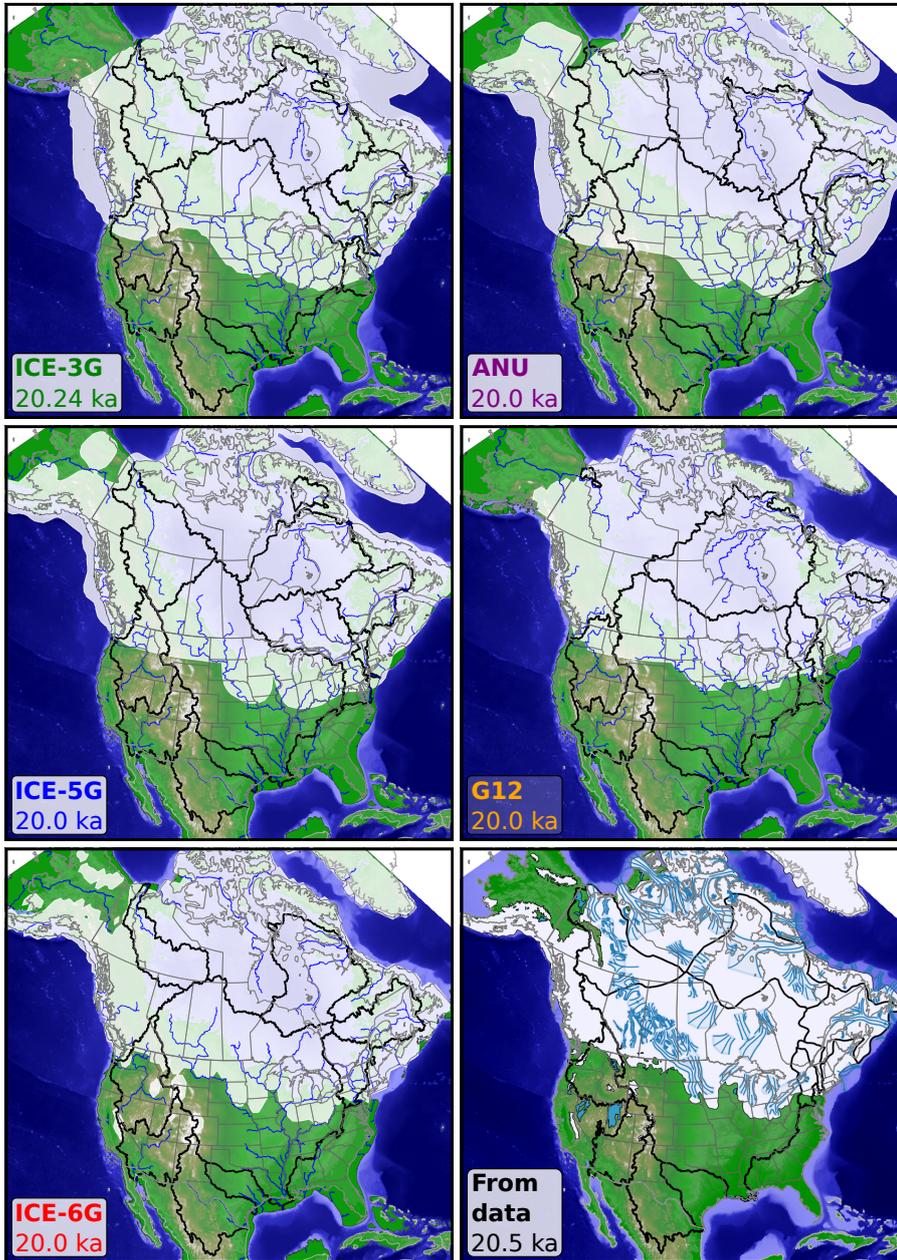
**Figure 7. End of the global Last Glacial Maximum.** North American drainage basins at the Last Glacial Maximum. Ice models are organized left to right, top to bottom, in the order of their publication age. Drainage basins are delimited in black. The model output plots contain blue rivers, which occur where the runoff calculations indicate streamflow that is $\geq 1000$ m$^3$ s$^{-1}$. The data-driven compilation indicates evidence of past ice streams in blue (Margold et al., 2014). The model- and data-driven reconstructions show generally a consistent trend of an enlarged Mississippi River drainage basin, ice flow via Hudson Strait into the North Atlantic, and ice-sheet meltwater routed down the Hudson and/or Susquehanna Rivers.
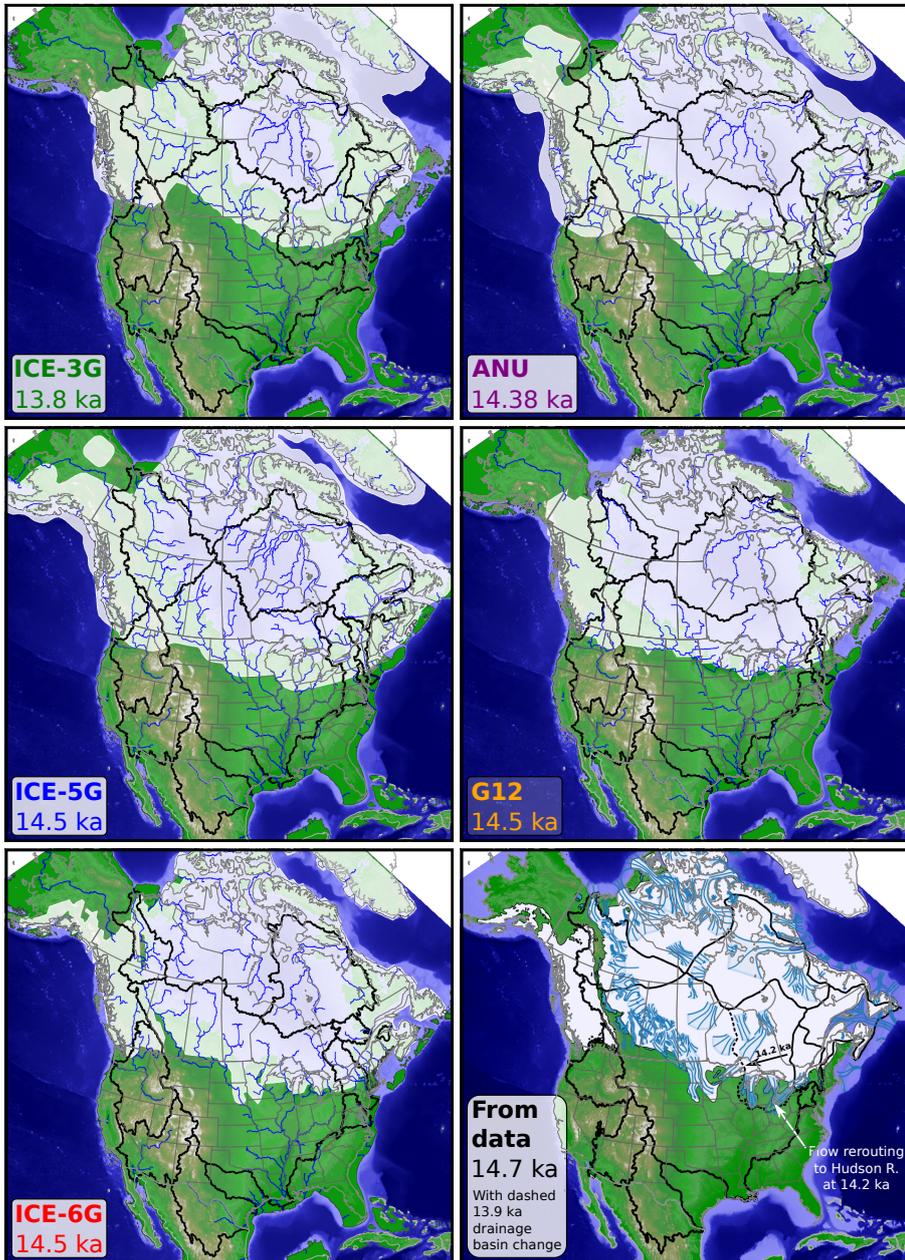
**Figure 8. Bølling-Allerød warm period** and (for all but ICE-3G and the data-driven reconstruction, for which the closest-available time-slice(s) was/were chosen) **Meltwater Pulse 1A.** The Bølling-Allerød warm period was the major period of warming between earlier near-LGM conditions and the later Younger Dryas cooling. The early part of the Bølling-Allerød encompasses Meltwater Pulse 1A, a period of 14–18 m sea level rise between 14.65 and 14.31 ka (Deschamps et al., 2012). Collapse of the ice saddle between the Laurentide and Cordilleran Ice Sheets at this time could be the dominant cause of Meltwater Pulse 1A (Gregoire et al., 2012). Note the expansion of the blue $\geq 1000$ m$^3$ s$^{-1}$ river lines for many of the ice models; this is representative of an increase in melt at this time.
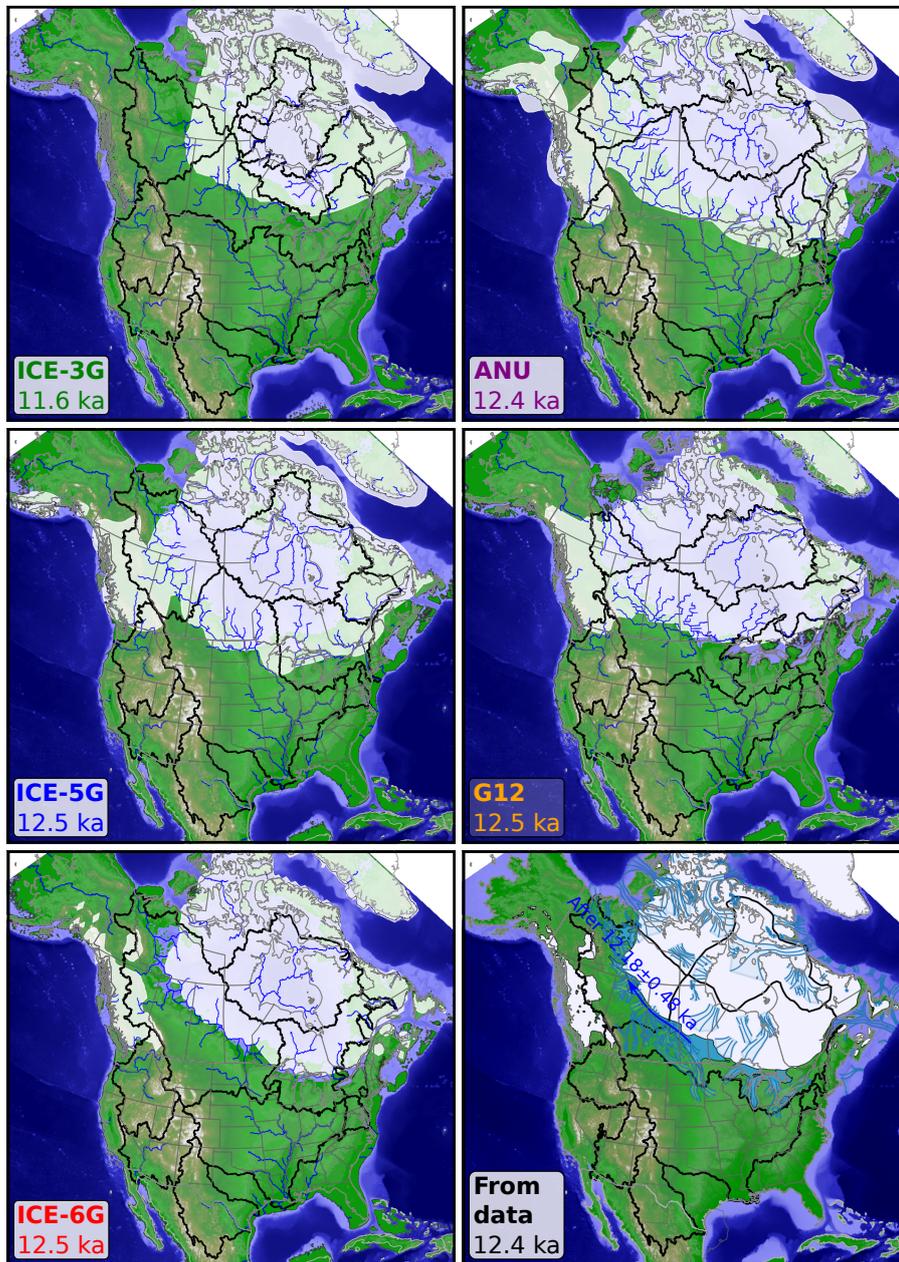
**Figure 9. Younger Dryas** (at transition to Holocene for ICE-3G). The Younger Dryas was a period of rapid cooling that corresponds with meltwater rerouting away from the Mississippi (Williams et al., 2012; Wickert et al., 2013) and enhanced meltwater output to the Mackenzie (Murton et al., 2010) and Saint Lawrence (Carlson et al., 2007a) rivers. Model predictions here vary widely, and properly matching this continental-scale drainage rerouting away from the Mississippi basin is a feature that all successful ice models should have. The routing of flow from Lake Agassiz, at the center of the continent, was not towards the Mississippi at this time (Wickert et al., 2013), but is otherwise unclear based on current data (e.g., Carlson and Clark, 2012; Lowell et al., 2013; Breckenridge, 2015).
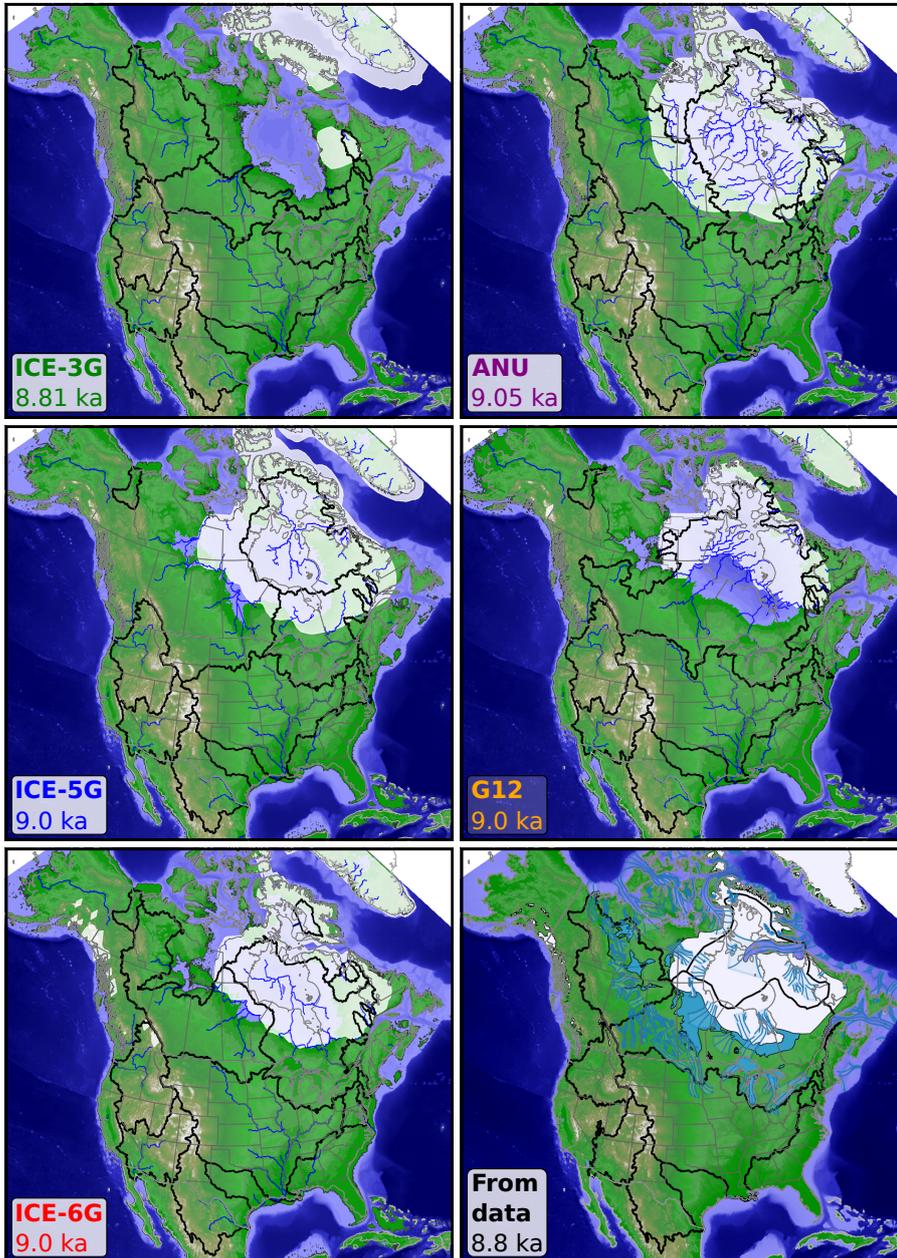
**Figure 10. Early Holocene.** The early Holocene was notable for its ice retreat and proglacial lake growth, which included enhanced flow down the St. Lawrence River and abrupt drainage of proglacial lakes Agassiz and Ojibway into Hudson Bay. Many other rivers no longer had ice-sheet input. In ICE-5G, the Upper Missouri river reoccupies its hypothesized preglacial channel in the Bismarck–Mandan area (Alden, 1932) and separates from the rest of the Mississippi system. This illustrates how sensitive mid-continental river systems can be to subtle tilts of the land surface.
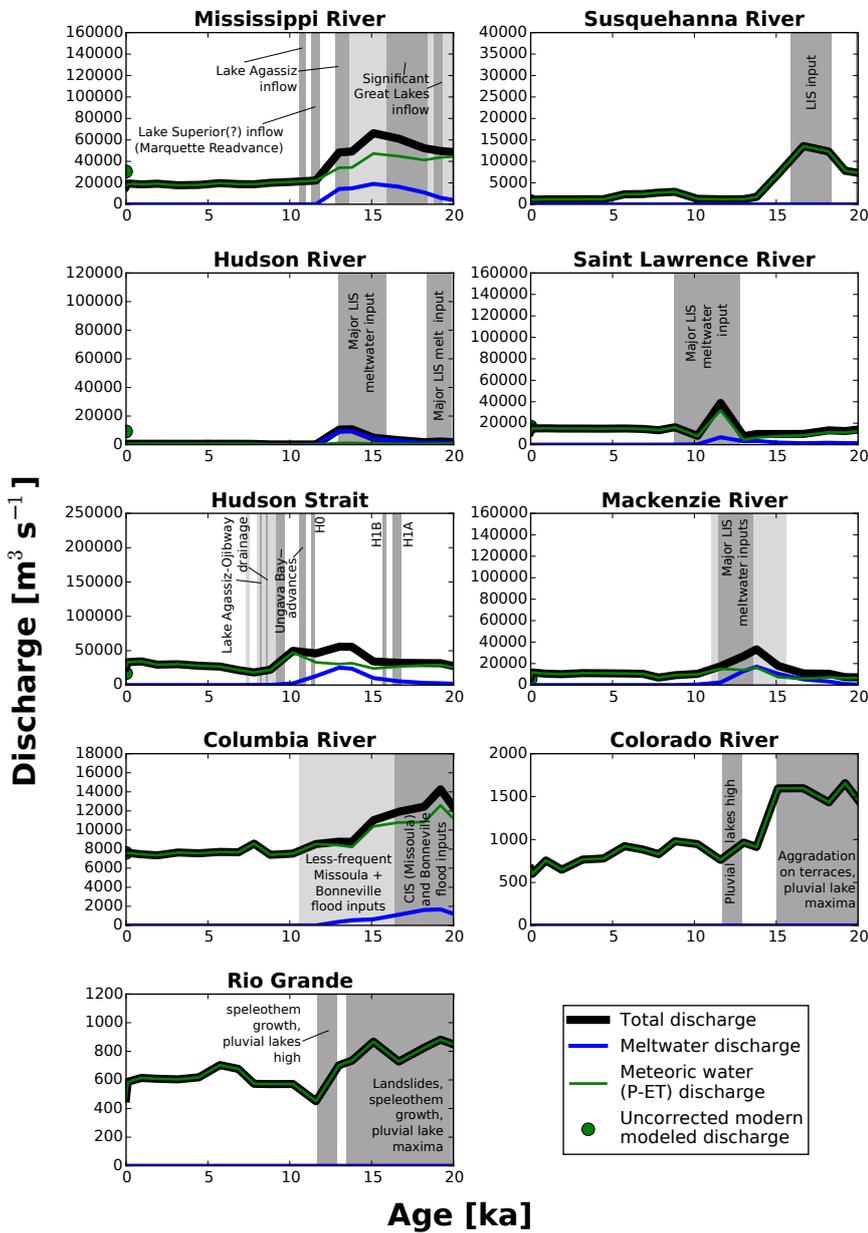
**Figure 11.** Computed discharge from ICE-3G/VM1 (Tushingham and Peltier, 1991), with gray shading at times of enhanced discharge based on the geologic record. Dark gray indicates a specific time of enhanced discharge, while light gray indicates inferred higher discharge from ice-sheet and landscape geometry or other factors, or, for the Columbia River, a time of enhanced discharge that is likely less-enhanced than earlier in the record. These are annotated here with the following abbreviations: LIS, Laurentide Ice Sheet; H0 (YD) and H1, Heinrich Events 0 (Younger Dryas) and 1; CIS, Cordilleran Ice Sheet.
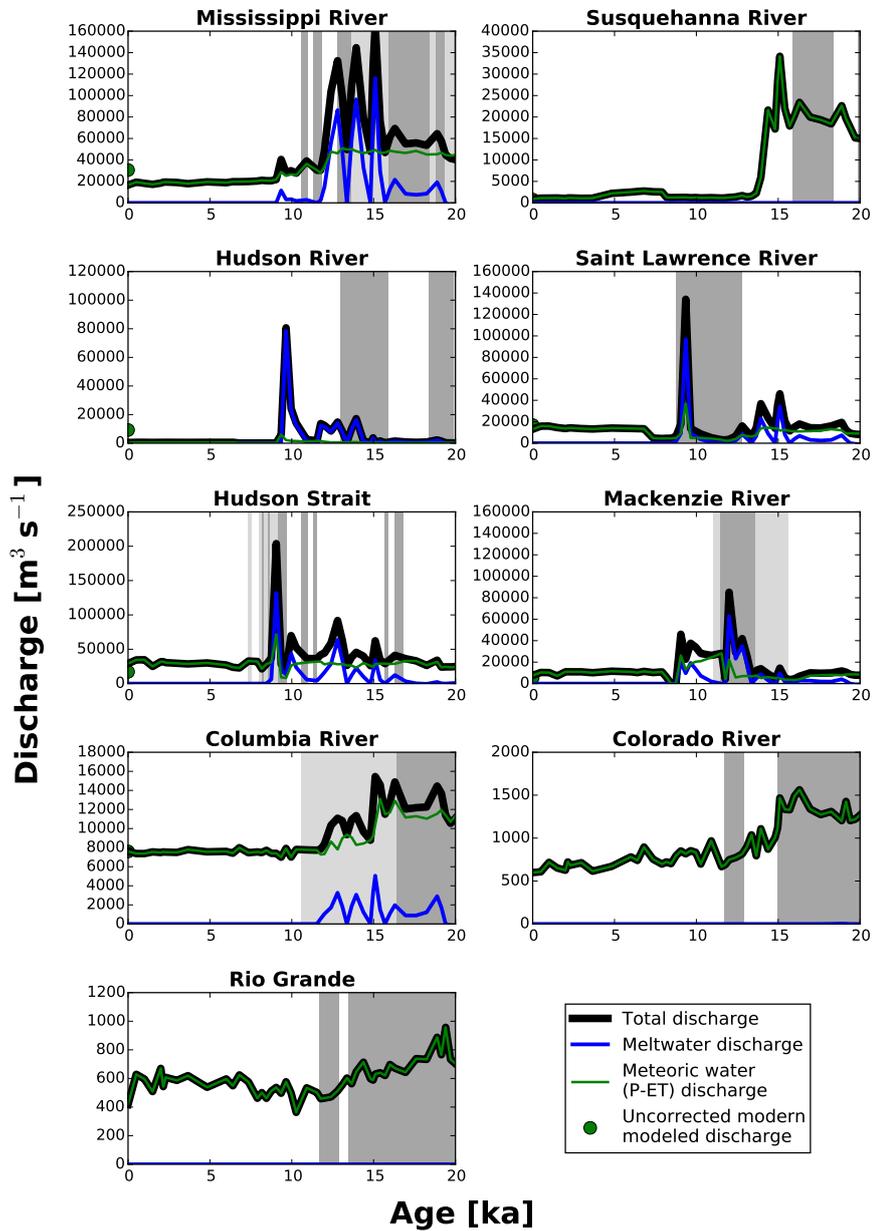
**Figure 12.** Computed discharge based on the ANU ice-sheet–solid-Earth model pair (Lambeck et al., 2002), compared to the geologic record of enhanced past discharge (gray shading: dark, specific; light, inferred and/or less discharge). Notes on the geologic record can be found in Fig. 11.
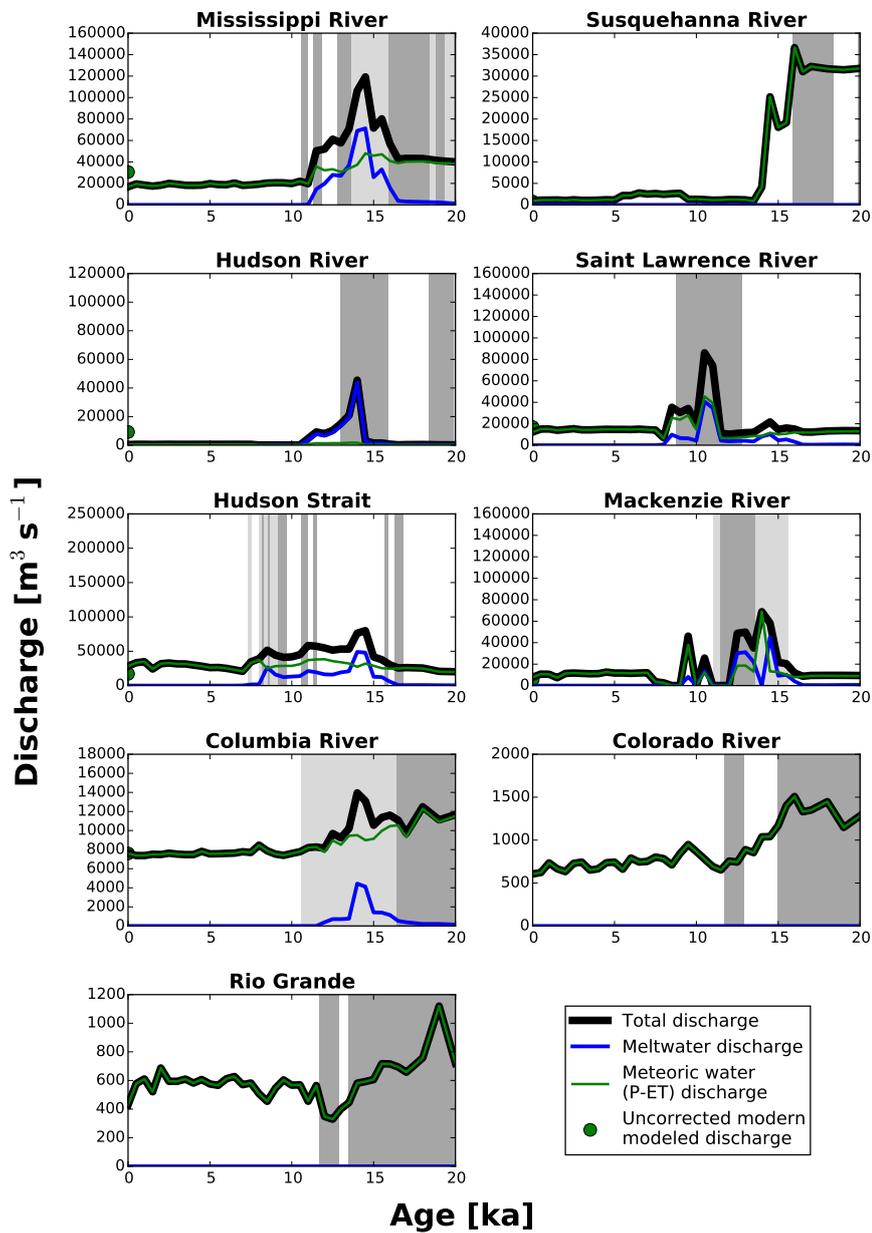
**Figure 13.** Computed discharge based on ICE-5G/VM2 (Peltier, 2004), compared to the geologic record of enhanced past discharge (gray shading: dark, direct record; light, inferred and/or less discharge). Notes on the geologic record can be found in Fig. 11.
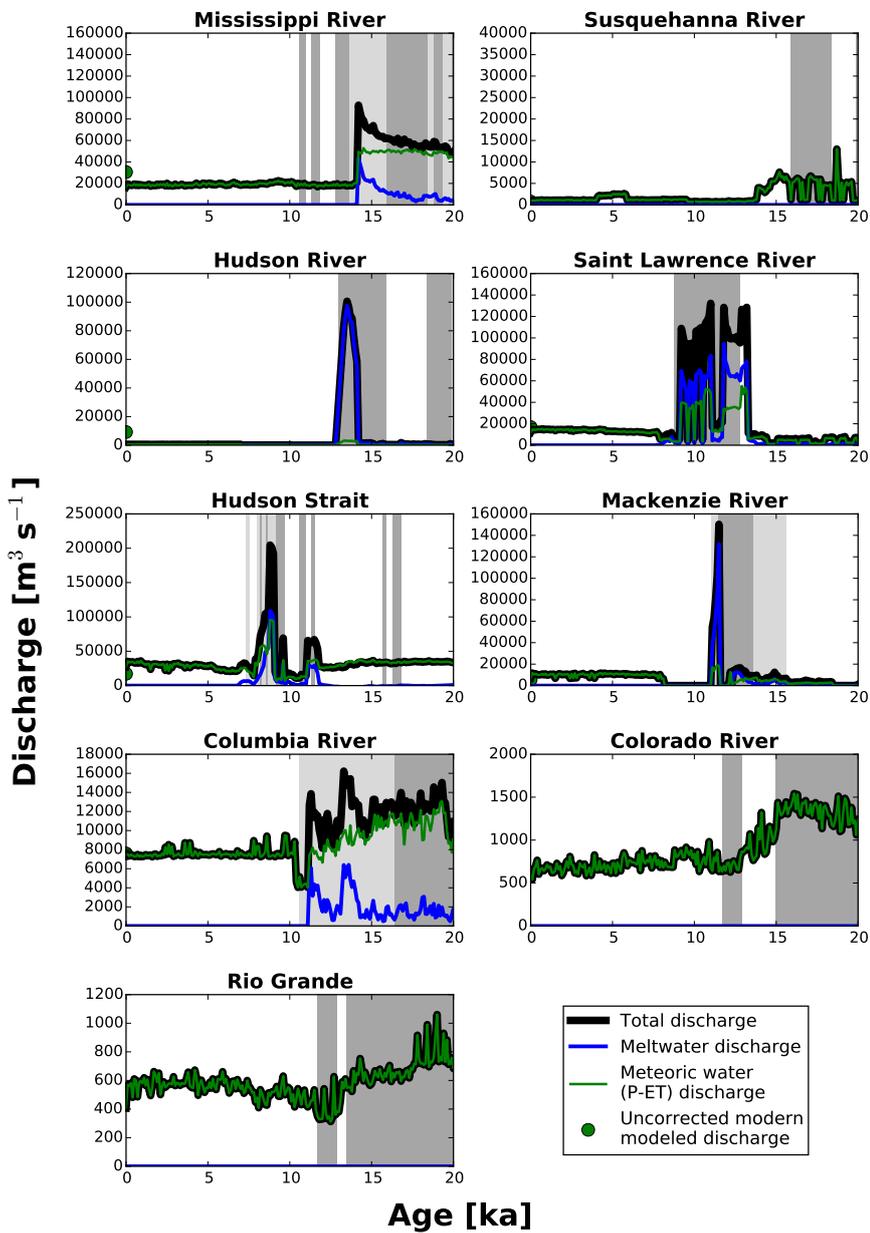
**Figure 14.** Computed discharge based on the G12/VM2 coupled ice-sheet–solid-Earth model (Gregoire et al., 2012; Peltier, 2004), compared to the geologic record of enhanced past discharge (gray shading: dark, direct record; light, inferred and/or less discharge). Notes on the geologic record can be found in Fig. 11.
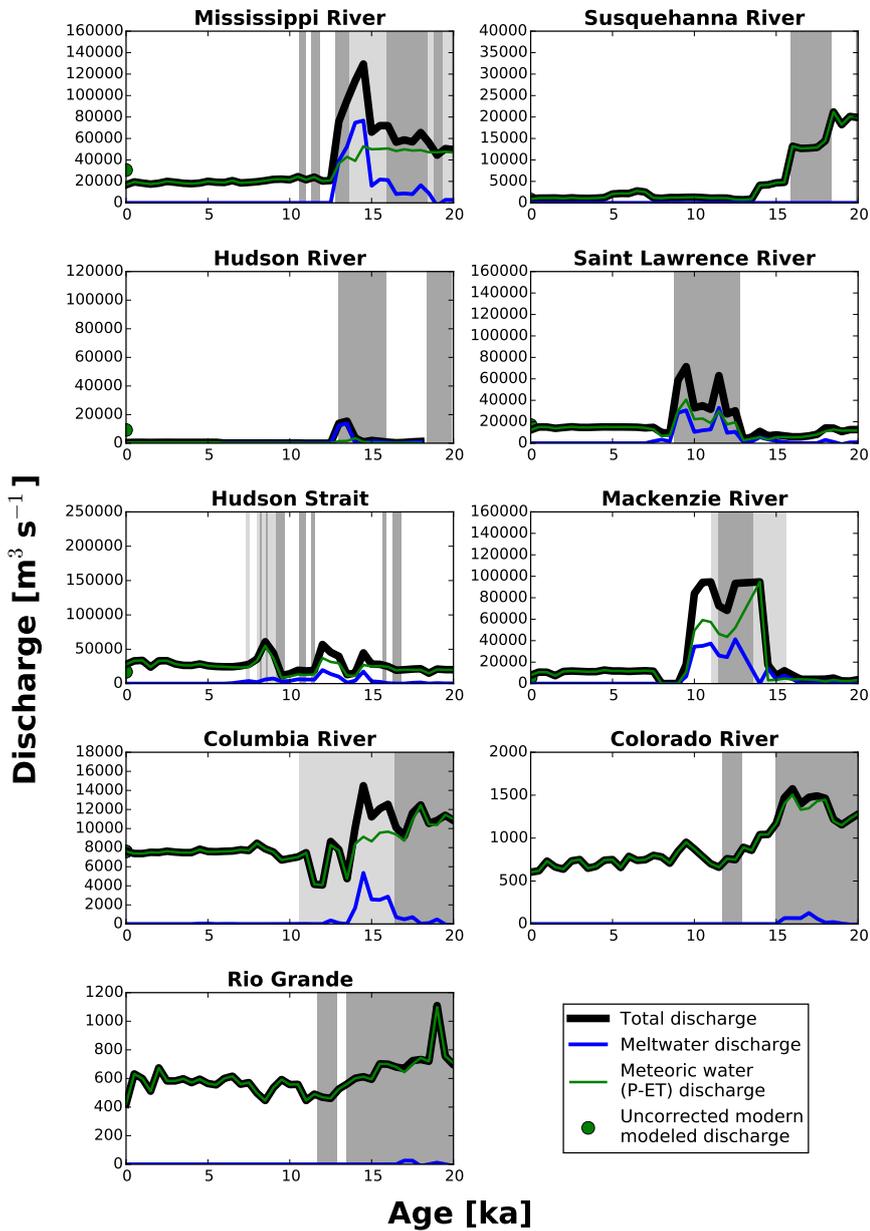
**Figure 15.** Computed discharge based on the ICE-6G/VM5a coupled ice-sheet–solid-Earth model (Argus et al., 2014; Peltier et al., 2015), compared to the geologic record of enhanced past discharge (gray shading: dark, direct record; light, inferred and/or less discharge). Notes on the geologic record can be found in Fig. 11.
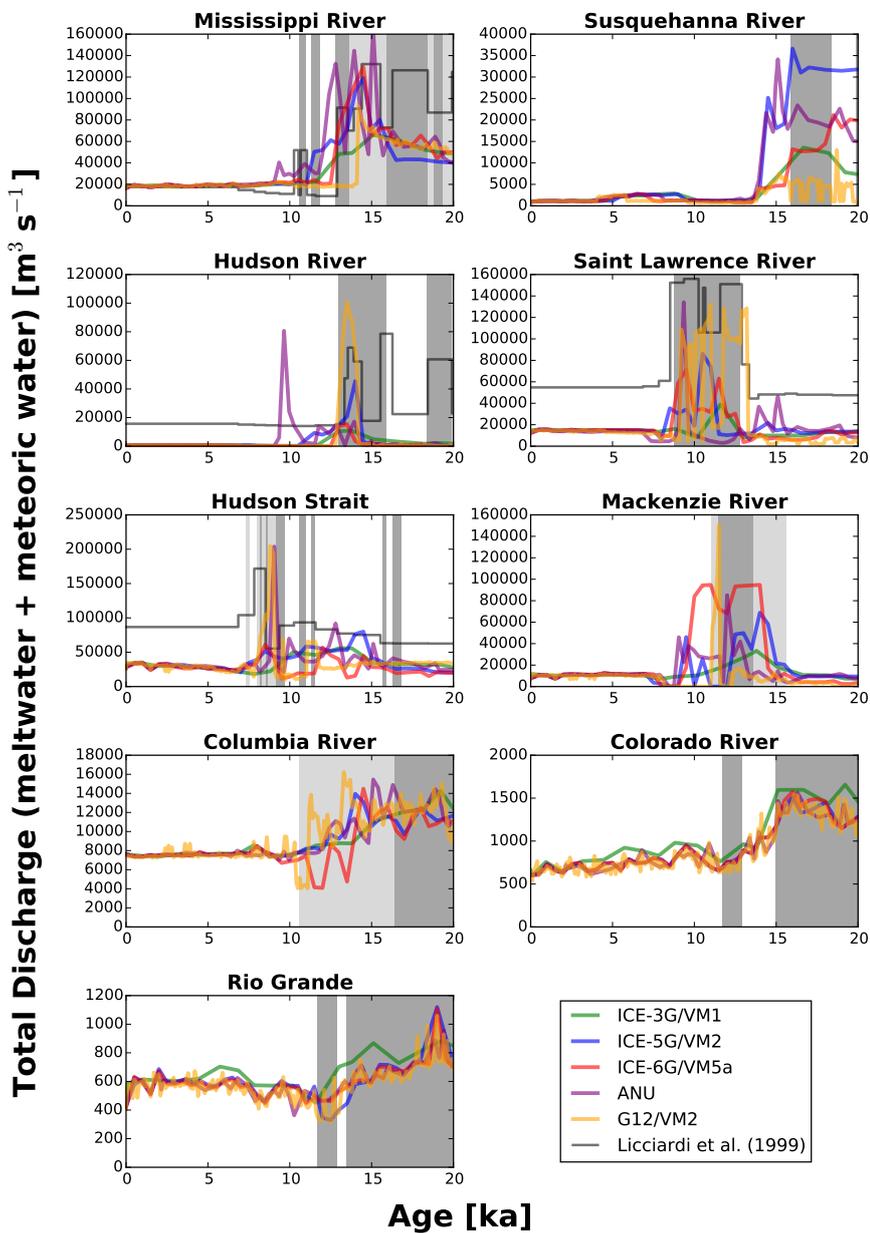
**Figure 16.** Total discharge from each river basin, represented on a single set of axes for comparison of timing and absolute magnitudes of meltwater discharge among the models, with the geologic record of enhanced past discharge (gray shading: dark, direct record; light, inferred and/or less discharge). Also shown here as a darker gray line, where available, is the data-driven discharge history of Licciardi et al. (1999), with its ages recalibrated using IntCal13.

Great Lakes was split between the Mississippi and Susquehanna Rivers (Ridge et al., 1991; Ridge, 1997; Licciardi et al., 1999). At 19.9 ka, ice retreat associated with the Erie Interstade opened the Mohawk valley in New York, which became a preferential pathway for all of the meltwater formerly sent to the Susquehanna River, as well as water from the Lake Erie and western Lake Ontario basins that formerly drained to the Mississippi (Ridge, 1997). In spite of the loss of Mississippi-routed meltwater inputs, deposits of the Kankakee Outwash Plain (Knox, 2007) indicate increased meltwater outflow to the Mississippi River from the Lake Michigan basin ~19.3–18.8 ka, with a major flood ~19 ka (Curry et al., 2014). Following the end of the Erie Interstade, at 18.4 ka (Licciardi et al., 1999; Reimer et al., 2013; Wickert, 2014b), the Port Bruce Stade advance produced the Valley Heads Glaciation in New York, sending flow back from the Hudson to the Susquehanna and Mississippi from 18.4–15.9 ka. As the ice again retreated during the 15.9–15.6 ka Mackinaw Interstade, the Hudson took all of the eastern outflow from the Great Lakes, reducing Mississippi discharge and removing ice-sheet inputs from the Susquehanna for the final time. Ice advanced again starting at 15.6 ka towards its Port Huron Stade maximum, at which point only Lake Ontario flowed towards the Hudson River (via the Mohawk Valley) and all other Great Lakes sent their outflow to the Mississippi (Hansel and Mickelson, 1988; Licciardi et al., 1999; Obbink et al., 2010). After 15.2 ka, the Great Lakes (except for Lake Superior) gradually shifted their flow away from the Mississippi and towards the Hudson River, though the Mississippi was augmented by increasing melt via the Des Moines Lobe, James Lobe, and Lake Agassiz (Patterson, 1997, 1998; Licciardi et al., 1999; Obbink et al., 2010; Sionneau et al., 2010).

Much of this early history stems from the continental record of ice advance and retreat. As such, it is a good predictor of changes in drainage basin area but somewhat less effective at predicting past river discharge, especially when that discharge is strongly influenced by ice-sheet melt. Discharge inferences continue to be aided by the growing database of paleoceanographic proxy records (e.g., Keigwin et al., 2006; Obbink et al., 2010; Williams et al., 2012; Hillaire-Marcel et al., 2013; Taylor et al., 2014; Gibb et al., 2014; Gil et al., 2015), improved geochemical techniques to produce richer records that also reduce or quantify uncertainties (e.g., Vetter, 2013; Spero et al., 2015; Khider et al., 2015; Vázquez Riveiros et al., 2016), and continuing work to provide quantitative freshwater discharge estimates based on these data (Carlson et al., 2007a; Carlson, 2009; Obbink et al., 2010; Wickert et al., 2013). Particularly important are records of past water isotopes, past water temperatures, and geochemical signatures of provenance. In addition to these sediment-based methods, continental-scale constraints on ice-sheet melt can be informed by sea-level fingerprinting (Gomez et al., 2015; Liu et al., 2015). In this work, we follow Licciardi et al. (1999) in correlating the terrestrial record of a large Mississippi River drainage basin with likely periods of enhanced Mississippi River discharge.

Meltwater discharge down the Mississippi decreased ~13.2 ka (Flower et al., 2004; Williams et al., 2012; Wickert et al., 2013), which correlates with a 13.2 ka increase in meltwater discharge

to the Gulf of Saint Lawrence (Carlson et al., 2007a; Rayburn et al., 2011). This initial phase of increased Saint Lawrence River outflow included two pulses of water input that probably record the discrete and stepwise eastward rerouting of the Great Lakes subbasins away from the glacial-stage Mississippi watershed (Carlson et al., 2007a; Rayburn et al., 2011). At 12.9 ka the Lake Agassiz drainage basin was rerouted away from the Mississippi River, with the most likely current chronology indicating that water from the Lake Agassiz subbasin first flowed east to the newly-ice-free Saint Lawrence (Broecker et al., 1989; Carlson et al., 2007a; Carlson and Clark, 2012; Levac et al., 2015; Leydet, 2016), and then, starting at 12.18±0.48 ka, to the northwest towards the Mackenzie River (Carlson et al., 2007a; Breckenridge, 2015). Two final periods of meltwater discharge down the Mississippi River occurred after the initial rerouting of Lake Agassiz flow. The first is recorded in a 11.8–11.3 ka $\delta^{18}$O spike in offshore sediments (Williams et al., 2012; Wickert, 2014a), whose age range encompasses the ∼11.6–11.5 ka Marquette Readvance of ice in the Lake Superior basin (Lowell et al., 1999) that temporarily separated the Great Lakes–Saint Lawrence river system from Lake Agassiz and may have sent meltwater from the Lake Superior basin back towards the Mississippi River (Breckenridge and Johnson, 2009). The second lasted ∼11.0 ka–10.6 ka (Fisher, 2003; Williams et al., 2012; Wickert, 2014a), and was the final pulse of ice-sheet meltwater to flow down the Mississippi.

Following the initial ∼13.2 ka increase in meltwater discharge to the Saint Lawrence River (Carlson et al., 2007a; Rayburn et al., 2011) and the dramatic 12.9 ka rerouting of Glacial Lake Agassiz that vastly increased its discharge (Carlson and Clark, 2012; Levac et al., 2015; Leydet, 2016), the Saint Lawrence continued to receive significant ice-sheet meltwater inputs via proglacial lakes. This lasted until sometime between ∼8.6 ka, when the combined Lake Agassiz-Ojibway level dropped in a partial drainage event (Breckenridge et al., 2012), and 8.2 ka, when the ice saddle in Hudson Bay collapsed, causing a massive flood that resulted in sea-surface freshening and the brief cooling of the 8.2 ka event (Barber et al., 1999; Carlson et al., 2009; Roy et al., 2011; Hoffman et al., 2012; Gregoire et al., 2012; Breckenridge et al., 2012; Stroup et al., 2013). While this ended meltwater inputs to the Saint Lawrence River, meltwater from the Québec–Labrador dome flowed down the Manicouagan River and into the Gulf of Saint Lawrence until ∼7.8 ka (Occhietti et al., 2004).

The record of ice and meltwater discharge from Hudson Bay and Hudson Strait that predates the Agassiz–Ojibway flood comes primarily from records of ice-rafted debris in marine sediment cores. This is because Hudson Strait was an ice-covered marine-terminating margin of a major ice stream of the Laurentide Ice Sheet (Margold et al., 2014). The largest of the post-LGM ice-rafted debris events was Heinrich Event 1, which occurred in two pulses: H1A (16.8–16.3 ka) and H1B (15.9–15.7 ka) (Gil et al., 2015). Heinrich Event 0, formerly thought to correspond to the Younger Dryas (12.8–12.3 ka (Andrews and Tedesco, 1992; Clark et al., 2001), has been recently shown to correlate with early Holocene warming and melt 11.5–11.3 ka (Pearce et al., 2015). Later ice-rafting events are related to ice advances of the Québec–Labrador dome into Ungava Bay (Kaufman and Miller,

1993; Metz et al., 2008; Rashid et al., 2014; Pearce, 2015; Jennings et al., 2015); these comprise the 11.0–10.6 ka Gold Cove advance (Pearce, 2015) and the 9.7–9.2 ka Noble Inlet advance (Jennings et al., 2015). Following these ice-rafting events, the merged Lake Agassiz–Ojibway released water into Hudson Bay in two major pulses. The first was the ~8.6 ka partial drainage of Lake Agassiz–Ojibway, identified by a low-water period in the varve record (Breckenridge et al., 2012). The second was the 8.2 ka complete drainage of Lake Agassiz–Ojibway (Breckenridge et al., 2012; Stroup et al., 2013) that is associated with collapse of the Laurentide Ice Sheet saddle that connected the Keewatin and Québec–Labrador domes (Gregoire et al., 2012). High carbonate concentrations and low $\delta^{18}O$ concentrations in sediments indicate consistent high discharge, even between these events, from the start of the Noble Inlet Advance at 9.7 ka until ~8.0 ka Jennings et al. (2015).

After 8.2 ka, Hudson Bay continued to receive a smaller meltwater input from the ablating remnant Laurentide ice caps (Carlson et al., 2008) that included one last ~200-year period period of enhanced discharge ~7.55–7.35 ka that appears in the $\delta^{18}O$ record of Jennings et al. (2015). The total volume of the 7.5–6.8 ka final ablation of the Laurentide Ice Sheet – comprising the Keewatin, Québec–Labrador, Baffin Island–Foxe ice domes – could have been up to 5 meters sea-level equivalent (SLE) (Carlson et al., 2007b; Jennings et al., 2015). Much of this melt would have flowed into Hudson Bay, but would not have been significant: the maximum estimate (5 m SLE and all melt entering Hudson Bay) results in an average discharge enhancement of 82 $m^3 \ s^{-1}$, which is small compared to the 30,900 $m^3 \ s^{-1}$ total modern discharge (Table 1). Therefore, background melt outside of the $\delta^{18}O$ excursion does not appear as a time of enhanced discharge on Figs. 11–16. Following final Laurentide Ice Sheet collapse, isostatic rebound with a time-averaged uplift rate of 1.3 cm $yr^{-1}$ (Lavoie et al., 2012) caused Hudson Bay to shrink to its modern size.

The main period of post-LGM high discharge down the Mackenzie River started ~15.6 ka with the retreat of the Mackenzie Lobe of the Laurentide Ice Sheet and associated meltwater production (Duk-Rodkin et al., 1994; Lemmen et al., 1994). Meltwater inputs increased at 13.6±0.2 ka (Smith, 1994), when glacial Lake McConnell formed in the Great Bear Lake Basin. Lake McConnell catastrophically flooded towards the Mackenzie River between ~13.6 and ~13.3 ka, possibly again at ~13.3 ka, and at ~13.1 ka. At ~13.1 ka, ice retreat rerouted Glacial Lake Peace, which formerly drained into the Missouri River (and hence, the Mississippi), towards the Mackenzie, significantly increasing its drainage area. At 12.18±0.48 ka, strandlines of Glacial Lake Agassiz indicate that it, too, started to flow to the north (Breckenridge, 2015). This age range is consistent with the 13.0±0.2 to 11.7±0.1 bounds on the age of gravel deposits that overlie a regional erosion surface on the Mackenzie River delta, presumably the result of a large flood associated with drainage rearrangement (Murton et al., 2010; Carlson and Clark, 2012). It also postdates the youngest dated material from Glacial Lake Mackenzie (13.0±0.3 ka), which drained when The Ramparts – the largest bedrock gorge in the Mackenzie River – incised (Mackay and Mathews, 1973). This incision may be related to drainage rerouting that increased inflow into Glacial Lake Mackenzie and caused it to overtop the

bedrock sill that dammed it to the north. Meltwater inputs to the Mackenzie River ended ∼11 ka when its eastern tributaries were temporarily rerouted eastward due to a combination of ice retreat and glacial-isostatic depression (see Section 5.1.3 and Keigwin et al., in prep.). Later northwestern drainage of Lake Agassiz during its high-water "Emerson" phase, 10.8–10.2 ka Fisher (2007), must therefore have reached Lake McConnell and then flowed towards the north near the retreating ice margin instead of entering the Mackenzie River drainage basin.

The Columbia River has an offshore record of rapid turbidite deposition that stretches 36.1–10.6 ka (Zuffa et al., 2000). Within this time, large floods associated with glacial Lake Missoula occurred 22.9–16.5 ka (Bretz, 1923, 1969; Waitt, 1980; Atwater, 1984; Benito and O'Connor, 2003; Lopes and Mix, 2009), and Lake Bonneville routed a portion of flow from the Great Basin to the Columbia River 18.2–16.4 ka (Gilbert, 1890; Godsey et al., 2005, 2011; McGee et al., 2012). The terrestrial record contains evidence for later, smaller outflows from glacial Lake Missoula 15.1–12.6 ka (Hanson et al., 2012), and intermittent overflow inputs from Lake Bonneville 16.4–14.8 ka (synthesis of Godsey et al., 2011; McGee et al., 2012).

Water discharge in Colorado River and the Rio Grande, while influenced by mountain glacier retreat, responded primarily to the cooler and wetter regional climate during the Last Glacial Maximum and Younger Dryas that was caused by changes in continental-scale moisture transport (e.g., Kutzbach and Wright, 1985; He, 2011). These cool, wet periods are marked by high pluvial lake levels (e.g., Currey et al., 1990; Matsubara and Howard, 2009; McGee et al., 2012), mountain glacier advances prior to the onset of the Bølling-Allerød (e.g., Owen et al., 2003; Guido et al., 2007; Orme, 2008), increased landsliding in the Rio Grande basin between ∼21.2 and ∼14.5 ka (Reneau and Dethier, 1996), deposition of valley fills in the Colorado River (Pederson et al., 2013), and speleothem growth (Polyak et al., 2004). The warmer Bølling-Allerød and Holocene are related to records of strath terrace formation (Anders et al., 2005; Cook et al., 2009) and mountain glacier retreat (Guido et al., 2007). While anomalous records, such as speleothem growth ∼14 ka during the Bølling-Allerød (Polyak et al., 2004), complicate the picture of past climate in the southwest, the general pattern of climate change closely mirrors that observed in the Greenland ice core records (Benson et al., 1997; Svensson et al., 2008; Asmerom et al., 2010; Wagner et al., 2010).

### 5.1.2 Comparison of data and models for river discharge

In order to determine how well, broadly, these different models were able to reproduce our observed record of discharge variability, I subdivided the computed discharges into events during known high-flow periods (light and dark gray regions on Figs.11–16 and those from the low-flow remainder of the record. I first compared the mean discharges during known high- and low-flow periods (Fig. 17A). For the five ice-sheet models and nine river systems, only twice did the known low-flow time produce a higher computed discharge: the Hudson River for the ANU model and Hudson Strait for ICE-3G. The ice-physics-based G12 performed the best in generating discharges during high-flow

periods that were much higher than those during low-flow periods, with ICE-5G and ICE-6G nearly

730  tied in second place. The strong performance of G12 may be because its input mass balance was
driven by a coupled ocean–atmosphere general circulation model (FAMOUS: Smith et al., 2008),
making its ice mass the result of a pre-computed hydrologic balance. I then generated histograms
for the high-flow and low-flow segments of the model results, and performed Kolmogorov–Smirnov
tests between the pairs of distributions for each ice model and river system to test how different

735  they are from one another (Fig. 17B). Here, the new GIA-based ICE-6G was a close second to
ICE-3G, though the latter is disqualified as a good fit to the North American ice sheet complex
by not including a large enough total ice mass. G12 reproduced many patterns of deglacial water
discharge well, including the pulses of iceberg/meltwater output from Hudson Strait (Figure 14), but
its goodness of fit is reduced by its short (but intense) pulse of meltwater down the Mackenzie River,

740  its lack of early meltwater delivery to the Hudson River, and a too-early switch of meltwater outflow
away from the Mississippi River because its climate forcing and dynamical ice response created a
Québec–Labrador dome that retreated too early. For both of these metrics, the inconsistent time steps
between ice-sheet reconstructions can affect the fits, as can be seen especially for the Rio Grande
and Columbia River, which should be the same for all runs as the same climate reconstruction was

745  employed in all cases. Therefore, these catchments were removed from the above analysis, the broad
strokes of which provide a useful template for comparison.

Across all model runs, Hudson Strait was the consistent site of the worst agreement between data
and the models. It is possible that this is due to data-collection issues (e.g., few organics) and data
sparsity (few settlements and fewer GPS monuments) in this formerly fully ice-covered region, lead-

750  ing to a lack of good regional constraints on ice-sheet thickness near the center of the Laurentide Ice
Sheet. However, recent data sets have brought more clarity to the Hudson Strait record (e.g., Rashid
et al., 2014; Gil et al., 2015; Pearce et al., 2015; Pearce, 2015; Jennings et al., 2015), furthering the
argument that this mismatch could be because the models do not accurately represent the dynamics
of the marine-terminating Hudson Strait ice catchment (e.g., MacAyeal, 1993). An additional com-

755  plication of Hudson Bay/Strait is that its drainage area was smaller at the Last Glacial Maximum,
but it had the potential to release a large amount of ice, as is observed in the Heinrich Events (e.g.,
Heinrich, 1988). A final potential issue is that Hudson Bay lies on the low-relief Canadian Shield in
the zone of maximum glacial-isostatic deformation, meaning that its computed drainage area during
deglaciation is sensitive to GIA (Fig. 10). In summary, a proper comparison requires both long-term

760  proxy discharge evidence and a mechanistic ice-sheet and GIA model that can explain the dynamics
of ice and solid Earth masses in Hudson Bay and Hudson Strait under a realistic climate forcing.
The Glimmer–CISM (Rutt et al., 2009) runs of Gregoire et al. (2012) are able to reconstruct the
general form of the pulsed meltwater releases seen in proxies (e.g., Jennings et al., 2015), putting
more weight behind approaches that involve ice physics to reconstruct past ice sheets (e.g., Tarasov

765  and Peltier, 2005; Tarasov et al., 2006, 2012; Gregoire et al., 2012; Wickert et al., 2013).

A comparison between these model results and data-driven drainage histories of Licciardi et al. (1999) (Fig. 16: Mississippi, Hudson, Saint Lawrence, Hudson Strait) includes both similarities and differences when compared to the river system reconstructions presented here. For the Mississippi River System, Licciardi et al. (1999) expect enhanced discharge between 18.4 and 16.3 ka and prior

770 to 19.9 ka – that is, at times when all Great Lakes flow was routed down the Mississippi River. The reconstructions analyzed here exhibit enhanced discharge over the entire time prior to 16.3 ka, but with no shorter-term periods of more enhanced discharge (Fig. 16: Mississippi). The discharges predicted by Licciardi et al. (1999) are higher than any produced here, and this is because they neglect evapotranspiration. Periodicity due to drainage rearrangement, predicted by Licciardi et al. (1999) is

775 seen (albeit with different timing) in the $\delta^{18}O$ record of the Gulf of Mexico (Williams et al., 2012; Wickert, 2014a), though this is more sensitive to the very negative $\delta^{18}O$ of meltwater discharge than to the overall freshwater discharge. The modeled Hudson River discharge does not exhibit the predicted Erie or Mackinaw Interstade periods of enhanced discharge in any of the computed discharge histories presented here. Compelling geological evidence that meltwater flowed through the Mohawk

780 Valley into the Hudson River during the Erie Interstade (Ridge, 1997) makes this omission a point to improve in future reconstructions of the southeastern Laurentide Ice Sheet. The Saint Lawrence River constraints from Licciardi et al. (1999) remain consistent in this work with the flow-routed G12 model Gregoire et al. (2012) and ICE-6G (Argus et al., 2014; Peltier et al., 2015) providing good fits to these constraints in spite of G12 rerouting meltwater discharge from the Mississippi

785 to the Saint Lawrence ∼1.1 ka too early (Wickert et al., 2013). The Hudson Strait Record is difficult to match because of its many episodic meltwater releases (e.g., Heinrich, 1988; Andrews and MacLean, 2003; Hemming, 2004; Gil et al., 2015; Jennings et al., 2015), and only the climate-forced and ice-physics-based G12 reproduces the general form of these events. These events are simplified or smoothed-over by Licciardi et al. (1999), but recent improvements in the age constraints on these

790 iceberg and/or meltwater release events (e.g., Rashid et al., 2014; Gil et al., 2015; Pearce et al., 2015; Pearce, 2015; Jennings et al., 2015) set the stage for forthcoming advances in reconstructions of the northeastern core of the Laurentide Ice Sheet.

### 5.1.3 Comparison of data and models for drainage basin extents

Any model-based reconstruction that employs a realistically-shaped North American ice sheet com-

795 plex will produce certain changes in continental-scale drainage. The most visible such pattern, consistent across all model-based reconstructions, is that the high Keewatin and Labrador domes of the Laurentide Ice Sheet and ice advance across the Great Lakes basins generated a new trans-continental drainage divide that added regions that currently flow into Hudson Bay and the Saint Lawrence River to the LGM Mississippi drainage basin (Fig. 7). The patterns of post-LGM drainage basin evolution,

800 as well as regional-scale changes in drainage basin extents, vary more significantly among model-
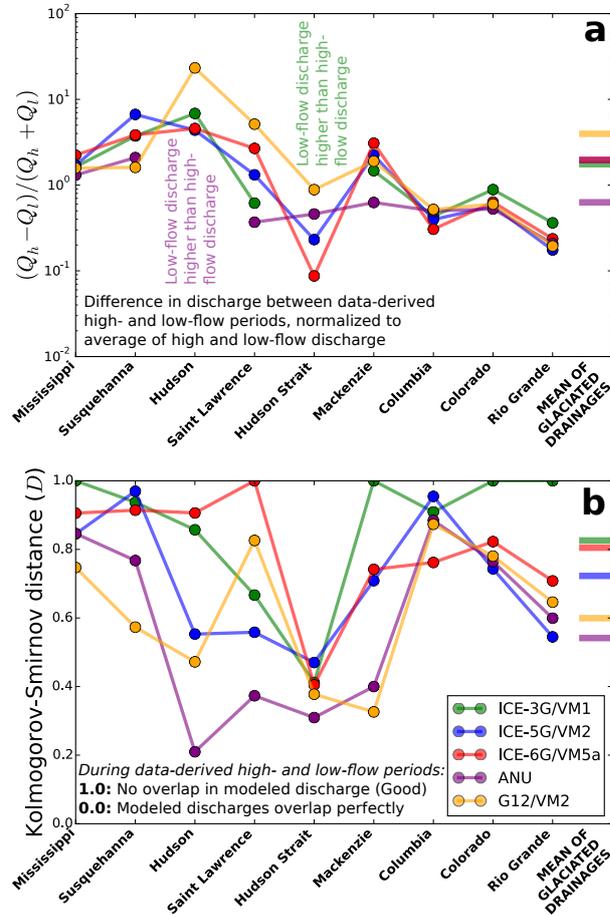
**Figure 17.** The computed discharge time-series is segmented into values corresponding with times of known high and low discharge. **a.** Normalized difference between known high and low discharge times. The greatest mean normalized difference is seen in G12, the ice-physics based model of Gregoire et al. (2012), and the least in the GIA-based model of Lambeck et al. (2002). **b.** The Kolmogorov–Smirnov test measures the distance between one-dimensional distributions; here I use it to compute the a metric of difference between the computed discharge histograms for each river system during the generalized data-derived times of high and low discharge (both light and dark gray in Figs. 11–16). A high distance value indicates a strong separation between the range of discharges during geologically-constrained high- and low-flow periods, and hence a good match between the data and model. Here, the GIA-based ICE-3G and ICE-6G models perform the best, with poor matches only to Hudson Bay. The ice-physics-based G12 performs poorly, due in part to the too-early demise of its Québec–Labrador dome, and the GIA-based ANU model performs the worst.

based reconstructions. Identifying differences between the model-driven and data-driven drainage basin reconstructions can guide efforts to produce a more accurate depiction of the last deglaciation.

At the Last Glacial Maximum, ICE-5G and G12 have the most severe misfits with data. ICE-5G sends a large fraction of what data indicate should be Mississippi-River-bound drainage to the Hudson River, an artifact fixed in ICE-6G with its more realistic ice-dome structure. G12 at the Last Glacial Maximum has Mackenzie River drainage routed towards the Yukon River, though time steps shortly before and after the LGM have the proper drainage routing. This is the result of its ice sheet briefly crossing a threshold that rerouted drainage. Such thresholds are the value of drainage routing in helping to discriminate between valid and invalid portions of ice-sheet reconstructions.

During Bølling-Allerød time, only ICE-6G and G12 properly show that ice retreated beyond the bounds of the Susquehanna River basin. All models simulate the Mississippi and Mackenzie catchments generally well, and close to what available data (e.g., Margold et al., 2014) would indicate.

During the early part of the Younger Dryas, the Mackenzie and Saint Lawrence Rivers both experienced periods of high discharge (de Vernal et al., 1996; Carlson et al., 2007a; Murton et al., 2010). While debate continues as to whether Lake Agassiz flowed towards the Mackenzie River in the northwest (e.g., Murton et al., 2010), towards the Saint Lawrence River in the east (e.g., Carlson and Clark, 2012), or, as one group has proposed, became a closed basin at this time due to regional drying (Lowell et al., 2013), evidence currently indicates that Lake Agassiz first drained east at the onset of the Younger Dryas (Carlson et al., 2007a; Rayburn et al., 2011; Carlson and Clark, 2012; Leydet, 2016) and then drained north at 12.18±0.48 ka (Breckenridge (2015), which is consistent with the data of Murton et al. (2010)). The drying hypothesis seems the least likely, as the model to simulate it (Lowell et al., 2013) creates a closed basin when at least two parameters seem unreasonable. These are: (1) evaporative loss that is generally >1.5 times today's observations, in spite of cooler temperatures and a longer lake-ice season, although katabatic winds may have increased evaporation somewhat over the open water (see Carlson and Clark, 2009, for more on the problem of too much evaporation), and (2) a temperature lapse rate that is 7.3 °C km$^{-1}$, outside of the error bars of the 5.1±1.2 °C km$^{-1}$ observed on modern ice sheets and ice caps Anderson et al. (2014), and resulting in a smaller melt-producing area of the Laurentide Ice Sheet. The drying hypothesis has received further critiques from Teller (2013) and Breckenridge (2015) based on field evidence, with strandline mapping by Breckenridge (2015) indicating that the level of Lake Agassiz dropped when it flowed to the northwest, though current evidence suggests that Lake Agassiz drawdown postdates the onset of the Younger Dryas. Regardless of where Lake Agassiz flowed, or whether it became a closed basin (the flow-routing presented here does not allow closed basins to exist: see Section 2.3.2), isotopic data from the Gulf of Mexico show unequivocally that meltwater discharge to the Mississippi ended ∼12.9 ka (Wickert et al., 2013). This means that the ICE-5G and ANU reconstructions miss the timing of the most major drainage rearrangement in the North American deglaciation. The G12 reconstruction has such intense isostatic adjustment when coupled with the

VM2 solid Earth model that there is marine inundation of the entire set of Great Lakes Basins. Extreme isostatic adjustment in both G12 and ICE-6G causes the Missouri River to flow towards the north. In G12, this is due in part to the too-early retreat of the southeastern Laurentide margin. Overall, ICE-3G and ICE-6G perform the best, with the latter sending Lake Agassiz meltwater to the Mackenzie River and Beaufort Sea and water from the Laurentide Great Lakes to the Gulf of Saint Lawrence, a scenario that is consistent with current geological evidence (e.g., de Vernal et al., 1996; Richard et al., 2005; Carlson et al., 2007a; Murton et al., 2010; Rayburn et al., 2011; Breckenridge, 2015).

The early Holocene in northern North America was characterized by retreat of the Laurentide Ice Sheet that led to expansion of proglacial lakes, setting the stage for the short-lived and rapid 8.2 ka cooling event (Breckenridge et al., 2012). G12 produced a saddle collapse that led to this flood (Gregoire et al., 2012), though with a somewhat different spatial pattern than what has been mapped (Dyke et al., 2003; Dyke, 2004). None of the models perform particularly well here. ICE-3G has altogether too much ice retreat. ICE-5G, ICE-6G, and ANU have a drainage divide that splits the east–west Saint Lawrence drainage basin, which at this time extended west to the Canadian Rockies (Teller and Leverington, 2004; Breckenridge et al., 2012; Stroup et al., 2013). G12 has this continuous drainage basin, but instead of flowing into the Saint Lawrence River, water in its drainage reconstruction flows to the Arctic Ocean via a gap at the Manitoba–Saskatchewan border along the southwest corner of the retreating ice-sheet (Fig. 10). While this could be a route for the ~8.6 ka flood associated with partial drainage of Lake Agassiz–Ojibway (Breckenridge, 2015), it is not the long-term drainage route for these lakes through the Kinojévis spillway system and into the Ottawa River (Vincent and Hardy, 1977; Veillette, 1994). It is notable that ICE-5G, ICE-6G, and G12 have a tiny early Holocene Mackenzie River basin, and the ANU model also produces a small Mackenzie drainage basin at 8.75 and 8.45 ka. In these models, rapid retreat of the western margin of the Laurentide Ice Sheet exposed an eastward-tilting isostatically-depressed land surface in the eastern portion of the modern Mackenzie River drainage basin, which drained to the Mackenzie River only after significant isostatic rebound. New cores from the Beaufort Sea record increased $\delta^{18}$O between 11 and 9 ka (Keigwin et al., manuscript in prep.) that cannot be reconciled with changing climate, but would be consistent with a decrease in drainage basin area. Each model output presented here (see supplementary videos) includes this reduced drainage basin area at different times. Therefore, the temporary reduction in Mackenzie River drainage area is sensitive to ice-sheet geometry and/or solid-Earth rheology, making it a useful constraint on ice-sheet reconstructions. G12 fit this timing the best of the models studied here by having a reduced Holocene drainage basin area from 11.0 to 8.2 ka, though it also exhibited a limited basin area at certain times before 11.5 ka.

### 5.2 Future directions: new ice-sheet reconstructions and coupling with hydrologic, climate, isotopic, archaeological, and sediment transport models and observations

The work presented here is a necessary starting point for future studies that investigate the inter-
875 actions between deglacial surface-water hydrology and other components of the integrated Earth
system. Combining these meltwater routing patterns with proglacial lakes and changing land cover
will allow equations designed to predict sediment yield from large catchments to be employed for a
continental-scale paleo-sediment-discharge reconstruction (following Overeem et al., 2005; Kettner
and Syvitski, 2008; Pelletier, 2012; Cohen et al., 2013), with modern control provided by present-day
880 sediment yields (Table 1). These sediment discharges can be compared with records of deposition
(e.g., Andrews and Dunhill, 2004; Breckenridge, 2007; Williams et al., 2010) and records of geo-
morphic change (e.g., Dury, 1964; Reusser et al., 2006; Knox, 2007; Anderson, 2015). The need to
properly compute past lake and land cover motivates continued work with climate- and water-balance
models (e.g., Collins et al., 2006; Matsubara and Howard, 2009; Liu et al., 2009; He, 2011; Blois
885 et al., 2013; Fan et al., 2013), which can in turn be used to improve past drainage basin and discharge
reconstructions. These, together with paleogeographic reconstructions such as those presented here,
can be used to reconstruct areas of archaeological interest, either as changes in shoreline positions
and topography (Clark et al., 2014) or as a wholesale landscape reconstruction that incorporates site-
potential modeling (Monteleone et al., 2013; Monteleone, 2013; Dixon and Monteleone, 2014). On
890 a global scale, several current flow-routing algorithms could be made global for better integration
with ice-sheet, climate, and GIA models (Metz et al., 2011; Qin and Zhan, 2012; Braun and Bezada,
2013; Huang and Lee, 2013; Schwanghart and Scherler, 2014), including the possibility to include
high-resolution flow routing as part of a transient coupled model run instead of an *a posteriori* anal-
ysis, as is presented here. Finally, high-resolution drainage routing schemes can connect models of
895 past climate, ice sheets, and drainage routing, to oxygen isotopes in sediment cores (Wickert et al.,
2013), and the increasingly-complete collection of such records from the North American continent
and continental margin (e.g., Hooke and Clausen, 1982; Remenda et al., 1994; Andrews et al., 1994;
de Vernal et al., 1996; Birks et al., 2007; Carlson et al., 2007a, 2009; Breckenridge and Johnson,
2009; Lopes and Mix, 2009; Obbink et al., 2010; Brown, 2011; Hoffman et al., 2012; Williams
900 et al., 2012; Gibb et al., 2014; Taylor et al., 2014; Ferguson and Jasechko, 2015; Hladyniuk and
Longstaffe, 2016) is opening new possibilities in isotopic studies of whole-ice-sheet mass balance.

Pursuit of these targets does not preclude the search for a more representative ice-sheet recon-
struction and better ways to integrate models and data. New reduced-complexity modeling rooted
in ice-margin mapping and ice physics (Gowan et al., 2016b, a) spans the gap between the empiri-
905 cal and modeling approaches highlighted here. Surface energy balance calculations (Ullman et al.,
2015) also elucidate which part of the ice sheet was melting, and when – providing a testable link
to records of glacial meltwater input. Continued development of numerical ice-sheet models (e.g.,
Cornford et al., 2013; Le Morzadec et al., 2015) provides new avenues to reconstruct past ice-sheets

that may be coupled directly with deglacial drainage evolution (Tarasov et al., 2006, 2012). Such fully-coupled models, if run at a high enough spatial and temporal resolution, have the potential to recreate short-term flooding events that have left a strong mark in the geologic record of deglaciation (e.g., Kehew et al., 1994; Breckenridge, 2007; Murton et al., 2010). Climate and ice-sheet models may also be isotope-enabled for comparison with isotopic data from geological archives (Caley et al., 2014; Ferguson and Jasechko, 2015; Gasson et al., 2016). Each of these approaches presents new opportunities to test deglacial drainage patterns and converge towards a solution for the shape and evolution of the North American ice-sheet complex that integrates data from glacial, fluvial, and marine systems.

## 6 Conclusions

Most ice-sheet reconstructions, including all those examined here, are built to fit sea-level records, glacial isostatic adjustment measurements, and/or moraine positions; some are built using ice-physics-based simulations. The models in this study were not calibrated to drainage basins or meltwater pathways, which leave behind geomorphic and stratigraphic markers that can be used to discriminate between hypothesized ice-thickness distributions and deglaciation histories.

Significant scatter in the data–model fit among the ice-sheet reconstructions tested leaves no clear "winner" among these models. Nevertheless, ICE-6G and G12 each perform well enough, and for distinct reasons, to be noted here. ICE-6G is based on GIA and ice margins, but also possesses an ice-dome structure that is consistent with geological evidence of ice-flow paths. Its generally good performance is likely tied to this combined geological and geophysical basis. G12, while only loosely calibrated to match the outlines of the North American Ice Sheet complex, nonetheless reproduces many changes in continental-scale drainage. Its basis in a process-based numerical model enhanced the separation between known high- and low-flow periods, as both the G12 ice sheet and the geological record were driven by climate forcings, and permitted tightly-spaced output time-steps that allow better comparison between the reconstruction and the geologic record.

Beyond the focus on deglaciation and ice-sheet geometry, the dynamic deglacial drainage basins of North America are significant in their own right. The new paleohydrographs presented here provide new insights into the ice-age legacy imprinted on the major rivers of the continent that quantifies the mid-20th-century observation that many North American rivers are "underfit" in their glacial-meltwater-carved valleys (Dury, 1964).

The goal of this work is to move towards a self-consistent paleogeographic framework within which models and geologic records may be quantitatively compared to build new insights into past glacial systems and climate–ice-sheet interactions. When integrated more broadly into studies of North American deglaciation, these time-varying deglacial drainage basins and paleohydrographs are poised to improve reconstructions of past climate and ice-sheet geometry.

*Acknowledgements.* Jerry Mitrovica provided GIA model outputs and Feng He supplied TraCE-21K GCM out-

945    puts, both of which were crucial to this work. CMAP Precipitation data were provided by the NOAA/OAR/ESRL

PSD, Boulder, Colorado, USA, from their web site at http://www.esrl.noaa.gov/psd/. Ruža Ivanović, Lauren

Gregoire, and Kelly Monteleone helped with stimulating discussion and ideas about where to take this work

in the future. Conversations with Bob Anderson about glacial impacts on the morphology of large rivers in-

spired this work, and reviews from Andy Breckenridge and Lev Tarasov as well as comments from Anders

950    Carlson improved the final publication. ADW was supported by the US Department of Defense through the

National Defense Science & Engineering Graduate Fellowship Program, the US National Science Foundation

Graduate Research Fellowship under Grant No. DGE 1144083, the Emmy Noether Programme of the Deutsche

Forschungsgemeinschaft (DFG) through funds awarded to T. Schildgen under Grant No. SCHI 1241/1-1, and

start-up funds from the University of Minnesota.

## References

Adler, R. F., Huffman, G. J., Chang, A., Ferraro, R., Xie, P.-P., Janowiak, J., Rudolf, B., Schneider, U., Curtis, S., Bolvin, D., Gruber, A., Susskind, J., Arkin, P., and Nelkin, E.: The Version-2 Global Precipitation Climatology Project (GPCP) Monthly Precipitation Analysis (1979–Present), Journal of Hydrometeorology, 4, 1147–1167, doi:10.1175/1525-7541(2003)004<1147:TVGPCP>2.0.CO;2, 2003.

Alden, W. C.: Physiography and glacial geology of western Montana and adjacent areas, vol. 231 of *Professional Paper 174*, United States Geological Survey, 1932.

Amante, C. and Eakins, B. W.: ETOPO1 1 Arc-Minute Global Relief Model: Procedures, Data Sources and Analysis, NOAA Technical Memorandum NESDIS NGDC-24, 2009.

Anders, M. D., Pederson, J. L., Rittenour, T. M., Sharp, W. D., Gosse, J. C., Karlstrom, K. E., Crossey, L. J., Goble, R. J., Stockli, L., and Yang, G.: Pleistocene geomorphology and geochronology of eastern Grand Canyon: linkages of landscape components during climate changes, Quaternary Science Reviews, 24, 2428–2448, doi:10.1016/j.quascirev.2005.03.015, 2005.

Anderson, J.: History of the Missouri River Valley from the Late Pleistocene to Present : Climatic vs . Tectonic Forcing on Valley Architecture, M.s. thesis, Texas Christian University, 2015.

Anderson, L. S., Roe, G. H., and Anderson, R. S.: The effects of interannual climate variability on the moraine record, Geology, 42, 55–58, doi:10.1130/G34791.1, 2014.

Anderson, R. C.: Reconstruction of preglacial drainage and its diversion by earliest glacial forebulge in the upper Mississippi Valley region, Geology, 16, 254, 1988.

Andersson, A., Fennig, K., Klepp, C., Bakan, S., Graß l, H., and Schulz, J.: The Hamburg Ocean Atmosphere Parameters and Fluxes from Satellite Data – HOAPS-3, Earth System Science Data, 2, 215–234, doi:10.5194/essd-2-215-2010, 2010.

Andersson, A., Klepp, C., Fennig, K., Bakan, S., Grassl, H., and Schulz, J.: Evaluation of HOAPS-3 Ocean Surface Freshwater Flux Components, Journal of Applied Meteorology and Climatology, 50, 379–398, doi:10.1175/2010JAMC2341.1, 2011.

Andrews, J. T. and Dunhill, G.: Early to mid-Holocene Atlantic water influx and deglacial meltwater events, Beaufort Sea slope, Arctic Ocean, Quaternary Research, 61, 14–21, doi:10.1016/j.yqres.2003.08.003, 2004.

Andrews, J. T. and MacLean, B.: Hudson Strait ice streams: a review of stratigraphy, chronology and links with North Atlantic Heinrich events, Boreas, 32, 4–17, doi:10.1080/03009480310001010, 2003.

Andrews, J. T. and Tedesco, K.: Detrital carbonate-rich sediments, northwestern Labrador Sea: Implications for ice-sheet dynamics and iceberg rafting (Heinrich) events in the North Atlantic, Geology, 20, 1087–1090, doi:10.1130/0091-7613(1992)020<1087:DCRSNL>2.3.CO;2, 1992.

Andrews, J. T., Erlenkeuser, H., Tedesco, K., Aksu, A. E., and Jull, A.: Late Quaternary (Stage 2 and 3) Meltwater and Heinrich Events, Northwest Labrador Sea, Quaternary Research, 41, 26–34, doi:10.1006/qres.1994.1003, 1994.

Andrews, J. T., Keigwin, L., Hall, F., and Jennings, A. E.: Abrupt deglaciation events and Holocene palaeoceanography from high-resolution cores, Cartwright Saddle, Labrador Shelf, Canada, Journal of Quaternary Science, 14, 383–397, doi:10.1002/(SICI)1099-1417(199908)14:5<383::AID-JQS464>3.0.CO;2-J, 1999.

Antevs, E.: The recession of the last ice sheet in New England, Research Series, American Geographical Society, 1922.

995     Argus, D. F. and Peltier, W. R.: Constraining models of postglacial rebound using space geodesy: a detailed assessment of model ICE-5G (VM2) and its relatives, Geophysical Journal International, 181, 697–723, doi:10.1111/j.1365-246X.2010.04562.x, 2010.

Argus, D. F., Peltier, W. R., Drummond, R., and Moore, A. W.: The Antarctica component of postglacial rebound model ICE-6G_C (VM5a) based on GPS positioning, exposure age dating of ice thicknesses, and

1000    relative sea level histories, Geophysical Journal International, 198, 537–563, doi:10.1093/gji/ggu140, 2014.

Asmerom, Y., Polyak, V. J., and Burns, S. J.: Variable winter moisture in the southwestern United States linked to rapid glacial climate shifts, Nature Geoscience, 3, 114–117, doi:10.1038/ngeo754, 2010.

Atwater, B. F.: Periodic floods from glacial Lake Missoula into the Sanpoil arm of glacial Lake Columbia, northeastern Washington, Geology, 12, 464–467, doi:10.1130/0091-7613(1984)12<464:PFFGLM>2.0.CO;2,

1005    1984.

Austermann, J., Mitrovica, J. X., Latychev, K., and Milne, G. A.: Barbados-based estimate of ice volume at Last Glacial Maximum affected by subducted plate, Nature Geoscience, 6, 553–557, doi:10.1038/ngeo1859, 2013.

Barber, D. C., Jennings, A. E., Andrews, J. T., Kerwin, M. W., and Morehead, M. D.: Forcing of the cold event

1010    of 8,200 years ago by catastrophic drainage of Laurentide lakes, Nature, 400, 13–15, doi:10.1038/22504, 1999.

Benito, G. and O'Connor, J. E.: Number and size of last-glacial Missoula floods in the Columbia River valley between the Pasco Basin, Washington, and Portland, Oregon, Geological Society of America Bulletin, 115, 624–638, doi:10.1130/0016-7606(2003)115<0624:NASOLM>2.0.CO;2, 2003.

1015    Benson, L., Burdett, J., Lund, S., Kashgarian, M., and Mensing, S.: Nearly synchronous climate change in the Northern Hemisphere during the last glacial termination, Nature, 388, 263–265, 1997.

Bentley, S.: Fluvial Sediment Delivery to Hudson Bay in a Changing Climate: Projections and Hypotheses, in: ArcticNet Annual Scientific Meeting, Victoria, British Columbia, Canada, 2006.

Birks, S. J., Edwards, T. W. D., and Remenda, V. H.: Isotopic evolution of Glacial Lake Agassiz: New insights

1020    from cellulose and porewater isotopic archives, Palaeogeography, Palaeoclimatology, Palaeoecology, 246, 8–22, doi:10.1016/j.palaeo.2006.10.024, 2007.

Blois, J. L., Williams, J. W., Fitzpatrick, M. C., Ferrier, S., Veloz, S. D., He, F., Liu, Z., Manion, G., and Otto-Bliesner, B.: Modeling the climatic drivers of spatial patterns in vegetation composition since the Last Glacial Maximum, Ecography, 36, 460–473, doi:10.1111/j.1600-0587.2012.07852.x, 2013.

1025    Bluemle, J. P.: Pleistocene Drainage Development in North Dakota, Geological Society of America Bulletin, 83, 2189, doi:10.1130/0016-7606(1972)83[2189:PDDIND]2.0.CO;2, 1972.

Blum, M. D., Guccione, M. J., Wysocki, D. A., Robnett, P. C., and Rutledge, E. M.: Late Pleistocene evolution of the lower Mississippi River valley, southern Missouri to Arkansas, Geological Society of America Bulletin, 112, 221–235, doi:10.1130/0016-7606(2000)112<221:LPEOTL>2.0.CO;2, 2000.

1030    Blumentritt, D. J., Wright, H. E., and Stefanova, V.: Formation and early history of Lakes Pepin and St. Croix of the upper Mississippi River, Journal of Paleolimnology, 41, 545–562, 2009.

Braun, C. and Bezada, M.: The History and Disappearance of Glaciers in Venezuela, Journal of Latin American Geography, 12, 85–124, doi:10.1353/lag.2013.0016, 2013.

Breckenridge, A.: The Lake Superior varve stratigraphy and implications for eastern Lake Agassiz outflow from 10,700 to 8900 cal ybp (9.5–8.0 ˆ{14}C ka), Palaeogeography, Palaeoclimatology, Palaeoecology, 246, 45–61, doi:10.1016/j.palaeo.2006.10.026, 2007.

Breckenridge, A.: The Tintah-Campbell gap and implications for glacial Lake Agassiz drainage during the Younger Dryas cold interval, Quaternary Science Reviews, 117, 124–134, doi:10.1016/j.quascirev.2015.04.009, 2015.

Breckenridge, A. and Johnson, T. C.: Paleohydrology of the upper Laurentian Great Lakes from the late glacial to early Holocene, Quaternary Research, 71, 397–408, doi:10.1016/j.yqres.2009.01.003, 2009.

Breckenridge, A., Lowell, T. V., Stroup, J. S., and Evans, G.: A review and analysis of varve thickness records from glacial Lake Ojibway (Ontario and Quebec, Canada), Quaternary International, 260, 43–54, doi:10.1016/j.quaint.2011.09.031, 2012.

Bretz, J. H.: The channeled scablands of the Columbia Plateau, The Journal of Geology, 31, 617–649, 1923.

Bretz, J. H.: The Lake Missoula floods and the channeled scabland, The Journal of Geology, 77, 505–543, 1969.

British Oceanographic Data Centre: The GEBCO_08 Grid, version 20100927, 2010.

Broecker, W. S., Kennett, J. P., Flower, B. P., Teller, J. T., Trumbore, S., Bonani, G., and Wolfli, W.: Routing of meltwater from the Laurentide Ice Sheet during the Younger Dryas cold episode, Nature, 341, 318–321, doi:10.1038/341318a0, 1989.

Brown, E. A.: Initial Ablation of the Laurentide Ice Sheet Based on Gulf of Mexico Sediments, M.s. thesis, University of South Florida, 2011.

Caley, T., Roche, D. M., Waelbroeck, C., and Michel, E.: Oxygen stable isotopes during the Last Glacial Maximum climate: Perspectives from data-model (iLOVECLIM) comparison, Climate of the Past, 10, 1939–1955, doi:10.5194/cp-10-1939-2014, 2014.

Carlson, A. E.: Geochemical constraints on the Laurentide Ice Sheet contribution to Meltwater Pulse 1A, Quaternary Science Reviews, 28, 1625–1630, 2009.

Carlson, A. E. and Clark, P. U.: Comment: Radiocarbon deglaciation chronology of the Thunder Bay, Ontario area and implications for ice sheet retreat patterns, Quaternary Science Reviews, 28, 2546–2547, doi:10.1016/j.quascirev.2009.02.025, 2009.

Carlson, A. E. and Clark, P. U.: Ice sheet sources of sea level rise and freshwater discharge during the last deglaciation, Reviews of Geophysics, 50, RG4007, doi:10.1029/2011RG000371, 2012.

Carlson, A. E., Clark, P. U., Haley, B. a., Klinkhammer, G. P., Simmons, K., Brook, E. J., and Meissner, K. J.: Geochemical proxies of North American freshwater routing during the Younger Dryas cold event., Proceedings of the National Academy of Sciences of the United States of America, 104, 6556–6561, doi:10.1073/pnas.0611313104, 2007a.

Carlson, A. E., Clark, P. U., Raisbeck, G. M., and Brook, E. J.: Rapid holocene deglaciation of the labrador sector of the Laurentide Ice Sheet, Journal of Climate, 20, 5126–5133, doi:10.1175/JCLI4273.1, 2007b.

Carlson, A. E., LeGrande, A. N., Oppo, D. W., Came, R. E., Schmidt, G. a., Anslow, F. S., Licciardi, J. M., and Obbink, E. a.: Rapid early Holocene deglaciation of the Laurentide ice sheet, Nature Geoscience, 1, 620–624, doi:10.1038/ngeo285, 2008.

Carlson, A. E., Clark, P. U., Haley, B. a., and Klinkhammer, G. P.: Routing of western Canadian Plains runoff during the 8.2 ka cold event, Geophysical Research Letters, 36, 1–5, doi:10.1029/2009GL038778, 2009.

Carriquiry, J. D. and Sánchez, A.: Sedimentation in the Colorado River delta and Upper Gulf of California after nearly a century of discharge loss, Marine Geology, 158, 125–145, doi:10.1016/S0025-3227(98)00189-3, 1999.

Carson, M. A., Jasper, J. N., and Conly, F. M.: Magnitude and sources of sediment input to the Mackenzie Delta, Northwest Territories, 1974–94, Arctic, 51, 116–124, 1998.

Chen, M., Xie, P., Janowiak, J. E., and Arkin, P. A.: Global Land Precipitation: A 50-yr Monthly Analysis Based on Gauge Observations, Journal of Hydrometeorology, 3, 249–266, doi:10.1175/1525-7541(2002)003<0249:GLPAYM>2.0.CO;2, 2002.

Clague, J. J. and James, T. S.: History and isostatic effects of the last ice sheet in southern British Columbia, Quaternary Science Reviews, 21, 71–87, doi:10.1016/S0277-3791(01)00070-1, 2002.

Clark, J., Mitrovica, J. X., and Alder, J.: Coastal paleogeography of the California–Oregon–Washington and Bering Sea continental shelves during the latest Pleistocene and Holocene: implications for the archaeological record, Journal of Archaeological Science, 52, 12–23, doi:10.1016/j.jas.2014.07.030, 2014.

Clark, P. U., Marshall, S. J., Clarke, G. K. C., Hostetler, S. W., Licciardi, J. M., and Teller, J. T.: Freshwater forcing of abrupt climate change during the last glaciation., Science (New York, N.Y.), 293, 283–7, doi:10.1126/science.1062517, 2001.

Clark, P. U., Dyke, A. S., Shakun, J. D., Carlson, A. E., Clark, J., Wohlfarth, B., Mitrovica, J. X., Hostetler, S. W., McCabe, A. M., Clark, P. U., Dyke, A. S., Shakun, J. D., Carlson, A. E., Clark, J., Wohlfarth, B., Mitrovica, J. X., Hostetler, S. W., and McCabe, A. M.: The Last Glacial Maximum., Science, 325, 710–714, doi:10.1126/science.1172873, 2009.

Cohen, M. J., Henges-Jeck, C., and Castillo-Moreno, G.: A preliminary water balance for the Colorado River delta, 1992–1998, Journal of Arid Environments, 49, 35–48, doi:10.1006/jare.2001.0834, 2001.

Cohen, S., Kettner, A. J., Syvitski, J. P. M., and Fekete, B. M.: WBMsed, a distributed global-scale riverine sediment flux model: Model description and validation, Computers and Geosciences, 53, 80–93, doi:10.1016/j.cageo.2011.08.011, 2013.

Collins, W. D., Bitz, C. M., Blackmon, M. L., Bonan, G. B., Bretherton, C. S., Carton, J. A., Chang, P., Doney, S. C., Hack, J. J., Henderson, T. B., Kiehl, J. T., Large, W. G., McKenna, D. S., Santer, B. D., and Smith, R. D.: The Community Climate System Model Version 3 (CCSM3), Journal of Climate, 19, 2122–2143, doi:10.1175/JCLI3761.1, 2006.

Condron, A. and Winsor, P.: Meltwater routing and the Younger Dryas, Proceedings of the National Academy of Sciences of the United States of America, 109, 19 928–19 933, doi:10.1073/pnas.1207381109, 2012.

Cook, K. L., Whipple, K. X., Heimsath, A. M., and Hanks, T. C.: Rapid incision of the Colorado River in Glen Canyon - insights from channel profiles, local incision rates, and modeling of lithologic controls, Earth Surface Processes and Landforms, 34, 994–1010, doi:10.1002/esp.1790, 2009.

Cornford, S. L., Martin, D. F., Graves, D. T., Ranken, D. F., Le Brocq, A. M., Gladstone, R. M., Payne, A. J., Ng, E. G., and Lipscomb, W. H.: Adaptive mesh, finite volume modeling of marine ice sheets, Journal of Computational Physics, 232, 529–549, doi:10.1016/j.jcp.2012.08.037, 2013.

Cuffey, K. M. and Paterson, W. S. B.: The physics of glaciers, Academic Press, Oxford, UK, 4th edn., 2010.

Currey, D. R., V, E. S. P. B., and City, S. L.: Quaternary palaeolakes in the evolution of semidesert basins, with special emphasis on Lake Bonneville and the Great Basin, U.S.A, Palaeogeography, Palaeoclimatology, Palaeoecology, 76, 189–214, doi:10.1016/0031-0182(90)90113-L, 1990.

1115 Curry, B. B.: Evidence at Lomax, Illinois, for Mid-Wisconsin (~40,000 yr B.P.) Position of the Des Moines Lobe and for Diversion of the Mississippi River by the Lake Michigan Lobe (20,350 yr B.P.), Quaternary Research, 50, 128–138, doi:10.1006/qres.1998.1985, 1998.

Curry, B. B., Hajic, E. R., Clark, J. A., Befus, K. M., Carrell, J. E., and Brown, S. E.: The Kankakee Torrent and other large meltwater flooding events during the last deglaciation, Illinois, USA, Quaternary Science
1120 Reviews, 90, 22–36, doi:10.1016/j.quascirev.2014.02.006, 2014.

de Vernal, A., Hillaire-Marcel, C., and Bilodeau, G.: Reduced meltwater outflow from the Laurentide ice margin during the Younger Dryas, Nature, 381, 774–777, doi:10.1038/381774a0, 1996.

Deschamps, P., Durand, N., Bard, E., Hamelin, B., Camoin, G., Thomas, A. L., Henderson, G. M., Okuno, J., and Yokoyama, Y.: Ice-sheet collapse and sea-level rise at the Bølling warming 14,600 years ago, Nature,
1125 483, 559–564, doi:10.1038/nature10902, 2012.

Dierckx, P.: Curve and surface fitting with splines, Curve and Surface Fitting with Splines, p. 308, doi:10.1093/imamat/1.2.164, 1993.

Dixon, J. E. and Monteleone, K.: Gateway to the Americas: Underwater Archeological Survey in Beringia and the North Pacific, in: Prehistoric Archaeology on the Continental Shelf, chap. 6, pp. 95–114, Springer New
1130 York, New York, NY, doi:10.1007/978-1-4614-9635-9_6, 2014.

Dolgopolova, E. N. and Isupova, M. V.: Water and sediment dynamics at Saint Lawrence River mouth, Water Resources, 38, 453–469, doi:10.1134/S009780781104004X, 2011.

Doyon, P.: Seasonal Structure of the Gulf of St. Lawrence Upper-Layer Thermohaline Fields during the Ice-free Months, Ms, McGill University, 1996.

1135 Duk-Rodkin, A., Hughes, O. L., Survey, G., and Calgary, S. N. W.: Tertiary-quaternary drainage of the Pre-glacial Mackenzie basin, Quaternary International, 22-23, 221–241, doi:10.1016/1040-6182(94)90015-9, 1994.

Dury, G. H.: Subsurface Exploration and Chronology of underfit streams, vol. General Th of *Professional Paper*, U.S. Geological Survey, Washington, D.C., 1964.

1140 Dutton, A. and Lambeck, K.: Ice Volume and Sea Level During the Last Interglacial, Science, 337, 216–219, doi:10.1126/science.1205749, 2012.

Dutton, A., Carlson, A. E., Long, A. J., Milne, G. A., Clark, P. U., DeConto, R., Horton, B. P., Rahmstorf, S., and Raymo, M. E.: Sea-level rise due to polar ice-sheet mass loss during past warm periods, 'Science, 349, aaa4019–aaa4019, doi:10.1126/science.aaa4019, 2015.

1145 Dyke, A. S.: An outline of North American deglaciation with emphasis on central and northern Canada, in: Quaternary Glaciations–Extent and Chronology — Part II: North America, edited by Ehlers, J. and Gibbard, P. L., vol. 2 of *Developments in Quaternary Sciences*, pp. 373–424, 2004.

Dyke, A. S. and Prest, V. K.: Late Wisconsinan and Holocene History of the Laurentide Ice Sheet, Géographie physique et Quaternaire, 41, 237, doi:10.7202/032681ar, 1987.

1150 Dyke, A. S., Moore, A., and Robertson, L.: Deglaciation of North America, Open File 1574, Natural Resources Canada, Ottawa, 2003.

Environment Canada: St. Lawrence River: http://www.ec.gc.ca/stl/, 2013.

Fairbanks, R. G.: A 17, 000-year glacio-eustatic sea level record: influence of glacial melting rates on the Younger Dryas event and deep-ocean circulation, Nature, 342, 637–642, 1989.

1155 Fan, Y., Li, H., and Miguez-Macho, G.: Global Patterns of Groundwater Table Depth, Science, 339, 940–943, doi:10.1126/science.1229881, 2013.

Ferguson, G. and Jasechko, S.: The isotopic composition of the Laurentide Ice Sheet and fossil groundwater, Geophysical Research Letters, 42, 1–6, doi:10.1002/2015GL064106.Received, 2015.

Fisher, T. G.: Chronology of glacial Lake Agassiz meltwater routed to the Gulf of Mexico, Quaternary Research,
1160 59, 271–276, 2003.

Fisher, T. G.: Abandonment chronology of glacial Lake Agassiz's Northwestern outlet, Palaeogeography, Palaeoclimatology, Palaeoecology, 246, 31–44, doi:10.1016/j.palaeo.2006.10.031, 2007.

Fisher, T. G. and Souch, C.: Northwest outlet channels of Lake Agassiz, isostatic tilting and a migrating continental drainage divide, Saskatchewan, Canada, Geomorphology, 25, 57–73, doi:10.1016/S0169-
1165 555X(98)00028-2, 1998.

Flower, B. P., Hastings, D. W., Hill, H. W., and Quinn, T. M.: Phasing of deglacial warming and Laurentide Ice Sheet meltwater in the Gulf of Mexico, Geology, 32, 597, doi:10.1130/G20604.1, 2004.

Galloway, W. E., Whiteaker, T. L., and Ganey-Curry, P.: History of Cenozoic North American drainage basin evolution, sediment yield, and accumulation in the Gulf of Mexico basin, Geosphere, 7, 938–973,
1170 doi:10.1130/GES00647.1, 2011.

Gasson, E., DeConto, R. M., Pollard, D., and Levy, R. H.: Dynamic Antarctic ice sheet during the early to mid-Miocene, Proceedings of the National Academy of Sciences, p. 201516130, doi:10.1073/pnas.1516130113, 2016.

Gates, L. D., Hagemann, S., and Golz, C.: Observed historical discharge data from major rivers for climate
1175 model validation, Tech. Rep. 307, Max-Planck-Institut für Meterologie, Hamburg, Germany, 2000.

Gibb, O. T., Hillaire-Marcel, C., and de Vernal, A.: Oceanographic regimes in the northwest Labrador Sea since Marine Isotope Stage 3 based on dinocyst and stable isotope proxy records, Quaternary Science Reviews, 92, 269–279, doi:10.1016/j.quascirev.2013.12.010, 2014.

Gil, I. M., Keigwin, L. D., and Abrantes, F.: The deglaciation over Laurentian Fan: History of diatoms, IRD,
1180 ice and fresh water, Quaternary Science Reviews, 129, 57–67, doi:10.1016/j.quascirev.2015.10.006, 2015.

Gilbert, G. K.: Lake Bonneville, U.S. Geological Survey Monograph, US Geological Survey, 1890.

Godsey, H. S., Currey, D. R., and Chan, M. a.: New evidence for an extended occupation of the Provo shoreline and implications for regional climate change, Pleistocene Lake Bonneville, Utah, USA, Quaternary Research, 63, 212–223, doi:10.1016/j.yqres.2005.01.002, 2005.

1185 Godsey, H. S., Oviatt, C. G., Miller, D. M., and Chan, M. a.: Stratigraphy and chronology of offshore to nearshore deposits associated with the Provo shoreline, Pleistocene Lake Bonneville, Utah, Palaeogeography, Palaeoclimatology, Palaeoecology, 310, 442–450, doi:10.1016/j.palaeo.2011.08.005, 2011.

Gomez, N., Gregoire, L. J., Mitrovica, J. X., and Payne, a. J.: Laurentide-Cordilleran Ice Sheet saddle collapse as a contribution to meltwater pulse 1A, Geophysical Research Letters, 42, 3954–3962,
1190 doi:10.1002/2015GL063960, 2015.

Gowan, E. J.: An assessment of the minimum timing of ice free conditions of the western Laurentide Ice Sheet, Quaternary Science Reviews, 75, 100–113, doi:10.1016/j.quascirev.2013.06.001, 2013.

Gowan, E. J., Tregoning, P., Purcell, A., Lea, J., Fransner, O. J., Noormets, R., and Dowdeswell, J. a.: ICESHEET 1.0: A program to produce paleo-ice sheet models with minimal assumptions, Geoscientific Model Development Discussions, pp. 1–18, doi:10.5194/gmd-2016-9, 2016a.

Gowan, E. J., Tregoning, P., Purcell, A., Montillet, J.-P., and McClusky, S.: A model of the western Laurentide Ice Sheet, using observations of glacial isostatic adjustment, Quaternary Science Reviews, 139, 1–16, doi:10.1016/j.quascirev.2016.03.003, 2016b.

GRASS Development Team: Geographic Resources Analysis Support System (GRASS GIS) Software, 2012.

Gregoire, L. J., Payne, A. J., and Valdes, P. J.: Deglacial rapid sea level rises caused by ice-sheet saddle collapses, Nature, 487, 219–222, doi:10.1038/nature11257, 2012.

Grimaldi, S., Nardi, F., Benedetto, F. D., Istanbulluoglu, E., and Bras, R. L.: A physically-based method for removing pits in digital elevation models, Advances in Water Resources, 30, 2151–2158, doi:10.1016/j.advwatres.2006.11.016, 2007.

Gross, M. G., Karweit, M., Cronin, W. B., Schubel, J. R., Gross, M. G., Karweit, M., Cronin, W. B., and Schubel, J. R.: Suspended sediment discharge of the Susquehanna River to northern Chesapeake Bay, 1966 to 1976, Estuaries, 1, 106–110, 1978.

Guido, Z. S., Ward, D. J., and Anderson, R. S.: Pacing the post–Last Glacial Maximum demise of the Animas Valley glacier and the San Juan Mountain ice cap, Colorado, Geology, 35, 739, doi:10.1130/G23596A.1, 2007.

Hager, B. H. and Richards, M. A.: Long-Wavelength Variations in Earth's Geoid: Physical Models and Dynamical Implications, Philosophical Transactions of the Royal Society A: Mathematical, Physical and Engineering Sciences, 328, 309–327, doi:10.1098/rsta.1989.0038, 1989.

Hansel, A. K. and Mickelson, D. M.: A reevaluation of the timing and causes of high lake phases in the Lake Michigan basin, Quaternary Research, 29, 113–128, doi:10.1016/0033-5894(88)90055-5, 1988.

Hanson, M. A., Lian, O. B., and Clague, J. J.: The sequence and timing of large late Pleistocene floods from glacial Lake Missoula, Quaternary Science Reviews, 31, 67–81, doi:10.1016/j.quascirev.2011.11.009, 2012.

Harmar, O. P. and Clifford, N. J.: Geomorphological explanation of the long profile of the Lower Mississippi River, Geomorphology, 84, 222–240, doi:10.1016/j.geomorph.2006.01.045, 2007.

Harris, I., Jones, P., Osborn, T., and Lister, D.: Updated high-resolution grids of monthly climatic observations - the CRU TS3.10 Dataset, International Journal of Climatology, 34, 623–642, doi:10.1002/joc.3711, 2014.

Hay, C., Mitrovica, J. X., Gomez, N., Creveling, J. R., Austermann, J., and Kopp, R. E.: The sea-level fingerprints of ice-sheet collapse during interglacial periods, Quaternary Science Reviews, 87, 60–69, doi:10.1016/j.quascirev.2013.12.022, 2014.

He, F.: Simulating Transiet Climate Evolution of the Last Deglaciation with CCSM3, Ph.d. dissertation, University of Wisconsin - Madison, 2011.

He, F., Shakun, J. D., Clark, P. U., Carlson, A. E., Liu, Z., Otto-Bliesner, B. L., and Kutzbach, J. E.: Northern Hemisphere forcing of Southern Hemisphere climate during the last deglaciation., Nature, 494, 81–85, doi:10.1038/nature11822, 2013.

1230    Hearty, P. J., Hollin, J. T., Neumann, a. C., O'Leary, M. J., and McCulloch, M.: Global sea-level fluctuations during the Last Interglaciation (MIS 5e), Quaternary Science Reviews, 26, 2090–2112, doi:10.1016/j.quascirev.2007.06.019, 2007.

Heinrich, H.: Origin and consequences of cyclic ice rafting in the Northeast Atlantic Ocean during the past 130,000 years, Quaternary Research, 29, 142–152, doi:10.1016/0033-5894(88)90057-9, 1988.

1235    Hemming, S. R.: Heinrich events: Massive late Pleistocene detritus layers of the North Atlantic and their global climate imprint, Reviews of Geophysics, 42, RG1005, doi:10.1029/2003RG000128, 2004.

Hillaire-Marcel, C., Maccali, J., Not, C., and Poirier, A.: Geochemical and isotopic tracers of Arctic sea ice sources and export with special attention to the Younger Dryas interval, Quaternary Science Reviews, 79, 184–190, doi:10.1016/j.quascirev.2013.05.001, 2013.

1240    Hladyniuk, R. and Longstaffe, F. J.: Oxygen-isotope variations in post-glacial Lake Ontario, Quaternary Science Reviews, 134, 39–50, doi:10.1016/j.quascirev.2016.01.002, 2016.

Hoffman, J. S., Carlson, A. E., Winsor, K., Klinkhammer, G. P., LeGrande, A. N., Andrews, J. T., and Strasser, J. C.: Linking the 8.2 ka event and its freshwater forcing in the Labrador Sea, Geophysical Research Letters, 39, doi:10.1029/2012GL053047, 2012.

1245    Holeman, J. N.: The Sediment Yield of Major Rivers of the World, Water Resources Research, 4, 737–747, doi:10.1029/WR004i004p00737, 1968.

Hooke, R. L. and Clausen, H. B.: Wisconsin and Holocene $\delta^{18}$O variations, Barnes Ice Cap, Canada, Geological Society of America Bulletin, 93, 784–789, doi:10.1130/0016-7606(1982)93<784:WAHOVB>2.0.CO;2, 1982.

1250    Huang, P.-c. and Lee, K. T.: An efficient method for DEM-based overland flow routing, Journal of Hydrology, 489, 238–245, doi:10.1016/j.jhydrol.2013.03.014, 2013.

Ivanović, R. F., Gregoire, L. J., Wickert, A. D., and Valdes, P. J.: How did the North American ice Saddle Collapse impact the climate 14,500 years ago?, in: AGU Fall Meeting Abstracts, American Geophysical Union, San Francisco, CA, USA, 2014.

1255    Ivanović, R. F., Gregoire, L. J., Kageyama, M., Roche, D. M., Valdes, P. J., Burke, A., Drummond, R., Peltier, W. R., and Tarasov, L.: Transient climate simulations of the deglaciation 21–9 thousand years before present; PMIP4 Core experiment design and boundary conditions, Geoscientific Model Development Discussions, 8, 9045–9102, doi:10.5194/gmdd-8-9045-2015, 2015.

Jennings, A., Andrews, J., Pearce, C., Wilson, L., and ??Lfasd??Tttir, S.: Detrital carbonate peaks on the
1260    Labrador shelf, a 13-7ka template for freshwater forcing from the Hudson Strait outlet of the Laurentide Ice Sheet into the subpolar gyre, Quaternary Science Reviews, 107, 62–80, doi:10.1016/j.quascirev.2014.10.022, 2015.

John, S., Branch, J. S., Branch, B. C. G. S., Resources, P., Columbia, B., Catto, N., Liverman, D. G. E., Bobrowsky, P. T., Rutter, N., John, S., Branch, J. S., Branch, B. C. G. S., Resources, P., Columbia, B., Catto, N.,
1265    Liverman, D. G. E., Bobrowsky, P. T., Rutter, N., John, S., Branch, J. S., Branch, B. C. G. S., Resources, P., Columbia, B., Catto, N., Liverman, D. G. E., Bobrowsky, P. T., Rutter, N., John, S., Branch, J. S., Branch, B. C. G. S., Resources, P., Columbia, B., Catto, N., Liverman, D. G. E., Bobrowsky, P. T., and Rutter, N.: Laurentide, cordilleran, and montane glaciation in the western Peace River — Grande Prairie region, Alberta and British Columbia, Canada, Quaternary International, 32, 21–32, doi:10.1016/1040-6182(95)00061-5, 1996.

1270    Kammerer, J. C.: Largest Rivers in the United States, Open-File Report, United States Geological Survey, Reston, Virginia, USA., 1990.

Kaufman, D. S. and Miller, G. H.: Abrupt early Holocene (9.9-9.6 ka) ice-stream advance at the mouth of Hudson Strait, Arctic Canada, Geology, 21, 1063–1066, doi:10.1130/0091-7613(1993)021<1063:AEHKIS>2.3.CO;2, 1993.

1275    Kehew, A. E., Teller, J. T., Tellert, J. T., and Teller, J. T.: History of late glacial runoff along the south-western margin of the Laurentide Ice Sheet, Quaternary Science Reviews, 13, 859–877, doi:10.1016/0277-3791(94)90006-X, 1994.

Keigwin, L. D., Donnelly, J. P., Cook, M. S., Driscoll, N. W., and Brigham-Grette, J.: Rapid sea-level rise and Holocene climate in the Chukchi Sea, Geology, 34, 861, doi:10.1130/G22712.1, 2006.

1280    Kendall, R. A., Mitrovica, J. X., and Milne, G. A.: On post-glacial sea level–II. Numerical formulation and comparative results on spherically symmetric models, Geophysical Journal International, 161, 679–706, doi:10.1111/j.1365-246X.2005.02553.x, 2005.

Kettner, A. J. and Syvitski, J. P. M.: HydroTrend v. 3.0: A climate-driven hydrological transport model that simulates discharge and sediment load leaving a river system, Computers & Geosciences, 34, 1170–1183, 1285    2008.

Khider, D., Huerta, G., Jackson, C., Stott, L. D., and Emile-Geay, J.: A Bayesian, multivariate cal-ibration for G lobigerinoides ruber Mg/Ca, Geochemistry, Geophysics, Geosystems, 16, 2916–2932, doi:10.1002/2015GC005844, 2015.

Kirby, J. F. and Swain, C. J.: A reassessment of spectral T_e estimation in continental interiors: The case of 1290    North America, Journal of Geophysical Research, 114, B08 401, doi:10.1029/2009JB006356, 2009.

Knox, J. C.: The Mississippi River System, in: Large rivers: geomorphology and management, edited by Gupta, A., pp. 145–182, Wiley, 2007.

Kujau, A., Nürnberg, D., Zielhofer, C., Bahr, A., and Röhl, U.: Mississippi River discharge over the last ˜560,000years — Indications from X-ray fluorescence core-scanning, Palaeogeography, Palaeoclimatology, 1295    Palaeoecology, 298, 311–318, doi:10.1016/j.palaeo.2010.10.005, 2010.

Kutzbach, J. E. and Wright, H. E.: Simulation of the climate of 18,000 years BP: Results for the North Ameri-can/North Atlantic/European sector and comparison with the geologic record of North America, Quaternary Science Reviews, 4, 147–187, doi:10.1016/0277-3791(85)90024-1, 1985.

Lambeck, K., Yokoyama, Y., and Purcell, T.: Into and out of the Last Glacial Maximum: sea-level change during 1300    Oxygen Isotope Stages 3 and 2, Quaternary Science Reviews, 21, 343–360, 2002.

Lambeck, K., Rouby, H., Purcell, A., Sun, Y., and Sambridge, M.: Sea level and global ice volumes from the Last Glacial Maximum to the Holocene, Proceedings of the National Academy of Sciences, doi:10.1073/pnas.1411762111, 2014.

Lavoie, C., Allard, M., and Duhamel, D.: Deglaciation landforms and C-14 chronology of the Lac Guillaume-1305    Delisle area, eastern Hudson Bay: A report on field evidence, Geomorphology, 159-160, 142–155, doi:10.1016/j.geomorph.2012.03.015, 2012.

Le Morzadec, K., Tarasov, L., Morlighem, M., and Seroussi, H.: A new sub-grid surface mass balance and flux model for continental-scale ice sheet modelling: Testing and last glacial cycle, Geoscientific Model Development, 8, 3199–3213, doi:10.5194/gmd-8-3199-2015, 2015.

1310    Lehner, B., Verdin, K., and Jarvis, A.: HydroSHEDS Technical Documentation Version 1.2, vol. 89, 2013.

Lemieux, J.-M., Sudicky, E. a., Peltier, W. R., and Tarasov, L.: Dynamics of groundwater recharge and seepage over the Canadian landscape during the Wisconsinian glaciation, Journal of Geophysical Research, 113, 1–18, doi:10.1029/2007JF000838, 2008.

Lemmen, D. S. D. D. S., Duk-Rodkin, A., and Bednarski, J. M. A. N. M.: Late glacial drainage systems along

1315    the northwestern margin of the Laurentide Ice Sheet, Quaternary Science Reviews, 13, 805–828, 1994.

Leopold, L. B. and Maddock, T.: The hydraulic geometry of stream channels and some physiographic implications, Professional Paper, United States Geological Survey, Washington, D.C., 1953.

Levac, E., Lewis, M., Stretch, V., Duchesne, K., and Neulieb, T.: Evidence for meltwater drainage via the St. Lawrence River Valley in marine cores from the Laurentian Channel at the time of the Younger Dryas, Global

1320    and Planetary Change, 130, 47–65, doi:10.1016/j.gloplacha.2015.04.002, 2015.

Lewis, C. F. M. and Teller, J. T.: Glacial runoff from North America and its possible impact on oceans and climate, in: Glacier Science and Environmental Change, chap. Chapter Tw, pp. 138–150, Blackwell Publishing, Malden, MA, USA, doi:10.1002/9780470750636.ch28, 2006.

Leydet, D. J.: Eastward Routing of Glacial Lake Agassiz Runoff caused the Younger Dryas Cold Event Abstract,

1325    M.s., Oregon State University, 2016.

Licciardi, J. M., Teller, J. T., and Clark, P. U.: Freshwater routing by the Laurentide Ice Sheet during the last deglaciation, in: Mechanisms of global climate change at millennial time scales, edited by Clark, U., Webb, S., and Keigwin, D., vol. 112 of *Geophysical Monograph*, pp. 177–201, American Geophysical Union, doi:10.1029/gm112p0177, 1999.

1330    Liu, J., Curry, J. a., Wang, H., Song, M., and Horton, R. M.: Correction for " Impact of declining Arctic sea ice on win- ter snowfall, " by Jiping Liu, Judith A. Curry, Huijun Wang, Mirong Song, and Radley M. Horton, which appeared in issue 11, March 13, 2012, of Proc Natl Acad Sci USA, Proceedings of the National Academy of Sciences, 109, 4074–9, doi:10.1073/pnas.1114910109, 2012.

Liu, J., Milne, G. A., Kopp, R. E., Clark, P. U., and Shennan, I.: Sea-level constraints on the amplitude and

1335    source distribution of Meltwater Pulse 1A, Nature Geoscience, pp. 6–12, doi:10.1038/ngeo2616, 2015.

Liu, Z., Otto-Bliesner, B. L., He, F., Brady, E. C., Tomas, R., Clark, P. U., Carlson, A. E., Lynch-Stieglitz, J., Curry, W., Brook, E., Erickson, D., Jacob, R., Kutzbach, J., and Cheng, J.: Transient simulation of last deglaciation with a new mechanism for Bolling-Allerod warming., Science (New York, N.Y.), 325, 310–314, doi:10.1126/science.1171041, 2009.

1340    Livingstone, S. J., Storrar, R. D., Hillier, J. K., Stokes, C. R., Clark, C. D., and Tarasov, L.: An ice-sheet scale comparison of eskers with modelled subglacial drainage routes, Geomorphology, 246, 104–112, doi:10.1016/j.geomorph.2015.06.016, 2015.

Lopes, C. and Mix, a. C.: Pleistocene megafloods in the Northeast Pacific, Geology, 37, 79–82, doi:10.1130/G25025A.1, 2009.

1345    Lowell, T. V., Larson, G. J., Hughes, J. D., and Denton, G. H.: Age verification of the Lake Gribben forest bed and the Younger Dryas Advance of the Laurentide Ice Sheet, Canadian Journal of Earth Sciences, 36, 383–393, doi:10.1139/e98-095, 1999.

Lowell, T. V., Applegate, P. J., Fisher, T. G., and Lepper, K.: What caused the low-water phase of glacial Lake Agassiz?, Quaternary Research, 80, 370–382, doi:10.1016/j.yqres.2013.06.002, 2013.

1350    MacAyeal, D. R.: Binge/purge oscillations of the Laurentide Ice Sheet as a cause of the North Atlantic's Heinrich events, Paleoceanography, 8, 775, doi:10.1029/93PA02200, 1993.

Maccali, J., Hillaire-Marcel, C., Carignan, J., and Reisberg, L. C.: Geochemical signatures of sediments documenting Arctic sea-ice and water mass export through Fram Strait since the Last Glacial Maximum, Quaternary Science Reviews, 64, 136–151, doi:10.1016/j.quascirev.2012.10.029, 2013.

1355    Mackay, J. R. and Mathews, W. H.: Geomorphology and Quaternary History of the Mackenzie River Valley near Fort Good Hope, N.W.T., Canada, Canadian Journal of Earth Sciences, 10, 26–41, doi:10.1139/e73-003, 1973.

Margold, M., Stokes, C. R., Clark, C. D., and Kleman, J.: Ice streams in the Laurentide Ice Sheet : a new mapping inventory, Journal of Maps, 16, 9669, doi:10.1080/17445647.2014.912036, 2014.

1360    Margold, M., Stokes, C. R., and Clark, C. D.: Ice streams in the Laurentide Ice Sheet: Identification, characteristics and comparison to modern ice sheets, Earth-Science Reviews, 143, 117–146, doi:10.1016/j.earscirev.2015.01.011, 2015.

Marshall, S. J. and Clarke, G. K. C.: Modeling North American freshwater runoff through the last glacial cycle, Quaternary Research, 52, 300–315, 1999.

1365    Matsubara, Y. and Howard, A. D.: A spatially explicit model of runoff, evaporation, and lake extent: Application to modern and late Pleistocene lakes in the Great Basin region, western United States, Water Resources Research, 45, W06425, doi:10.1029/2007WR005953, 2009.

McGee, D., Quade, J., Edwards, R. L., Broecker, W. S., Cheng, H., Reiners, P. W., and Evenson, N.: Lacustrine cave carbonates: Novel archives of paleohydrologic change in the Bonneville Basin (Utah, USA), Earth and
1370    Planetary Science Letters, 351-352, 182–194, doi:10.1016/j.epsl.2012.07.019, 2012.

Meissner, K. J. and Clark, P. U.: Impact of floods versus routing events on the thermohaline circulation, Geophysical Research Letters, 33, L15704, doi:10.1029/2006GL026705, 2006.

Metz, J. M., Dowdeswell, J., and Woodworth-Lynas, C. M. T.: Sea-floor scour at the mouth of Hudson Strait by deep-keeled icebergs from the Laurentide Ice Sheet, Marine Geology, 253, 149–159,
1375    doi:10.1016/j.margeo.2008.05.004, 2008.

Metz, M., Mitasova, H., and Harmon, R. S.: Efficient extraction of drainage networks from massive, radar-based elevation models with least cost path search, Hydrology and Earth System Sciences, 15, 667–678, doi:10.5194/hess-15-667-2011, 2011.

Milliman, J. and Farnsworth, K.: River discharge to the coastal ocean: a global synthesis, Cambridge University
1380    Press, 2013.

Milliman, J. D. and Meade, R. H.: World-wide delivery of river sediment to the oceans, The Journal of Geology, 91, 1–21, 1983.

Mitrovica, J. X.: Haskell [1935] revisited, Journal of Geophysical Research, 101, 555–569, doi:10.1029/95JB03208, 1996.

1385    Mitrovica, J. X. and Forte, A. M.: A new inference of mantle viscosity based upon joint inversion of convection and glacial isostatic adjustment data, Earth and Planetary Science Letters, 225, 177–189, 2004.

Mitrovica, J. X. and Milne, G. A.: On post-glacial sea level: I. General theory, Geophysical Journal International, 154, 253–267, doi:10.1046/j.1365-246X.2003.01942.x, 2003.

Monteleone, K., Dixon, E. J., and Wickert, A. D.: Lost Worlds: A predictive model to locate submerged ar-
1390  chaeological sites in SE Alaska, USA, in: Archaeology in the Digital Era: Papers from the 40th Annual Con-
ference of Computer Applications and Quantitative Methods in Archaeology (CAA), Southampton, 26-29
March 2012, edited by Earl, G., Sly, T., Chrysanthi, A., Murrieta-Flores, P., Papadopoulos, C., Romanowska,
I., and Wheatley, D., pp. 1–12, Amsterdam University Press, Southampton, UK, 2013.

Monteleone, K. R.: Lost worlds: Locating submerged archaeological sites in Southeast Alaska, Ph.d. disserta-
1395  tion, The University of New Mexico, 2013.

Montero-Serrano, J. C., Bout-Roumazeilles, V., Tribovillard, N., Sionneau, T., Riboulleau, A., Bory, A., and
Flower, B.: Sedimentary evidence of deglacial megafloods in the northern Gulf of Mexico (Pigmy Basin),
Quaternary Science Reviews, 28, 3333–3347, doi:10.1016/j.quascirev.2009.09.011, 2009.

Moore, T. C., Walker, J. C. G., Rea, D. K., Lewis, C. F. M., Shane, L. C. K., and Smith, A. J.: Younger Dryas In-
1400  terval and outflow from the Laurentide Ice Sheet, Paleoceanography, 15, 4–18, doi:10.1029/1999PA000437,
2000.

Mu, Q., Heinsch, F. A., Zhao, M., and Running, S. W.: Development of a global evapotranspiration algo-
rithm based on MODIS and global meteorology data, Remote Sensing of Environment, 111, 519–536,
doi:10.1016/j.rse.2007.04.015, 2007.

1405  Mu, Q., Zhao, M., and Running, S. W.: Improvements to a MODIS global terrestrial evapotranspiration algo-
rithm, Remote Sensing of Environment, 115, 1781–1800, doi:10.1016/j.rse.2011.02.019, 2011.

Murton, J. B., Bateman, M. D., Dallimore, S. R., Teller, J. T., and Yang, Z.: Identification of Younger Dryas
outburst flood path from Lake Agassiz to the Arctic Ocean., Nature, 464, 740–743, doi:10.1038/nature08954,
2010.

1410  Neteler, M., Bowman, M. H., Landa, M., and Metz, M.: GRASS GIS: A multi-purpose open source GIS,
Environmental Modelling & Software, 31, 124–130, doi:10.1016/j.envsoft.2011.11.014, 2012.

Nordman, M., Milne, G., and Tarasov, L.: Reappraisal of the Ångerman River decay time estimate and its
application to determine uncertainty in Earth viscosity structure, Geophysical Journal International, 201,
811–822, doi:10.1093/gji/ggv051, 2015.

1415  Nowak, K. C.: Stochastic streamflow simulation at interdecadal time scales and implications to water resources
management in the Colorado River Basin, Ph.d. thesis, University of Colorado, 2011.

Obbink, E. A., Carlson, A. E., and Klinkhammer, G. P.: Eastern North American freshwater discharge during
the Bolling-Allerod warm periods, Geology, 38, 171–174, doi:10.1130/G30389.1, 2010.

Occhietti, S., Govare, E., Klassen, R., Parent, M., and Vincent, J.-S.: Late Wisconsinan–Early Holocene
1420  deglaciation of Québec-Labrador, in: Quaternary Glaciations – Extent and Chronology — Part II: North
America, edited by Ehlers, J. and Gibbard, P. L., Developments in Quaternary Sciences, pp. 243–273, 2004.

Ó Cofaigh, C., Evans, D. J. A., and Smith, I. R.: Large-scale reorganization and sedimentation of terrestrial ice
streams during late Wisconsinan Laurentide Ice Sheet deglaciation, Geological Society of America Bulletin,
122, 743–756, doi:10.1130/B26476.1, 2010.

1425  Orme, A. R.: Pleistocene pluvial lakes of the American West: a short history of research, Geological Society,
London, Special Publications, 301, 51–78, doi:10.1144/SP301.4, 2008.

Overeem, I., Syvitski, J. P. M., Hutton, E. W. H., and Kettner, A. J.: Stratigraphic variability due to uncertainty in model boundary conditions: A case-study of the New Jersey Shelf over the last 40,000 years, Marine Geology, 224, 23–41, doi:10.1016/j.margeo.2005.06.044, 2005.

1430    Owen, L. A., Finkel, R. C., Minnich, R. A., and Perez, A. E.: Extreme southwestern margin of late Quaternary glaciation in North America: Timing and controls, Geology, 31, 729, doi:10.1130/G19561.1, 2003.

Patterson, C. J.: Southern Laurentide ice lobes were created by ice streams: Des Moines Lobe in Minnesota, USA, Sedimentary Geology, 111, 249–261, doi:10.1016/S0037-0738(97)00018-3, 1997.

Patterson, C. J.: Laurentide glacial landscapes: The role of ice streams, Geology, 26, 643, doi:10.1130/0091-
1435    7613(1998)026<0643:LGLTRO>2.3.CO;2, 1998.

Pearce, C.: The timing of the Gold Cove glacial event: A comment on "Signature of the Gold Cove event (10.2ka) in the Labrador Sea", Quaternary International, 377, 157–159, doi:10.1016/j.quaint.2015.02.067, 2015.

Pearce, C., Andrews, J. T., Bouloubassi, I., Hillaire-Marcel, C., Jennings, A. E., Olsen, J., Kuijpers, A., and
1440    Seidenkrantz, M.-S. S.: Heinrich 0 on the east Canadian margin: Source, distribution, and timing, Paleoceanography, 30, 1613–1624, doi:10.1002/2015PA002884, 2015.

Pederson, J. L., Cragun, W. S., Hidy, A. J., Rittenour, T. M., and Gosse, J. C.: Colorado River chronostratigraphy at Lee's Ferry, Arizona, and the Colorado Plateau bull's-eye of incision, Geology, 41, 427–430, doi:10.1130/G34051.1, 2013.

1445    Pelletier, J. D.: A spatially distributed model for the long-term suspended sediment discharge and delivery ratio of drainage basins, Journal of Geophysical Research, 117, F02 028, doi:10.1029/2011JF002129, 2012.

Peltier, W. R., Argus, D. F., and Drummond, R.: Space geodesy constrains ice age terminal deglaciation: The global ICE-6G\_C (VM5a)model, Journal of Geophysical Research: Solid Earth, 120, 450–487, doi:10.1002/2014JB011176, 2015.

1450    Peltier, W. R. R.: Global Glacial Isostasy and the Surface of the Ice-Age Earth: The ICE-5G (VM2) Model and GRACE, Annual Review of Earth and Planetary Sciences, 32, 111–149, doi:10.1146/annurev.earth.32.082503.144359, 2004.

Polyak, V. J., Rasmussen, J. B. T., and Asmerom, Y.: Prolonged wet period in the southwestern United States through the Younger Dryas, Geology, 32, 5, doi:10.1130/G19957.1, 2004.

1455    Prairie, J. and Callejo, R.: Natural Flow And Salt Computation Methods: Calendar Years 1971-1995, December, U.S. Department of the Interior, Bureau of Reclamation, Salt Lake City, UT, and Boulder City, NV, 2005.

Prince, P. S. and Spotila, J. A.: Evidence of transient topographic disequilibrium in a landward passive margin river system: knickpoints and paleo-landscapes of the New River basin, southern Appalachians, Earth Surface Processes and Landforms, 38, 1685–1699, doi:10.1002/esp.3406, 2013.

1460    Qin, C.-z. and Zhan, L.: Parallelizing flow-accumulation calculations on graphics processing units—From iterative DEM preprocessing algorithm to recursive multiple-flow-direction algorithm, Computers & Geosciences, 43, 7–16, doi:10.1016/j.cageo.2012.02.022, 2012.

Rashid, H., Piper, D. J. W., Mansfield, C., Saint-Ange, F., and Polyak, L.: Signature of the Gold Cove event (10.2ka) in the Labrador Sea, Quaternary International, 352, 212–221, doi:10.1016/j.quaint.2014.06.063,
1465    2014.

Rayburn, J. A., K. Knuepfer, P. L., and Franzi, D. A.: A series of large, Late Wisconsinan meltwater floods through the Champlain and Hudson Valleys, New York State, USA, Quaternary Science Reviews, 24, 2410–2419, doi:10.1016/j.quascirev.2005.02.010, 2005.

Rayburn, J. A., Franzi, D. A., and Knuepfer, P. L. K.: Evidence from the Lake Champlain Valley for a later onset of the Champlain Sea and implications for late glacial meltwater routing to the North Atlantic, Palaeogeography, Palaeoclimatology, Palaeoecology, 246, 62–74, doi:10.1016/j.palaeo.2006.10.027, 2007.

Rayburn, J. A., Cronin, T. M., Franzi, D. A., Knuepfer, P. L. K., and Willard, D. A.: Timing and duration of North American glacial lake discharges and the Younger Dryas climate reversal, Quaternary Research, 75, 541–551, doi:10.1016/j.yqres.2011.02.004, 2011.

Reimer, P. J., Bard, E., Bayliss, A., Beck, J. W., Blackwell, P. G., Ramsey, C. B., Grootes, P. M., Guilderson, T. P., Haflidason, H., Hajdas, I., Hatté, C., Heaton, T. J., Hoffmann, D. L., Hogg, A. G., Hughen, K. A., Kaiser, K. F., Kromer, B., Manning, S. W., Niu, M., Reimer, R. W., Richards, D. A., Scott, E. M., Southon, J. R., Staff, R. A., Turney, C. S. M., van der Plicht, J., and van der Plicht, J.: IntCal13 and Marine13 Radiocarbon Age Calibration Curves 0–50,000 Years cal BP, Radiocarbon, 55, 1869–1887, doi:10.2458/azu_js_rc.55.16947, 2013.

Remenda, V. H., Cherry, J. A., and Edwards, T. W. D.: Isotopic Composition of Old Ground Water from Lake Agassiz: Implications for Late Pleistocene Climate, Science (New York, N.Y.), 266, 1975–8, doi:10.1126/science.266.5193.1975, 1994.

Reneau, S. L. and Dethier, D. P.: Late Pleistocene landslide-dammed lakes along the Rio Grande, White Rock Canyon, New Mexico, Geological Society of America Bulletin, 108, 1492–1507, doi:10.1130/0016-7606(1996)108<1492:LPLDLA>2.3.CO;2, 1996.

Reusser, L., Bierman, P., Pavich, M., Larsen, J., and Finkel, R.: An episode of rapid bedrock channel incision during the last glacial cycle, measured with 10Be, American Journal of Science, 306, 69–102, doi:10.2475/ajs.306.2.69, 2006.

Richard, P. J. H., Occhietti, S., T, P. J. H. R., Occhietti, S., Richard, P. J. H., and Occhietti, S.: 14C chronology for ice retreat and inception of Champlain Sea in the St. Lawrence Lowlands, Canada, Quaternary Research, 63, 353–358, doi:10.1016/j.yqres.2005.02.003, 2005.

Ridge, J. C.: Shed Brook Discontinuity and Little Falls Gravel: Evidence for the Erie interstade in central New York, Geological Society of America Bulletin, 109, 652–665, doi:10.1130/0016-7606(1997)109<0652:SBDALF>2.3.CO;2, 1997.

Ridge, J. C., Franzi, D. A., and Muller, E. H.: Late Wisconsinan, pre-Valley Heads glaciation in the western Mohawk Valley, central New York, and its regional implications, Geological Society of America Bulletin, 103, 1032–1048, doi:10.1130/0016-7606(1991)103<1032:LWPVHG>2.3.CO;2, 1991.

Rittenour, T. M., Goble, R. J., and Blum, M. D.: An optical age chronology of Late Pleistocene fluvial deposits in the northern lower Mississippi valley, Quaternary science reviews, 22, 1105–1110, 2003.

Rittenour, T. M., Goble, R. J., and Blum, M. D.: Development of an OSL chronology for Late Pleistocene channel belts in the lower Mississippi valley, USA, Quaternary Science Reviews, 24, 2539–2554, doi:10.1016/j.quascirev.2005.03.011, 2005.

Rittenour, T. M., Blum, M. D., and Goble, R. J.: Fluvial evolution of the lower Mississippi River valley during the last 100 ky glacial cycle: Response to glaciation and sea-level change, Bulletin of the Geological Society of America, 119, 586, 2007.

Roberts, G. G., White, N. J., Martin-Brandis, G. L., and Crosby, A. G.: An uplift history of the Colorado Plateau and its surroundings from inverse modeling of longitudinal river profiles, Tectonics, 31, 1–2, doi:10.1029/2012TC003107, 2012.

Rohling, E. J., Grant, K., Hemleben, C. H., Siddall, M., Hoogakker, B. A. A., Bolshaw, M., and Kucera, M.: High rates of sea-level rise during the last interglacial period, Nature Geoscience, 1, 38–42, doi:10.1038/ngeo.2007.28, 2007.

Ross, M., Campbell, J. E., Parent, M., and Adams, R. S.: Palaeo-ice streams and the subglacial landscape mosaic of the North American mid-continental prairies, Boreas, 38, 421–439, doi:10.1111/j.1502-3885.2009.00082.x, 2009.

Roy, M., Dell'Oste, F., Veillette, J. J., de Vernal, a., Hélie, J.-F., and Parent, M.: Insights on the events surrounding the final drainage of Lake Ojibway based on James Bay stratigraphic sequences, Quaternary Science Reviews, 30, 682–692, doi:10.1016/j.quascirev.2010.12.008, 2011.

Rutt, I. C., Hagdorn, M., Hulton, N. R. J., and Payne, a. J.: The Glimmer community ice sheet model, Journal of Geophysical Research, 114, F02 004, doi:10.1029/2008JF001015, 2009.

Schmidt, J. C., Schmidt, B. J. C., and Schmidt, J. C.: A Watershed Perspective of Changes in Streamflow , Sediment Supply , and Geomorphology of the Colorado River, in: Proceedings of the Colorado River Basin Science and Resource Management Symposium, November 18–20, 2008, Scottsdale, Arizona, edited by Melis, T. S., Hamill, J. F., Bennett, G. E., Lewis G. Coggins, J., Grams, P. E., Kennedy, T. A., Kubly, D. M., and Ralston, B. E., vol. 2009 of *USGS Scientific Investigations Report*, pp. 51–76, United States Geological Survey, Scottsdale, Arizona, USA, 2010.

Schneider-Vieira, F., Baker, R., and Lawrence, M.: The Estuaries of Hudson Bay: A Case Study of the Physical and Biological Characteristics of Selected Sites, North/South Consultants Inc., Winnipeg, Manitoba, Canada, 1994.

Schwanghart, W. and Scherler, D.: Short Communication: TopoToolbox 2 – MATLAB-based software for topographic analysis and modeling in Earth surface sciences, Earth Surface Dynamics, 2, 1–7, doi:10.5194/esurf-2-1-2014, 2014.

Sionneau, T., Bout-Roumazeilles, V., Biscaye, P. E., Van Vliet-Lanoe, B., and Bory, A.: Clay mineral distributions in and around the Mississippi River watershed and Northern Gulf of Mexico: sources and transport patterns, Quaternary Science Reviews, 27, 1740–1751, doi:10.1016/j.quascirev.2008.07.001, 2008.

Sionneau, T., Bout-Roumazeilles, V., Flower, B. P., Bory, A., Tribovillard, N., Kissel, C., Van Vliet-Lanoë, B., and Montero Serrano, J. C.: Provenance of freshwater pulses in the Gulf of Mexico during the last deglaciation, Quaternary Research, 74, 235–245, doi:10.1016/j.yqres.2010.07.002, 2010.

Smith, D. G.: Glacial lake McConnell: Paleogeography, age, duration, and associated river deltas, mackenzie river basin, western Canada, Quaternary Science Reviews, 13, 829–843, doi:10.1016/0277-3791(94)90004-3, 1994.

Smith, R. S., Gregory, J. M., and Osprey, a.: A description of the FAMOUS (version XDBUA) climate model and control run, Geoscientific Model Development, 1, 53–68, doi:10.5194/gmd-1-53-2008, 2008.

Spero, H. J., Eggins, S. M., Russell, A. D., Vetter, L., Kilburn, M. R., and H??nisch, B.: Timing and mechanism for intratest Mg/Ca variability in a living planktic foraminifer, Earth and Planetary Science Letters, 409, 32–42, doi:10.1016/j.epsl.2014.10.030, 2015.

Stokes, C. R., Clark, C. D., and Storrar, R.: Major changes in ice stream dynamics during deglaciation of the north-western margin of the Laurentide Ice Sheet, Quaternary Science Reviews, 28, 721–738, doi:10.1016/j.quascirev.2008.07.019, 2009.

Storrar, R. D., Stokes, C. R., and Evans, D. J.: A map of large Canadian eskers from Landsat satellite imagery, Journal of Maps, 9, 456–473, doi:10.1080/17445647.2013.815591, 2013.

Stroup, J. S., Lowell, T. V., and Breckenridge, A.: A model for the demise of large, glacial Lake Ojibway, Ontario and Quebec, Journal of Paleolimnology, 50, 105–121, doi:10.1007/s10933-013-9707-9, 2013.

Svensson, A., Andersen, K. K., Bigler, M., Clausen, H. B., Dahl-Jensen, D., Davies, S. M., Johnsen, S. J., Muscheler, R., Parrenin, F., Rasmussen, S. O., Röthlisberger, R., Seierstad, I., Steffensen, J. P., and Vinther, B. M.: A 60 000 year Greenland stratigraphic ice core chronology, Climate of the Past, 4, 47–57, doi:10.5194/cp-4-47-2008, 2008.

Syvitski, J. P. M., Peckham, S. D., Hilberman, R., and Mulder, T.: Predicting the terrestrial flux of sediment to the global ocean: a planetary perspective, Sedimentary Geology, 162, 5–24, doi:10.1016/S0037-0738(03)00232-X, 2003.

Tarasov, L. and Peltier, W. R.: Arctic freshwater forcing of the Younger Dryas cold reversal., Nature, 435, 662–665, doi:10.1038/nature03617, 2005.

Tarasov, L., Peltier, W. R. R., Ã, L. T., Peltier, W. R. R., Tarasov, L., and Peltier, W. R. R.: A calibrated deglacial drainage chronology for the North American continent: evidence of an Arctic trigger for the Younger Dryas, Quaternary Science Reviews, 25, 659–688, doi:10.1016/j.quascirev.2005.12.006, 2006.

Tarasov, L., Dyke, A. S., Neal, R. M., and Peltier, W. R.: A data-calibrated distribution of deglacial chronologies for the North American ice complex from glaciological modeling, Earth and Planetary Science Letters, 315-316, 30–40, doi:10.1016/j.epsl.2011.09.010, 2012.

Taylor, M., Hendy, I., and Pak, D.: Deglacial ocean warming and marine margin retreat of the Cordilleran Ice Sheet in the North Pacific Ocean, Earth and Planetary Science Letters, 403, 89–98, doi:10.1016/j.epsl.2014.06.026, 2014.

Teller, J. T.: Preglacial (Teays) and Early Glacial Drainage in the Cincinnati Area, Ohio, Kentucky, and Indiana, Geological Society of America Bulletin, 84, 3677, doi:10.1130/0016-7606(1973)84<3677:PTAEGD>2.0.CO;2, 1973.

Teller, J. T.: Meltwater and precipitation runoff to the North Atlantic, Arctic, and Gulf of Mexico from the Laurentide Ice Sheet and adjacent regions during the Younger Dryas, Paleoceanography, 5, 897–905, doi:10.1029/PA005i006p00897, 1990a.

Teller, J. T.: Lake Agassiz during the Younger Dryas, Quaternary Research, 80, 361–369, doi:10.1016/j.yqres.2013.06.011, 2013.

Teller, J. T. and Leverington, D. W.: Glacial Lake Agassiz: A 5000 yr history of change and its relationship to the $\delta 18O$ record of Greenland, Geological Society of America Bulletin, 116, 729, doi:10.1130/B25316.1, 2004.

Teller, J. T., Leverington, D. W., and Mann, J. D.: Freshwater outbursts to the oceans from glacial Lake Agassiz and their role in climate change during the last deglaciation, Quaternary Science Reviews, 21, 879–887, doi:10.1016/S0277-3791(01)00145-7, 2002.

Teller, J. T. J. T.: Volume and routing of late-glacial runoff from the southern Laurentide Ice Sheet, Quaternary Research, 34, 12–23, doi:10.1016/0033-5894(90)90069-W, 1990b.

Tesauro, M., Kaban, M. K., and Cloetingh, S. A. P. L.: Global strength and elastic thickness of the lithosphere, Global and Planetary Change, 90-91, 51–57, doi:10.1016/j.gloplacha.2011.12.003, 2012.

Tight, W. G.: Drainage modifications in southeastern Ohio and adjacent parts of West Virginia and Kentucky, US Geological Survey Professional Paper, US Geological Survey, Reston, Virginia, USA., 1903.

Tripsanas, E. K., Bryant, W. R., Slowey, N. C., Bouma, A. H., Karageorgis, A. P., and Berti, D.: Sedimentological history of Bryant Canyon area, northwest Gulf of Mexico, during the last 135 kyr (Marine Isotope Stages 1–6): A proxy record of Mississippi River discharge, Palaeogeography, Palaeoclimatology, Palaeoecology, 246, 137–161, doi:10.1016/j.palaeo.2006.10.032, 2007.

Tripsanas, E. K., Karageorgis, A. P., Panagiotopoulos, I. P., Koutsopoulou, E., Kanellopoulos, T. D., Bryant, W. R., and Slowey, N. C.: Paleoenvironmental and paleoclimatic implications of enhanced Holocene discharge from the Mississippi River Based on the sedimentology and geochemistry of a deep core (JPC-26) from the Gulf Of Mexico, PALAIOS, 28, 623–636, doi:10.2110/palo.2012.p12-060r, 2014.

Tucker, G. E. and Hancock, G. R.: Modelling landscape evolution, Earth Surface Processes and Landforms, 35, 28–50, doi:10.1002/esp.1952, 2010.

Tucker, G. E. and Whipple, K. X.: Topographic outcomes predicted by stream erosion models: Sensitivity analysis and intermodel comparison, Journal of Geophysical Research, 107, 1–16, doi:10.1029/2001JB000162, 2002.

Tushingham, A. M. and Peltier, W. R.: Ice-3G: A new global model of Late Pleistocene deglaciation based upon geophysical predictions of post-glacial relative sea level change, Journal of Geophysical Research, 96, 4497, doi:10.1029/90JB01583, 1991.

Ullman, D. J., LeGrande, A. N., Carlson, A. E., Anslow, F. S., and Licciardi, J. M.: Assessing the impact of Laurentide Ice Sheet topography on glacial climate, Climate of the Past, 10, 487–507, doi:10.5194/cp-10-487-2014, 2014.

Ullman, D. J., Carlson, A. E., Anslow, F. S., Legrande, A. N., and Licciardi, J. M.: Laurentide ice-sheet instability during the last deglaciation, Nature Geoscience, 8, 534–537, doi:10.1038/NGEO2463, 2015.

U.S. Bureau of Reclamation: Report on the Water Supply of the Lower Colorado River, Project Planning Report, 1952.

van Andel, T. H.: Recent marine sediments of the Gulf of California, in: Marine Geology of the Gulf of California: A Symposium, edited by van Andel, T. J. and Shor, G. G., Memoir, pp. 216–310, American Association of Petroleum Geologists, 1964.

van Hise, C. R. and Leith, C. K.: The geology of the Lake Superior region, Monographs, United States Geological Survey, Washington, D.C., 1911.

Vázquez Riveiros, N., Govin, A., Waelbroeck, C., Mackensen, A., Michel, E., Moreira, S., Bouinot, T., Caillon, N., Orgun, A., and Brandon, M.: Mg/Ca thermometry in planktic foraminifera: Improving paleotem-

perature estimations for G. bulloides and N. pachyderma left, Geochemistry, Geophysics, Geosystems, doi:10.1002/2015GC006234, 2016.

Veillette, J. J.: Evolution and paleohydrology of glacial Lakes Barlow and Ojibway, Quaternary Science Reviews, 13, 945–971, doi:10.1016/0277-3791(94)90010-8, 1994.

Vening Meinesz, F. A.: Une nouvelle methode pour la reduction isostatique regionale de l'intensite de la pesanteur, Bulletin Géodésique (1922-1941), 29, 33–51, 1931.

Ver Steeg, K.: The Teays River, The Ohio Journal of Science, 46, 297–307, 1946.

Vetter, L.: Combined Stable Isotope and Trace Element Analyses on Single Planktic Foraminifer Shells: Insights from Live Culture Experiments and Paleoceanographic Applications, Ph.d. dissertation, University of California, Davis, 2013.

Vincent, J.-S. and Hardy, L.: L'évolution et l'extension des lacs glaciaires Barlow et Ojibway en territoire québécois, Géographie physique et Quaternaire, 31, 357–372, doi:10.7202/1000283ar, 1977.

Wagner, J. D. M., Cole, J. E., Beck, J. W., Patchett, P. J., Henderson, G. M., and Barnett, H. R.: Moisture variability in the southwestern United States linked to abrupt glacial climate change, Nature Geoscience, 3, 110–113, doi:10.1038/ngeo707, 2010.

Waitt, R. B. J.: About forty last-glacial Lake Missoula jökulhlaups through southern Washington, The Journal of Geology, 88, 653–679, 1980.

Wall, G. R., Nystrom, E. A., and Litten, S.: Suspended Sediment Transport in the Freshwater Reach of the Hudson River Estuary in Eastern New York, Estuaries and Coasts, 31, 542–553, doi:10.1007/s12237-008-9050-y, 2008.

Wickert, A. D.: The ALog: Inexpensive, Open-Source, Automated Data Collection in the Field, Bulletin of the Ecological Society of America, 95, 68–78, doi:10.1890/0012-9623-95.2.68, 2014a.

Wickert, A. D.: Impacts of Pleistocene glaciation and its geophysical effects on North American river systems, Ph.d. dissertation, University of Colorado Boulder, 2014b.

Wickert, A. D., Mitrovica, J. X., Williams, C., and Anderson, R. S.: Gradual demise of a thin southern Laurentide ice sheet recorded by Mississippi drainage, Nature, 502, 668–671, doi:10.1038/nature12609, 2013.

Willgoose, G.: Mathematical Modeling of Whole Landscape Evolution, Annual Review of Earth and Planetary Sciences, 33, 443–459, doi:10.1146/annurev.earth.33.092203.122610, 2005.

Williams, C., Flower, B. P., Hastings, D. W., Guilderson, T. P., Quinn, K. A., and Goddard, E. A.: Deglacial abrupt climate change in the Atlantic Warm Pool: A Gulf of Mexico perspective, Paleoceanography, 25, PA4221, doi:10.1029/2010PA001928, 2010.

Williams, C., Flower, B. P., and Hastings, D. W.: Seasonal Laurentide Ice Sheet melting during the "Mystery Interval" (17.5-14.5 ka), Geology, 40, 955–958, doi:10.1130/G33279.1, 2012.

Wright, H.: Tunnel valleys, glacial surges, and subglacial hydrology of the Superior Lobe, Minnesota, Geological Society of America Memoir, 136, 251–276, 1973.

Wright, H. E. J.: Synthesis: the land south of the ice sheets, in: North America and Adjacent Oceans During the Last Deglaciation, edited by Ruddiman, W. F. and Wright, H. E. J., Geology of North America, pp. 479–488, Geological Society of America, Boulder, Colorado, USA, 1987.

1660 Xie, P. and Arkin, P. A.: Global Precipitation: A 17-Year Monthly Analysis Based on Gauge Observations, Satellite Estimates, and Numerical Model Outputs, Bulletin of the American Meteorological Society, 78, 2539–2558, doi:10.1175/1520-0477(1997)078<2539:GPAYMA>2.0.CO;2, 1997.

Yeager, S. G., Shields, C. A., Large, W. G., and Hack, J. J.: The low-resolution CCSM3, Journal of Climate, 19, 2545–2566, doi:10.1175/JCLI3744.1, 2006.

1665 Zuffa, G., Normark, W., Serra, F., and Brunner, C.: Turbidite megabeds in an oceanic rift valley recording jökulhlaups of late Pleistocene glacial lakes of the western United States, The Journal of Geology, 108, 253–274, 2000.